US Army Corps
of Engineers®
Fort Worth District

October 2018

Draft Environmental Impact Statement

Lake Ralph Hall Regional Water Supply Reservoir Project

Volume II

Table of Contents

Volume II

Appendix A- Alternative Analysis Supporting Documents

Appendix B- Geotechnical Data Report and Conceptual Design

Appendix C- Fluvial Geomorphology Study Report

Appendix D- Hydrologic and Hydraulic Studies

Appendix E- Jurisdictional Determination of Waters of the U.S

Appendix F- Biological and Habitat Studies

Appendix G- Hazardous Materials Radius Report

Appendix H- Tribal Consultation Letters

Appendix I- Final Lake Ralph Hall Water Resources Technical Report

Appendix J- Final Order from Court of Appeals

Appendix K- Draft Operations Plan

Appendix L- Mitigation Plan

Appendix M- Draft Programmatic Agreement

Appendix C

Fluvial Geomorphology Study Report

ATTACHMENT 8
FLUVIAL GEOMORPHOLOGY STUDY REPORT

PREPARED BY
MUSSETTER ENGINEERING, INC.

UPPER TRINITY
REGIONAL WATER DISTRICT

Geomorphic and Sedimentation Evaluation of North Sulphur River and Tributaries for the Lake Ralph Hall Project

Submitted to:

Chiang Patel & Yerby, Inc.
1820 Regal Row, Suite 200
Dallas, Texas 75235

Submitted by:

Mussetter Engineering, Inc.
1730 S. College Avenue, Suite 100
Fort Collins, Colorado 80525

October 23, 2006

EXECUTIVE SUMMARY

ES.1. INTRODUCTION

The Upper Trinity Regional Water District (UTRWD) is proposing to build a 160,235-acre-foot (ac-ft) water supply reservoir, Lake Ralph Hall, on the North Sulphur River (NSR) about 3.5 miles north of Ladonia in Fannin County, Texas (Figure 1.1). Fannin County is located within the Texas Blackland Prairie physiographic area (NRCS, 2001). The NSR and its tributaries, within the boundaries of the proposed reservoir, as well as upstream and downstream, are deeply incised and eroding. Current conditions are the result of channelization and straightening of the sinuous, meandering river and the lower reaches of its tributaries to prevent frequent overbank flooding on the NSR floodplain in the late 1920s (Williams, 1928; Avery, 1974). Prior to channelization, the NSR was a sinuous (1.7) meandering stream with a slope of about 4.3 ft/mi. In the vicinity of the proposed dam site, the natural channel was about 48 feet wide and 6 feet deep and had a hydraulic capacity of between 700 and 1,000 cfs. The channelized and straightened channel had a top width of 16 to 30 feet, and a depth of 9 to 12 feet with a slope of 6.5 ft/mile (Avery, 1974; Chiang, Patel & Yerby, Inc., 2004; AR Consultants, Inc., 2005) and a hydraulic capacity of about 700 cfs. Currently, at the proposed dam site the NSR is 300 feet wide and about 40 feet deep, the bed and lower portions of the banks of the channel are composed of erodible shale (Ozan Formation), and the channel contains flows well in excess of the 100-year flood peak (38,000 cfs). Between the late 1920s and the present, about 28M tons of sediment have been eroded from the mainstem NSR and its tributaries upstream of the proposed dam site. At the time of the channelization in the late 1920's about 75 percent of the watershed was under cultivation (Williams, 1928), and consequently soil erosion rates were probably very high (up to 16 t/ac/yr) (Baird, 1948, 1964), which may have contributed to loss of channel capacity and increased frequency of overbank flooding that occasioned the channelization. Currently about 21 percent of the watershed that contributes water and sediment to the proposed reservoir is cultivated (Texas State Soil and Water Conservation Board, 1997).

ES.2. OBJECTIVES

The primary objectives of this geomorphic and sedimentation study of the Lake Ralph Hall project, that was conducted by Mussetter Engineering, Inc. (MEI) for the UTRWD under subcontract to Chiang Patel & Yerby, Inc. (CP&Y), were:

1. Quantification of the sediment delivery to the reservoir site for the 50-year project life under pre- and post-project conditions,
2. Evaluation of the downstream effects of the dam on channel conditions and flow capacity, and
3. Assessment of the potential for reducing or managing the upstream sediment supply to the reservoir.
4. Assessment of future conditions in the North Sulphur River and tributaries upstream of the dam site in the absence of the project.

ES.3. METHODOLOGY

Future loss of reservoir capacity due to sedimentation is the primary issue of concern for this investigation of the Lake Ralph Hall project and, therefore, estimates of sediment yield from the 100-square-mile watershed upstream of the proposed dam were required. Potential sources of sediment identified included channel erosion in the mainstem NSR and the incised tributaries (bed and banks) and watershed erosion (sheet, rill, ephemeral gully). Hydrologic analyses of the gage record at the USGS North Sulphur River near Cooper gage (USGS Gage No. 07343000) and HEC-1 models were used to estimate peak flow frequencies (Figures 3.7 and 3.9), mean daily durations and flow volumes (Figure 3.10) for the dam site and the tributaries. One–dimensional HEC-RAS models were developed for the mainstem and for the major tributaries based on the 2-foot contour interval Digital Terrain Model (DTM) provided by CP&Y, and the models were calibrated to field-measured high-water marks for the 2002 (10-year event) and 2003 (25-year event) peak flows. Reach-averaged hydraulic output (effective width, hydraulic depth and average velocity) from the HEC-RAS models was used to compute sediment transport.

ES.4. CHANNEL MORPHOLOGY AND EVOLUTION

Field observations of the NSR and its tributaries indicated that in common with other incised streams, the morphological adjustments of the river and the larger tributaries can be described by a geomorphic model of incised channel evolution (Schumm et al., 1984; Simon and Hupp, 1986; Simon, 1989). A channel evolution model (NSRCEM) was developed for the NSR and its tributaries (Figure 2.19). The model varies substantially from those developed for alluvial streams (Figure 2.4) in that it does not predict an equilibrium end point because both vertical and lateral erosion of the exposed shale outcrop is controlled by wetting and drying cycles (Tinkler and Parish, 1989; Allen et al., 2002) and not hydraulic processes. There is little doubt that following channelization in the late 1920s the NSR incised and widened (Avery, 1974) and followed the typical channel evolution sequence while the channel boundary materials were composed of alluvium (Types I through V). However, exposure of the shale added a significant complicating factor to the evolution of the channel. Based on the flow record at the USGS gage on the NSR near Cooper, there are an average of six wetting and drying cycles per year (Figure 2.3). Flow events in the channel remove the weathering products and re-initiate vertical and lateral erosion into the shale. As a rule, lateral erosion rates exceed vertical erosion rates in bedrock and result in the formation of gravel-covered strath surfaces that become terraces when vertical erosion of the bed occurs (Leopold et al., 1964; Schumm, 1977) (Type VI). Deep-seated slump failures of the overlying alluvium bury the strath surfaces (Type VII) and prevent lateral erosion of the shale. Resulting channel narrowing may actually accelerate erosion of the shale exposed in the bed, which in turn leads to undercutting of the erosion-resistant, root-reinforced alluvium, thereby leading to re-exposure of the shale in the toe of the banks and ongoing lateral retreat of the shale (Type VIII). It is likely that over time the incision into the shale will induce further mass failure of the alluvial valley fill and a Type VII condition will be reestablished at a lower bed elevation and there will be additional channel widening. The NSRCEM applies equally to the larger tributaries that have eroded into the shale.

Between the FM 904 bridge and the upstream end of the watershed, the NSR was subdivided into 10 subreaches (Table 2.2). Based on the NSRCEM, Subreaches 1 through 3 were classified as Type VI, Subreach 4 was classified as Type VII, Subreaches 5 through 8 were classified as Type VIII, and Subreaches 9 and 10 were classified as Type VII. Similar sequences are present in the larger tributaries. Incision in the headwaters of the NSR and the major north-side tributaries has been limited by outcrop of reasonably erosion resistant Roxton/Gober Chalk (Figure 2.2). Currently, the incised channel has the ability to convey in

excess of the 100-year flood in-bank (Figures 2.5 through 2.18), the bed of the river is composed of shale, and therefore, the current supply of sediment to the channel is far less than the transport capacity.

ES.5. SEDIMENT TRANSPORT AND YIELD

The primary sources of bed-material size sediment are the exposed shale outcrops in the bed and banks of the river and the tributaries. Based on studies of the erosion of the shale (Allen et al., 2002; Crawford, in prep) and the results of analysis of stage-discharge rating curves for the Cooper gage (Figure 2.36) and comparative bridge profiles (Figure 2.34), erosion rates for shale exposed in the bed and banks of the channel are on the order of 2 to 4 in./yr, respectively. Transport and slaking of the shale clasts results in a temporal and spatial transformation of initially gravel-sized material, which is transported as bed material, to silt-clay-sized wash load (Figure 2.40) that has little or no morphological significance. At the upstream end of the NSR about 80 percent of the bed material that forms a thin veneer over in-situ shale slakes to silt-clay-sized material, whereas in the downstream reaches only about 10 percent of the bed-material slakes (Figure 2.42). Based on a supply-limited model of sediment-transport capacity, calibrated to the area of the bed covered by depositional bars, and incorporating the transformation of the bed material to wash load, the best estimate of sediment yield from channel sources to the dam site under pre-project conditions is 93,100 t/yr. Based on a somewhat unrealistic transport capacity-limited model, the worst-case estimate of sediment yield from channel sources to the dam site is 292,000 t/yr. With the dam in place, the best-case estimate of annual sediment yield from all channel sources to the reservoir is 35,600 tons, and the worst–case estimate is 59,600 tons. The reduced amount of sediment is because the reservoir inundates a high proportion of the contributing channel area and eliminates it as a contributing source.

Estimates of the sheet-and-rill erosion on the watershed were developed with the Modified Universal Soil Equation (MUSLE) with appropriate parameters based on the subbasin topography and soil types (clays and loams) determined from the Soil Survey of Fannin County (NRCS, 2001). Application of the MUSLE with the appropriate parameters underestimated reported gross sheet-and-rill erosion rates on the Blackland Prairie soils (2 t/ac/yr), and therefore the alpha coefficient for the MUSLE was increased by a factor of 2.7. Ephemeral gully erosion for the cropland portions of the watershed was estimated to be equivalent to the sheet-and-rill gross erosion rates on the basis of the soil erosion literature (Laflen et al., 1986). Sediment delivery ratios (SDR) for the sheet-and-rill erosion were estimated with Equation 5.4 (Renfro, 1975) that yields the highest SDR values. For the ephemeral gully erosion the SDR was estimated to be 0.67 (Alan Plummer Associates, 2005). Worst-case watershed sediment yields were estimated with an assumption of 100-percent cropping in the watershed with a gross erosion rate of 3.74 t/ac/yr (Richardson, 1993). The best conservative estimate of the current annual watershed sediment yield at the dam site is about 81,000 t/yr which reduces to about 69,000 t/yr with the reservoir in place. Under worst-case conditions the existing annual watershed sediment yield to the dam site is about 147,000 t/yr, and this reduces to about 90,000 t/yr with the reservoir in place. When placed in the context of reported sediment yields in the Blackland Prairie (Table 5.4), these estimates are very conservative especially because a 100 percent trap efficiency has been assumed for the reservoir.

Although estimated sediment yields to the Lake Ralph Hall reservoir are relatively low, the sediment yields could be further reduced by implementation of soil conservation measures on the watershed and by reducing the exposure of shale in the mainstem of the NSR and the tributaries between the upstream end of the conservation pool and the Roxton/Gober Chalk outcrop (Figure 2.2).

ES.6. DOWNSTREAM IMPACTS

The potential downstream effects of the Lake Ralph Hall project on channel conditions and channel capacity are a concern. Potential problems could include sediment accumulation in the bed of the channel since operation of the reservoir will affect the magnitude and frequency of flows in the downstream channel, but will not affect sediment supply from the watershed, tributary and channel sources below the dam. Field and helicopter reconnaissance of the NSR from its confluence with the South Sulphur River to the headwaters indicates that the channel of the NSR is deeply incised for its entire length, and that the bed of the channel is composed of shale bedrock. Since the rates of bedrock erosion are controlled by the number of wetting and drying cycles (Allen et al., 2002), and not by hydraulic processes, the upstream dam is unlikely to have any effects on bedrock erosion rates. On an average annual basis, the shale will continue to erode vertically at a rate of about 2 inches per year and laterally at a rate of about 4 inches per year. Locally, near the mouths of some of the large tributaries downstream of the dam site (e.g., Hickory and Big Sandy Creeks) there are alternate bars in the bed of the channel, but these reflect local sediment supply and do not extend downstream for any distance. Under existing conditions, the best estimate of the annual total sediment yield to the dam site is about 174,000 tons (Figure 5.8), but only about 25 percent is composed of bed material, the remainder being wash load. Therefore, construction of the dam will reduce the morphologically-significant sediment yield to the channel downstream of the dam by about 25 percent, which will have an insignificant effect on the channel morphology in this sediment supply-limited system.

Based on the geologic map (Figure 2.2), and field observations, the characteristics of the shale exposed in the mainstem NSR and tributaries downstream of the dam site are similar to those upstream of the site, and therefore, it can be assumed that the sediment characteristics are also similar. This being the case, the bulk of the sediments being delivered to the NSR by the tributaries downstream of the dam will be composed of shale clasts that break down into wash-load-sized materials as they are exposed to transport and weathering processes (slaking). Furthermore, the NSR is a supply-limited system that has the capacity to transport considerably more bed material than is currently being supplied to the channel. Consequently, it is unlikely that significant amounts of sediment will accumulate in the bed of the river downstream of the dam. If sediment accumulation does occur it is highly unlikely that there will be significant loss of channel capacity. Even with the loss of channel capacity, flows far greater than the 100-year flood peak can be conveyed in-bank.

ES.7. CONCLUSIONS

The geomorphic, hydrologic, hydraulic and sediment-transport studies conducted for this investigation of the Lake Ralph Hall project allow the following to be concluded:

1. Channelization-induced degradation and widening of the NSR and its principal tributaries upstream of the dam site has resulted in the erosion of about 28M tons of sediment since the late 1920s. Current channel erosion rates are controlled by slaking rates of the exposed shale and not by hydraulic processes and are, therefore, less than historic rates.
2. The conservative estimate of total annual sediment yield to the dam site under pre-project conditions is 86 ac-ft (174,000 tons). With the reservoir in place, the contributing watershed area is reduced, as is the length of channel that is supplying sediment, and therefore, the total annual sediment yield to the reservoir reduces to 51.4 ac-ft (104,000 tons). Therefore, estimated sediment delivery to the 160,235-ac-ft reservoir over a 50-

year period, assuming 100-percent trap efficiency, is about 2,570 ac-ft, which represents a loss of reservoir storage capacity of approximately 1.6 percent.

3. Under the assumptions of the worst-case watershed (100 percent of the watershed under cultivation with no soil conservation measures) and channel sediment yields (transport capacity limited assumption) the estimated total annual sediment yield to the dam site is 217 ac-ft (439,000 tons). With the reservoir in place, the worst-case reduces to an annual sediment yield to the reservoir of 74 ac-ft (150,000 tons). Under these circumstances, estimated sediment delivery to the 160,235 ac-ft reservoir over a 50-year period, assuming 100-percent trap efficiency, is about 3,700 ac-ft, which represents a loss of reservoir storage capacity of approximately 2.3 percent.

4. In the absence of the Lake Ralph Hall project there will be continued erosion of the NSR and its tributaries. On average, where shale is exposed in the bed and banks of the channels, the channel depth will increase by about 8 feet and the channel bottom widths will increase by about 16 feet over a 50-year period. Increased channel depths are also likely to cause further mass failure of the alluvial portions of the banks, thereby increasing channel top widths, as well.

5. No adverse downstream impacts on channel morphology or capacity are expected as a result of sediment trapping in the reservoir, or operation of the reservoir.

6. Watershed sediment yields could be reduced by implementation of best soil conservation management practices, reduction in the area under cultivation and re-establishment of riparian buffer areas along the channel margins where they have been cleared.

7. Channel sediment yields between the elevation of the top of the conservation pool and the downstream extent of the Roxton/Gober Chalk could be reduced by construction of in-channel structures that pond water and prevent weathering of the shale outcrop. Given the existing hydraulic capacity of the channels there is little likelihood that the in-channel structures would cause out-of-bank flooding.

Table of Contents

Page

EXECUTIVE SUMMARY ii

ES.1. INTRODUCTION ii
ES.2. OBJECTIVES ii
ES.3. METHODOLOGY iii
ES.4. CHANNEL MORPHOLOGY AND EVOLUTION iii
ES.5. SEDIMENT TRANSPORT AND YIELD iv
ES.6. DOWNSTREAM IMPACTS v
ES.7. CONCLUSIONS v

1. INTRODUCTION 1.1

1.1. Background 1.1
1.2. Project Objectives 1.3
1.3. Data and Information Sources 1.3
1.4. Authorization 1.4

2. GEOLOGY AND GEOMORPHOLOGY 2.1

2.1. Geology 2.1
2.2. Geomorphology 2.4

2.2.1. Incised Channel Evolution Models 2.6
2.2.2. Channel Evolution in the North Sulphur River 2.8

2.2.2.1. North Sulphur River Channel Evolution Model 2.16

2.2.3. Existing Channel Morphology 2.18
2.2.4. Channel Incision Rates 2.32
2.2.5. Sediment Sources and Bed-material Gradations 2.34

3. HYDROLOGY 3.1

3.1. USGS Gage near Cooper, Texas 3.1

3.1.1. Annual Flow Volume and Mean Daily Flow-duration Analysis 3.1
3.1.2. Peak Flood Frequency Analysis 3.1
3.1.3. Annual Flow Frequency 3.1

3.2. Hydrology at the Proposed Dam Site 3.6

3.2.1. Regional Regressional Relationships 3.6
3.2.2. Hydrologic (HEC-1) Models 3.7

3.2.2.1. RJ Brandes Company Model 3.7

3.2.3. Modified HEC-1 Models for Contributing Watershed to Proposed Dam Site 3.9
3.2.4. HEC-1 Models for Tributary Basins 3.12
3.2.5. With-Dam Downstream Impacts 3.15

4. HYDRAULICS 4.1

4.1. Hydraulic Model for the North Sulphur River 4.1

4.1.1. Model Calibration 4.1
4.1.2. Reach-averaged Hydraulics 4.3

4.2. Hydraulic Models for the Primary Tributaries 4.12

4.2.1. Reach-averaged Hydraulics 4.12

5. SEDIMENT TRANSPORT 5.1

5.1. Watershed Sediment Yield 5.1

5.1.1. Soil Characteristics, Cover and Management Practices 5.1
5.1.2. Modified Universal Soil Loss Equation 5.2
5.1.3. Ephemeral Gully Erosion 5.5
5.1.4. Sediment Delivery Ratios 5.5
5.1.5. Existing Conditions Watershed Sediment Yield 5.6
5.1.6. With-Dam Sediment Yield 5.6
5.1.7. Worst-Case Sediment Yield 5.6

5.2. Total Sediment Yield 5.6

5.2.1. Bed-material Capacity Calculations 5.9
5.2.2. Sediment-Routing Analysis 5.9
5.2.3. Capacity-Limited Sediment-Continuity Analysis 5.17
5.2.4. Worst-Case Watershed Sediment Yield and Summary of Total Sediment Yields 5.17
5.2.5. Summary 5.20

6. SEDIMENT MANAGEMENT 6.1

6.1. Watershed Sediment Reduction 6.1
6.2. Channel Sediment Reduction 6.1

7. SUMMARY AND CONCLUSIONS 7.1

7.1. Summary 7.1
7.2. Conclusions 7.4

8. REFERENCES 8.1

APPENDIX A: Photographs of North Sulphur River and Tributaries ..... ---
APPENDIX B: Sediment Sample Analysis Report (Kleinfelder, 2006) ..... ---
APPENDIX C: HEC-1 Models for the Mainstem North Sulphur River and the Primary Tributaries ..... ---
APPENDIX D: HEC-RAS Models for the Mainstem North Sulphur River and the Primary Tributaries ..... ---
APPENDIX E: Fine Sediment Yield Calculations (Best Estimate and Worst Case; Existing Conditions) ..... ---

List of Figures

Figure 1.1. Map showing the location of the proposed Lake Ralph Hall on the North Sulphur River in Fannin County, Texas. 1.2

Figure 2.1. Geologic map of the North Sulphur River Basin (after Texas Bureau of Economic Geology, 1966, 1967). 2.2

Figure 2.2. Map of the North Sulphur River basin showing the locations of the downstream limits of exposed Roxton/Gober Chalk in the headwaters of the North Sulphur River and the north-side tributaries. 2.3

Figure 2.3. Number of continuous periods with flows less than 1 cfs at the USGS gage near Cooper, Texas. On average there are about 6 wetting and drying cycles per year (Q <1 cfs). 2.5

Figure 2.4. Incised channel evolution model (after Schumm et al., 1984). 2.7

Figure 2.5. Cross section of North Sulphur River in Subreach 1, Sta 604+27. ..... 2.9

Figure 2.6. Cross section of North Sulphur River in Subreach 2, Sta 562+44. ..... 2.9

Figure 2.7. Cross section of North Sulphur River in Subreach 3, Sta 530+93. ..... 2.10

Figure 2.8. Cross section of North Sulphur River in Subreach 3, Sta 496+42. ..... 2.10

Figure 2.9. Cross section of North Sulphur River in Subreach 3, Sta 468+60. ..... 2.11

Figure 2.10. Cross section of North Sulphur River in Subreach 3, Sta 453+04. ..... 2.11

Figure 2.11. Cross section of North Sulphur River in Subreach 4, Sta 390+34. ..... 2.12

Figure 2.12. Cross section of North Sulphur River in Subreach 5, Sta 344+08. ..... 2.12

Figure 2.13. Cross section of North Sulphur River in Subreach 6, Sta 303+01 ..... 2.13

Figure 2.14. Cross section of North Sulphur River in Subreach 7, Sta 273+25. ..... 2.13

Figure 2.15. Cross section of North Sulphur River in Subreach 7, Sta 246+13. ..... 2.14

Figure 2.16. Cross section of North Sulphur River in Subreach 8, Sta 187+60. ..... 2.14

Figure 2.17. Cross section of North Sulphur River in Subreach 9, Sta 88+77. ..... 2.15

Figure 2.18. Cross section of North Sulphur River in Subreach 10, Sta 32+36. ..... 2.15

Figure 2.19. Channel evolution model (NSRCEM) for the North Sulphur River. 2.17

Figure 2.20. Existing and adjusted effective widths and shear stresses for the 10 subreaches of the North Sulphur River at the 2-year peak flow assuming that velocities would have to be < 2 ft/s to induce sediment deposition on the bed. 2.19

Figure 2.21. Longitudinal profiles of the bed and valley floor of the North Sulphur River between FM 904 Bridge and upstream of Allen Creek. 2.20

Figure 2.22. Plot of channel top widths along the North Sulphur River between FM 904 Bridge and upstream of Allen Creek. 2.22

Figure 2.23. Longitudinal profiles of the bed and valley floor of Merrill Creek. 2.23

Figure 2.24. Longitudinal profiles of the bed and valley floor of Bralley Pool Creek..... 2.24

Figure 2.25. Longitudinal profiles of the bed and valley floor of Leggetts Branch. 2.25

Figure 2.26. Longitudinal profiles of the bed and valley floor of Davis Creek..... 2.26

Figure 2.27. Longitudinal profiles of the bed and valley floor Pickle Creek. 2.27

Figure 2.28. Longitudinal profiles of the bed and valley floor of Brushy Creek..... 2.28

Figure 2.29. Longitudinal profiles of the bed and valley floor Bear Creek. 2.29

Figure 2.30. Longitudinal profiles of the bed and valley floor of Allen Creek..... 2.30

Figure 2.31. Longitudinal profiles of the bed and valley floor of Long Creek..... 2.31

Figure 2.32. Bridge cross section profiles for the FM 2990 crossing of the North Sulphur River 2.33

Figure 2.33. Bridge cross section profiles for the FM 1550 crossing of Merrill Creek. 2.33

Figure 2.34. Bed degradation rates at the 7 evaluated bridges in the upper North Sulphur River basin. 2.35

Figure 2.35. Stage-discharge rating curves from 1950 to 2005 for the USGS gage on the North Sulphur River, near Cooper, Texas (USGS Gage No. 07343000). 2.36

Figure 2.36. Stage-discharge rating curves from 1971 to 2005 for the USGS gage on the North Sulphur River, near Cooper, Texas (USGS Gage No. 07343000). 2.37

Figure 2.37. Map showing the locations of the bed-material samples in the North Sulphur River and the tributaries. 2.39

Figure 2.38. Dry-sieved gradation curves for the bed-material samples collected in the North Sulphur River. 2.40

Figure 2.39. Wet-sieved gradations for the bed-material samples collected in the North Sulphur River. 2.41

Figure 2.40. Comparison of dry- and wet-sieved gradations for sample NSR4 located about 1,500 feet downstream of the Brushy Creek confluence..... 2.42

Figure 2.41. Dry- and wet-sieved gradation curves for the tributary samples. 2.43

Figure 2.42. Changes in the median sizes of the dry- and wet-sieved bed-material samples of the North Sulphur River as well as the silt-clay content of the samples following slaking arranged from upstream to downstream. 2.44

Figure 3.1. Mean annual flow volumes between 1950 and 2004 at the North Sulphur River near Cooper, Texas, gage. 3.2

Figure 3.2. Computed flow duration curve at the North Sulphur River near Cooper, Texas, gage. 3.3

Figure 3.3. Measured annual peak flows (1950-2004) at the North Sulphur River near Cooper, Texas, gage. 3.4

Figure 3.4. Computed peak flow frequency curve at the North Sulphur River near Cooper, Texas, gage. 3.5

Figure 3.5. Computed frequency curves at the Cooper gage using the measured peak flow values (HEC-FFA) and using the regional regression equations for Region 10 (Asquith and Slade, 1997). 3.8

Figure 3.6. Number of days preceding measured peak discharges at the USGS gage near Cooper with rainfall exceeding 0.1 inches at the Honey Grove weather station. 3.10

Figure 3.7. Flood-frequency curves based on the computed peak discharges from the MEI HEC-1 models (using wet antecedent runoff conditions), from the HEC-1 models using normal antecedent runoff conditions, from the regional regression equations, and based on the unit discharge at the Cooper gage location. Also shown is the computed frequency curve at the USGS gage near Cooper, Texas. 3.11

Figure 3.8. Delineated subbasins for the contributing watershed to the proposed Lake Ralph Hall dam site near Ladonia, Texas, and the primary tributary basins that were modeled using HEC-1 ..... 3.13

Figure 3.9. Computed peak discharges from the HEC-1 models for the primary tributaries as a function of contributing drainage area, and the resulting regression equations. 3.14

Figure 3.10. Computed storm volumes from the HEC-1 models for the primary tributaries as a function of contributing drainage area, and the resulting regression equations. 3.14

Figure 4.1. Measured high-water marks and computed water-surface elevations for the 2002 (Q=60,400 cfs) and the 2003 (72,200 cfs) flood peaks. 4.2

Figure 4.2. Subreach breakdown for the subreach-averaged hydraulic computations. 4.4

Figure 4.3. Subreach-averaged main channel velocities (bar graphs) for each of the subreaches for the 2- 10-, and 100-year peak flows. Also shown are the peak discharges (curves) 4.5

Figure 4.4. Subreach-averaged hydraulic depth (bar graphs) for each of the subreaches for the 2-, 10-, and 100-year peak flows. Also shown are the peak discharges (curves). 4.6

Figure 4.5. Subreach-averaged effective width (bar graphs) for each of the subreaches for the 2-, 10-, and 100-year peak flows. Also shown are the peak discharges (curves) 4.7

Figure 4.6. Subreach-averaged total shear stress (bar graphs) for each of the subreaches for the 2-, 10-, and 100-year peak flows. Also shown are the peak discharges (curves) 4.8

Figure 4.7. Computed total stream power along the modeled reach of the North Sulphur River for the 2-, 10-, and 100-year peak discharges 4.9

Figure 4.8. Computed unit stream power along the modeled reach of the North Sulphur River for the 2-, 10-, and 100-year peak discharges. 4.10

Figure 4.9. Subreach-averaged critical grain size (bar graphs) for each of the subreaches for the 2-, 10-, and 100-year peak flows. Also shown are the peak discharges (curves). 4.11

Figure 5.1. Cumulative total watershed sediment yield from the contributing basin at various locations within the project reach under existing and with-dam conditions. 5.7

Figure 5.2. Cumulative total watershed sediment yield from the contributing basin at various locations within the project reach for the worst-case watershed sediment yields under existing and with-dam conditions. 5.8

Figure 5.3. Computed bed-material transport capacity rating curves for the 10 subreaches in the mainstem North Sulphur River using MPM-Einstein equation 5.11

Figure 5.4. Computed bed-material transport capacity rating curves for the primary tributaries to the North Sulphur River using MPM-Einstein equation 5.12

Figure 5.5. Flow chart for the sediment routing computations 5.13

Figure 5.6. Measured percent area composed of depositional bars and the ratio (as percentage) of computed annual bed-material load to the hydraulic capacity for each subreach from the sediment routing analysis. 5.16

Figure 5.7. Computed upstream and tributary bed-material supply, hydraulic capacity, and the resulting aggradation/degradation volume for the sediment-continuity analysis (worst-case channel sediment yield with no supply limitations). 5.18

Figure 5.8. Summary of total sediment yield to the proposed location of the dam for the best-estimates and worst-case watershed and channel sediment yields under existing and with-dam conditions. 5.19

Figure A.1. Upstream view of Roxton/Gober Chalk outcrop providing grade control for the upper reaches of the North Sulphur River. A.1

Figure A.2. Upstream view of Roxton/Gober Chalk outcrop providing grade control for the upper reaches of Merrill Creek. The outcrop coincides with the top of the conservation pool at an elevation of 551 ft msl A.1

Figure A.3. Upstream view of exposed bed of Merrill Creek showing weathering of the Roxton/Gober Chalk. A.2

Figure A.4. Low specific gravity sand and gravels produced by weathering of Roxton/ Gober Chalk outcrop in the bed of Merrill Creek. A.2

Figure A.5. Mass failed blocks of shale exposed in bed of Baker Creek. A.3

Figure A.6. Slaked shale in mass failed blocks shown in Figure A.5. ....A.3

Figure A.7. Eroded shale in the bed of North Sulphur River upstream of FM 904 Bridge. ...A.4

Figure A.8. Mass failure of weathered shale (upper bank) and weathering of more recently exposed shale (lower bank) in the north bank of the North Sulphur River. A.4

Figure A.9. Plucking erosion along bedding planes of shale exposed in the bed of North Sulphur River. A.5

Figure A.10. Three inches of weathered (slaked) shale over intact shale bedrock in the bed of the North Sulphur River. A.5

Figure A.11. Upstream view of North Sulphur River showing the bed of the river mantled by unweathered shale clasts following a flow of about 15,000 cfs in March 2006. ....A.6

Figure A.12. Close up view of unweathered shale (grey) clasts transported during a flow of about 15,000 cfs in the North Sulphur River. A.6

Figure A.13. Downstream view showing a 30-foot thick section of the alluvial valley fill on the south bank of the North Sulphur River. A.7

Figure A.14. Downstream view showing a 10-foot thick section of the alluvial valley fill on the south bank of the North Sulphur River. Note limestone stringers forming localized grade control in the bed of the river. A.7

Figure A.15. Groundwater seepage at contact between shale and alluvium has caused mass failure of the overlying alluvium. A.8

Figure A.16. Downstream view of the North Sulphur River about 6 miles downstream of the dam site showing well vegetated channel banks and bed-material accumulation. A.8

Figure A.17. Downstream view of actively widening reach of the North Sulphur River about 5 miles upstream of the dam site. A.9

Figure A.18. Upstream view of the North Sulphur River from FM 904 showing well vegetated and apparently stable banks with exposed shale bedrock in the bed. A.9

Figure A.19. Upstream view of the lower reaches of Baker Creek showing well vegetated banks and some sediment accumulation in the bed....A.10

Figure A.20. Upstream view of Bralley Pool Creek showing active bank erosion and channel widening....A.10

Figure A.21. Upstream view of knickzone formed in shale in Baker Creek. A.11

Figure A.22. Upstream view of recently installed grade-control structure downstream of FM 1550 Bridge across Brushy Creek....A.11

Figure A.23. Downstream view of the North Sulphur River (Figure 2.5; Subreach 1) showing the channel incised into shale with a veneer of sediment (weathered shale) over the shale in the bedrock bed....A.12

Figure A.24. Downstream view of the North Sulphur River (Figure 2.6; Subreach 2) showing the channel incised into the shale, a veneer of sediment over the shale in the bed, and steep mass failing banks....A.12

Figure A.25. Downstream view of the North Sulphur River (Figure 2.7; Subreach 3) showing the channel incised into the shale, a veneer of sediment over the shale in the bed, steep mass failing left bank and a less steep right bank....A.13

Figure A.26. Downstream view of the North Sulphur River (Figure 2.8; Subreach 3) showing the channel incised into the shale, a veneer of sediment over the shale in the bed, and steep, mass failing left and right banks....A.13

Figure A.27. Downstream view of the North Sulphur River (Figure 2.9; Subreach 3) showing the channel incised into the shale, and an asymmetrical cross-section profile with a steep, actively mass failing left bank and a more rounded right bank formed by deeper seated slump failures in the alluvial fill. A.14

Figure A.28. Upstream view of the North Sulphur River (Figure 2.10; Subreach 3) showing the channel incised into the shale, and an asymmetrical cross-section profile with a steep, actively mass failing left descending bank and a more rounded right descending bank formed by deeper seated slump failures in the alluvial fill. A.14

Figure A.29. Downstream view of the North Sulphur River (Figure 2.11; Subreach 4) showing the channel incised into the shale, and asymmetrical cross-section profile with flatter, more convex slopes on both banks formed by deep seated slump failures of the alluvial fill. A.15

Figure A.30. Downstream view of the North Sulphur River (Figure 2.12; Subreach 5) showing deep incision into the shale, a thin veneer of sediment over the shale in the channel bed, and very steep eroding banks. A.15

Figure A.31. Downstream view of the North Sulphur River (Figure 2.13; Subreach 6) showing incision into the shale, a thin veneer of sediment over the shale in the bed, and actively failing, steep banks. A.16

Figure A.32. Downstream view of the North Sulphur River (Figure 2.14; Subreach 7) showing incision into the shale and erosion and retreat of the mass failed alluvial materials that form the toes of both banks. A.16

Figure A.33. Downstream view of the North Sulphur River (Figure 2.15; Subreach 7) showing incision into the shale, a veneer of sediment over shale in the bed, and retreat of the toes of both banks formed in mass failed alluvium that is exposing the underlying shale in the lower banks. A.17

Figure A.34. Downstream view of the North Sulphur River (Figure 2.16; Subreach 8) showing incision into the shale, a veneer of coarser sediment over the shale in the bed, and exposure of the shale in the toes of both banks formed by mass failure of the overlying alluvium A.17

Figure A.35. Downstream view of the North Sulphur River (Figure 2.17; Subreach 9) showing a veneer of sediment over the shale in the bed, and apparently very stable, low angle, vegetated banks in mass failed alluvium. A.18

Figure A.36. Downstream view of the North Sulphur River (Figure 2.18; Subreach 10) showing a veneer of sediment over shale in the bed, and apparently stable, low angle, vegetated banks formed in mass failed alluvium A.18

Figure A.37. Downstream view of North Sulphur River from Highway 32 Bridge showing erosion of previously failed alluvium and re-exposure of the shale in the lower banks. A.19

Figure A.38. View of eroded mass failed alluvium that has exposed shale outcrop in the toe of the north bank, upstream of FM904 Bridge. A.19

Figure A.39. Upstream view of north bank of North Sulphur River from FM 904 bridge showing multiple mass failure deposits in the alluvial fill that overlies the shale that have contributed to increasing the top width of the river A.20

Figure A.40. View of pier 4 at FM 2990 bridge on the North Sulphur River. Approximately 7 feet of scour has occurred at the pier. A.20

Figure A.41. Upstream view showing shale exposed in the bed of the North Sulphur River at the USGS gage on Highway 32 ..... A.21

Figure A.42. Deep-seated slump failure in alluvium on south bank of North Sulphur River near the proposed dam site. A.21

Figure A.43. Gravel and cobble size shale clasts plucked from exposed outcrop in the toe of the North Sulphur River near the FM 904 Bridge. A.22

Figure A.44. Detrital cone of weathered shale at the base of exposed shale outcrop in the lower bank region of Bralley Pool Creek. A.22

Figure A.45. Erosion of limestone stringers in the exposed shale outcrop delivers gravel and cobble size clasts to the North Sulphur River. A.23

Figure A.46. Weathered and poorly cemented gravels exposed by erosion of shale are a source of gravel sized sediments to the North Sulphur River. A.23

Figure A.47. Dune bedform composed of sand and fine gravel size shale particles on the bed of the North Sulphur River downstream of the FM 904 Bridge. A.24

Figure A.48. Bed-material sample NSR2 located upstream of Allen Creek is composed primarily of shale clasts. A.24

Figure A.49. Bed-material sample NSR0, located just downstream of the Bralley Pool Creek confluence has a lower percentage of shale clasts and a higher percentage of non-shale material. A.25

Figure A.50. Bed-material sample NSR8, located upstream of FM 904 Bridge is composed primarily of non-shale material. A.25

List of Tables

Table 2.1. Lengths of eroding channel between top of conservation pool extent and Roxton/Gober Chalk outcrop 2.4

Table 2.2. Summary of subreach information for mainstem of North Sulphur River 2.8

Table 3.1. Summary of results from the flood-frequency analysis at the Cooper gage. 3.6

Table 3.2. Summary of computed peak flows at the location of the proposed dam from the HEC-1 model with wet antecedent runoff conditions. 3.12

Table 4.1. Summary of subreach delineations used for the reach-averaged hydraulic calculations. 4.3

Table 4.2. Summary of hydraulic model information for the primary tributaries in the project reach. 4.12

Table 4.3. Summary of reach-averaged hydraulic conditions for the 2-, 10-, and 100-year events for subreaches of the primary tributaries. 4.14

Table 5.1. Summary of MUSLE factors for the individual subbasins in the project watershed. 5.3

Table 5.2. Summary of selected C-factors for the individual land-use types in the project watershed. 5.4

Table 5.3. Summary of gradation information used in the sediment-transport analysis 5.10

Table 5.4. Comparison of estimated sediment yields from Texas Blackland Prairie watersheds 5.20

1. INTRODUCTION

1.1. Background

The Upper Trinity Regional Water District (UTRWD) is proposing to build a 160,235-acre-foot (ac-ft) water supply reservoir, Lake Ralph Hall, on the North Sulphur River (NSR) about 3.5 miles north of Ladonia in Fannin County, Texas (**Figure 1.1**). The NSR and its tributaries, up- and downstream of the proposed reservoir, are deeply incised and eroding. Current conditions are the result of channelization and straightening of the very sinuous (1.7) meandering river and the lower reaches of its tributaries to prevent frequent overbank flooding on the NSR floodplain in the late 1920s (Avery, 1974). Estimates of the initial configuration of the channelized mainstem of the NSR vary from a top width of 16 to 30 feet, and a depth of 9 to 12 feet with a slope of 6.5 ft/mile (Avery, 1974; Chiang, Patel & Yerby, Inc., 2004; AR Consultants, Inc., 2005). It is of interest to note that Mr. Z.F Williams, the State Reclamation Engineer, predicted that the channelization would *cause high velocities and subsequent erosion, and will result in a substantial enlargement to the section as cut* (Williams, 1928). As predicted, the NSR has incised through the alluvial valley fill into the underlying shale bedrock, and currently has a depth and width at the dam site of 40 and 300 feet, respectively. The channel incision and widening caused the loss of agricultural lands, damages to bridges and other utilities, lowering of the water table, loss of riparian habitat and channel biodiversity. Additionally, this has resulted in baselevel lowering for tributaries that were not channelized, that have in turn incised and widened.

Based on measurements of remnants of the natural channel of NSR on the now abandoned floodplain, the width was about 48 feet, the depth was about 6 feet and the slope was about 3.8 ft/mile. Normal-depth calculations based on the geometry of the remnant channel segments indicate that the natural channel of the NSR had a flow capacity of between 700 and 1,000 cfs in the vicinity of the dam site, the channelized river had a flow capacity of about 700 cfs, and the current channel has a capacity in excess of the 100-year flood peak (~38,000 cfs; RJ Brandes Co., 2004). At the time of channelization of NSR, about 75 percent of the watershed was under cultivation (Williams, 1928). Based on Baird's (1948, 1964) estimates of annual gross soil erosion without any conservation measures for the Blackland Prairie Land Resource Area (14.3 to 16.6 t/ac), the annual sediment load at the dam site (100-square-mile drainage area) could have been as high as 1 million tons, which is about 10 times higher than the amount that would be predicted by more recent reservoir sedimentation surveys in the Blackland Prairie area (Alan Plummer and Associates, 2005). As occurred in many parts of the U.S., the high sediment loading from the watershed may have contributed to loss of channel capacity and the frequent (multiple times per year) overbank flooding that occasioned the channelization of NSR (Happ et al., 1940; Trimble, 1974; Schumm et al., 1984; Harvey and Watson, 1986).

Future loss of reservoir capacity due to sedimentation is an issue of concern for the Lake Ralph Hall project and, therefore, estimates of sediment yield from the 100-square-mile watershed upstream of the proposed dam are required. Potential sources of sediment include channel erosion (bed and banks) and watershed erosion (sheet, rill, ephemeral gully, gully). Incised channels generally follow a temporally and spatially based evolutionary sequence from instability back to some form of equilibrium between the supplied water and sediment load and the channel morphology that has been described by a geomorphic model, the Incised Channel Evolution Model (ICEM) (Schumm et al., 1984; Harvey and Watson, 1986; Simon and Hupp, 1986). During the course of the evolutionary sequence, sediment loads derived from erosion of the incised and widening channel can be extremely high (10^3 to 10^6 t/yr), but tend to decease

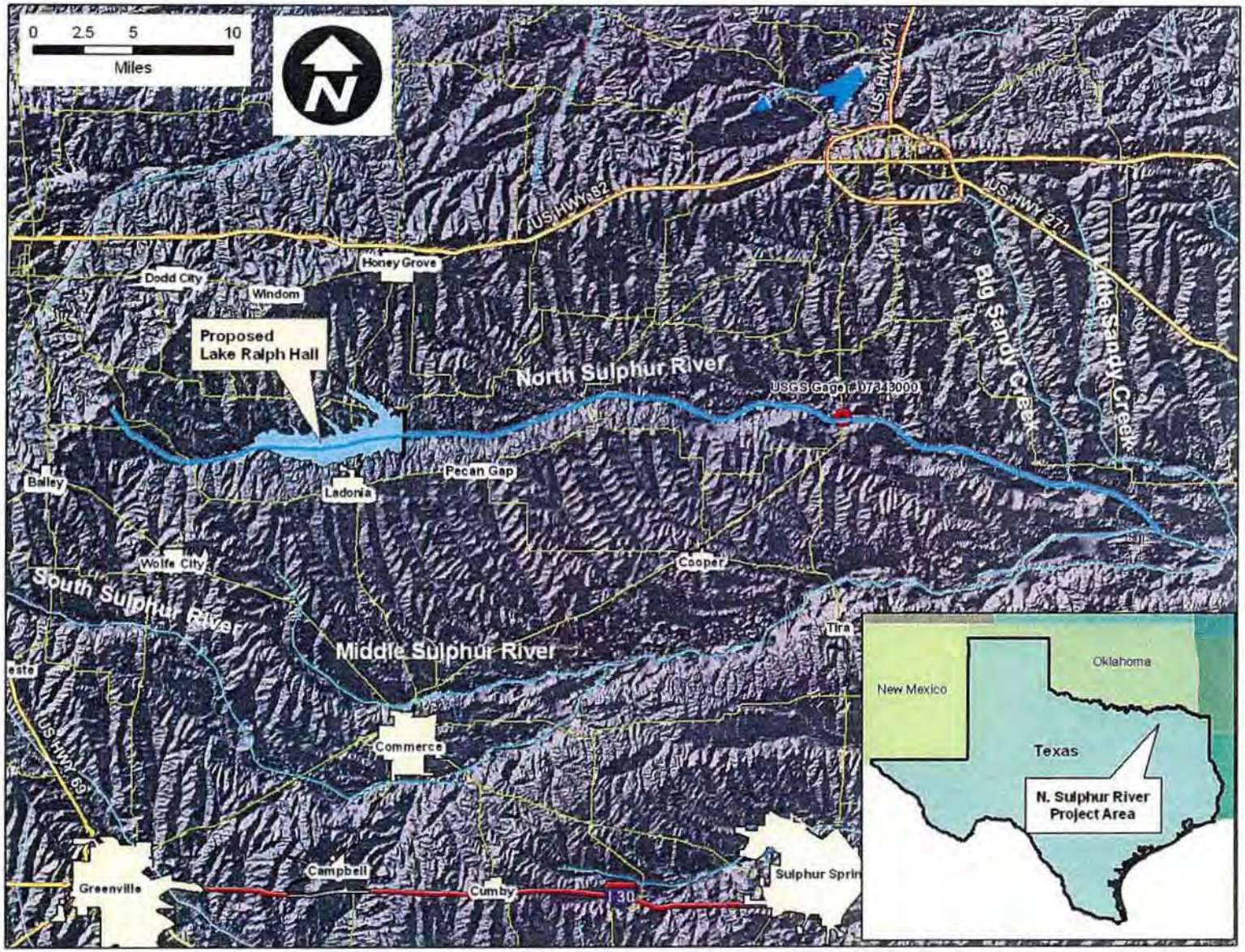

Figure 1.1. Map showing the location of the proposed Lake Ralph Hall on the NSR in Fannin County, Texas.

through time as a new state of equilibrium is approached (Harvey and Watson, 1986; Watson et al., 1986; Watson et al., 1988; Simon and Darby, 1999; Prosser et al., 2000). In the context of the NSR, the current sediment yield from the incised mainstem channel and the tributaries will depend on where these channels are in the evolutionary sequence. Sediment yield from the watershed is dependant on the land use within the watershed. Although approximately 75 percent of the watershed area was under cultivation for primarily row crops in the 1920s and 1930s, the current area in cropland is about 26 percent (Texas State Soil and Water Conservation Board, 1997).

1.2. Project Objectives

The primary objectives of this geomorphic and sedimentation study of the Lake Ralph Hall project conducted by Mussetter Engineering, Inc. (MEI) for Chiang, Patel & Yerby, Inc. (CP&Y) were:

1. Quantification of the sediment delivery to the reservoir site for the 50-year project life under pre- and post-project conditions,
2. Evaluation of the downstream effects of the dam on channel conditions and flow capacity,
3. Assessment of the potential for reducing or managing the upstream sediment supply to the reservoir, and
4. Assessment of future conditions in the North Sulphur River and tributaries upstream of the dam site in the absence of the project.

1.3. Data and Information Sources

Data and information used in this investigation were obtained from a number of sources. Previous project-related investigations that provided relevant information included:

1. Hydrologic and Hydraulic Studies of Lake Ralph Hall (RJ Brandes Co., 2004),
2. Geological Characteristics of Proposed Lake Ralph Hall (CP&Y, 2004),
3. Preliminary Subsurface Exploration, Ralph Hall Dam (Kleinfelder, 2005), and
4. Archaeology and Quaternary Geology at Lake Ralph Hall (AR Consultants, Inc., 2005).

Other data were obtained from a variety of sources, and included:

1. A 2-foot contour interval map and DTM of the proposed reservoir was provided by CP&Y.
2. Mean daily and annual peak flow data were obtained for the USGS North Sulphur River gage near Cooper, Texas (USGS Gage No. 07343000) for the period of record at the gage (1950-2005). Additionally, the 9207 summary discharge gaging data were obtained for the gage, and these were used to develop stage-discharge rating curves for different periods.
3. Bridge profiles were obtained by CP&Y for State Highway 34, FM 2990 and FM904 on the NSR; SH 34 and FM 1550 on Merrill Creek; FM 1550 on Bralley Pool Creek; FM 1550 on Baker Creek.
4. Aerial photography of the watershed for 1956 (1:20,000), 1969 (1:20,000), 1979 (1:40,000), 1989 (1:40,000), USDA.
5. Geologic Maps of Texas, Sherman (1967) and Texarkana (1966) sheets, Bureau of Economic Geology.

6. Soil Survey of Fannin County, Texas, NRCS (2001).

A 2-day helicopter and field reconnaissance of the channel and watershed of the NSR was conducted by Mr. John Levitt, P.E. (CP&Y) and Dr. Mike Harvey (MEI) in October 2005. During the field reconnaissance, four samples of bed material were collected from NSR (3) and Bralley Pool Creek (1) and provided to the Kleinfelder soils laboratory in McKinney, Texas. Because of the very high shale content of the samples, both dry and slaked gradations were determined for the samples. A more detailed field survey of the NSR and the principal tributaries upstream of the proposed dam site was conducted by Dr. Mike Harvey and Mr. Stuart Trabant (MEI) between December 12 and 16, 2005. Geomorphic and geologic features observed during the field survey were recorded, located with hand-held GPS units and photographed. Selected photographs are provided in **Appendix A**. During the course of this field work, a further 11 bed-material samples were collected, 8 in the NSR, 2 in Bralley Pool Creek, and 1 in Baker Creek. Wet and dry gradations and specific gravities were provided by Kleinfelder. All of the gradation data and specific gravities for the samples are provided in **Appendix B**.

1.4. Authorization

This study of the Lake Ralph Hall project was conducted for Chiang, Patel and Yerby, Inc. (CP&Y) and the Upper Trinity Regional Water District (UTRWD) by Mussetter Engineering, Inc. (MEI). CP&Y's project manager for this study was Mr. John Levitt, P.E. and MEI's project manager was Dr. Mike Harvey, P.G. Mr. Stuart Trabant, P.E. (Colorado) was the project engineer and Dr. Stanley A. Schumm, P.G. reviewed the report.

2. GEOLOGY AND GEOMORPHOLOGY

The dynamics of the NSR and its tributaries are intimately linked to the current geomorphic setting of the entrenched valley floor, and the characteristics of both the alluvial valley fill sediments and underlying bedrock that comprise the bed and banks of the incised channels. The details of the bedrock geology and the overlying alluvial valley fill have been described in detail elsewhere (CP&Y, 2004; AR Consultants, Inc., 2005). In the following section, the discussion of the bedrock geology and alluvial valley fill is tailored to their geomorphic significance.

2.1. Geology

The bedrock units that crop out in the North Sulphur River basin are from the Cretaceous-age Gulf Series. Both the land surface and the rock units dip slightly to the southeast (~0.5 degrees), which results in successively younger formations being exposed as the NSR flows east and southeast. From west to east, exposed in ascending order are the Austin and Taylor Groups (**Figure 2.1**). The Roxton Limestone and the Gober Chalk are the two uppermost units of the Austin Group that crop out along the north side of the NSR Basin. Although the geologic map shows a narrow band of Roxton Limestone on the north side of the NSR, field observation and mapping, and the respective lithologic descriptions of the Roxton Limestone and Gober Chalk (Texas Bureau of Economic Geology, 1966, 1967), suggest that it is the Gober Chalk that is actually observed in the beds of the headwaters of the NSR (**Figure A.1**) and the south flowing tributaries (Allen, Bear, Pot, Brushy, Pickle, Davis, Bralley Pool, Merrill, and Baker Creeks). For the purposes of this investigation, the outcrops are referred to as Roxton/Gober Chalk.

The downstream limit of the Roxton/Gober Chalk outcrop provides grade control for the upstream channel and thus limits the upstream extent of the baselevel lowering-induced incision in the tributaries (**Figure 2.2; Figure A.2**). The distance from the upstream extent of the top of the conservation pool elevation (551.0 ft msl) to the downstream limit of the Roxton/Gober Chalk outcrop provides an indication of the upstream extent of the channel incision and also the length of the incised channel that can contribute sediment to the reservoir once the dam is in place (**Table 2.1**). Erosion of the Roxton/Gober Chalk is primarily due to surficial weathering (**Figure A.3**), but the rate of erosion is low. Weathering and erosion tend to produce a low specific gravity (~2.4), sand- and gravel-sized sediment supply to the downstream incised channel (**Figure A.4**).

The uppermost unit of the Taylor Group is the Ozan Formation, a 425-foot thick dark gray calcareous, poorly bedded clay (shale) with varying amounts of silt and glauconite and some thin siltstone and limestone beds. The rock is compact, highly jointed, and highly erodible and ravels (**Figures A.5 and A.6**) when exposed to weathering (Kleinfelder, 2005). The Ozan Formation weathers in situ to a light gray shale and light yellow-brown shaly clay. The results of four borings across the valley at the proposed dam location (Kleinfelder, 2005) indicate that there is relief on the shale surface at the shale-valley fill contact.

Incision of the NSR and its tributaries has exposed the Ozan Formation in the bed (**Figure A.7**) and in the banks (**Figure A.8**) where the streams have eroded into the shale. Erosion into the shale takes place as a result of both hydraulic processes (abrasion, plucking, solution) (**Figure A.9**) and streambed weathering (slaking) (**Figure A.10**) (Howard, 1998; Tinkler and Parish, 1998; Allen et al., 2002). Slaking tests by Crawford (in preparation) indicate that the Taylor Marl has about a 50-percent weight slaking loss following a 2-cycle test. Rates of erosion into the

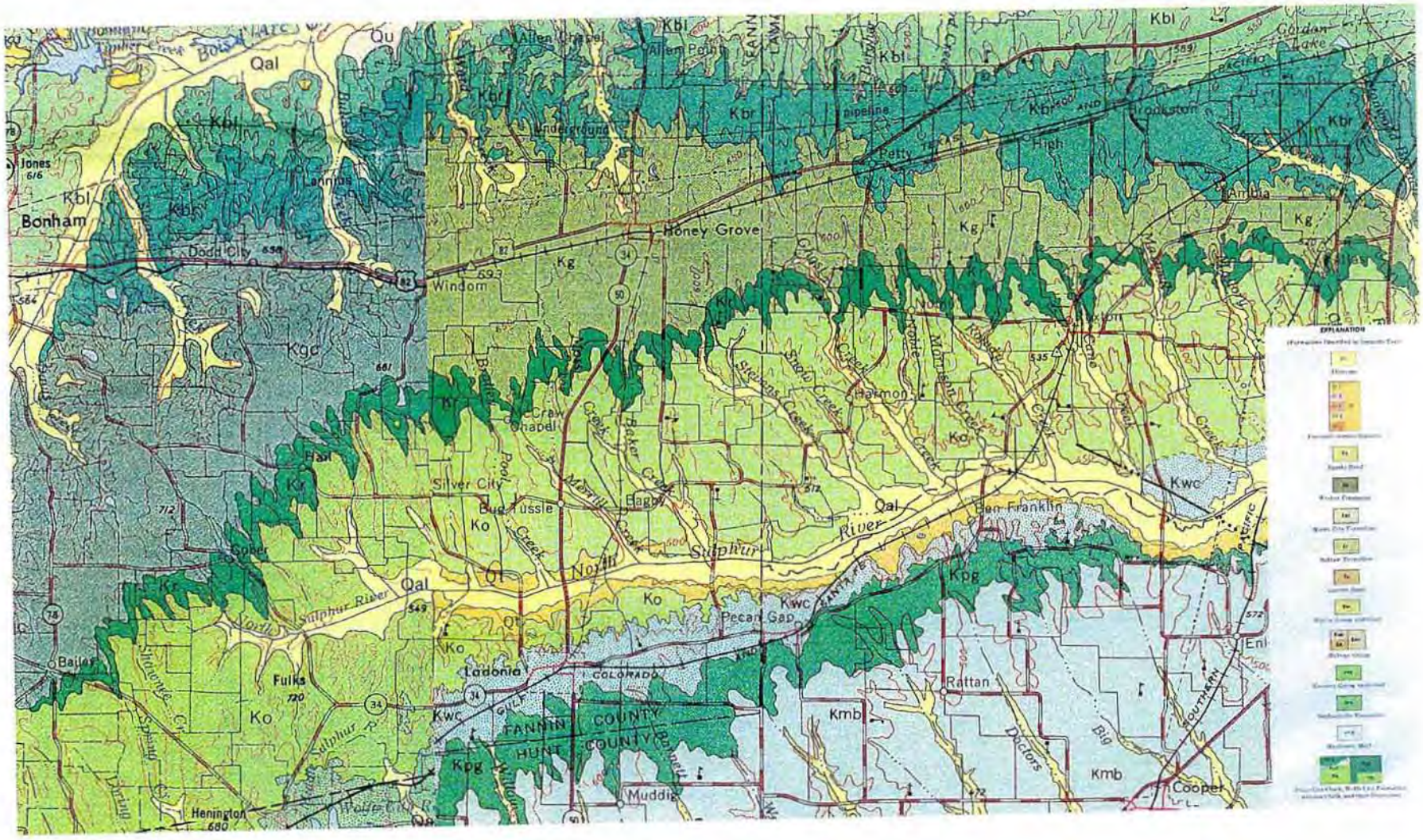

Figure 2.1. Geologic map of the North Sulphur River basin (after Texas Bureau of Economic Geology, 1966, 1967).

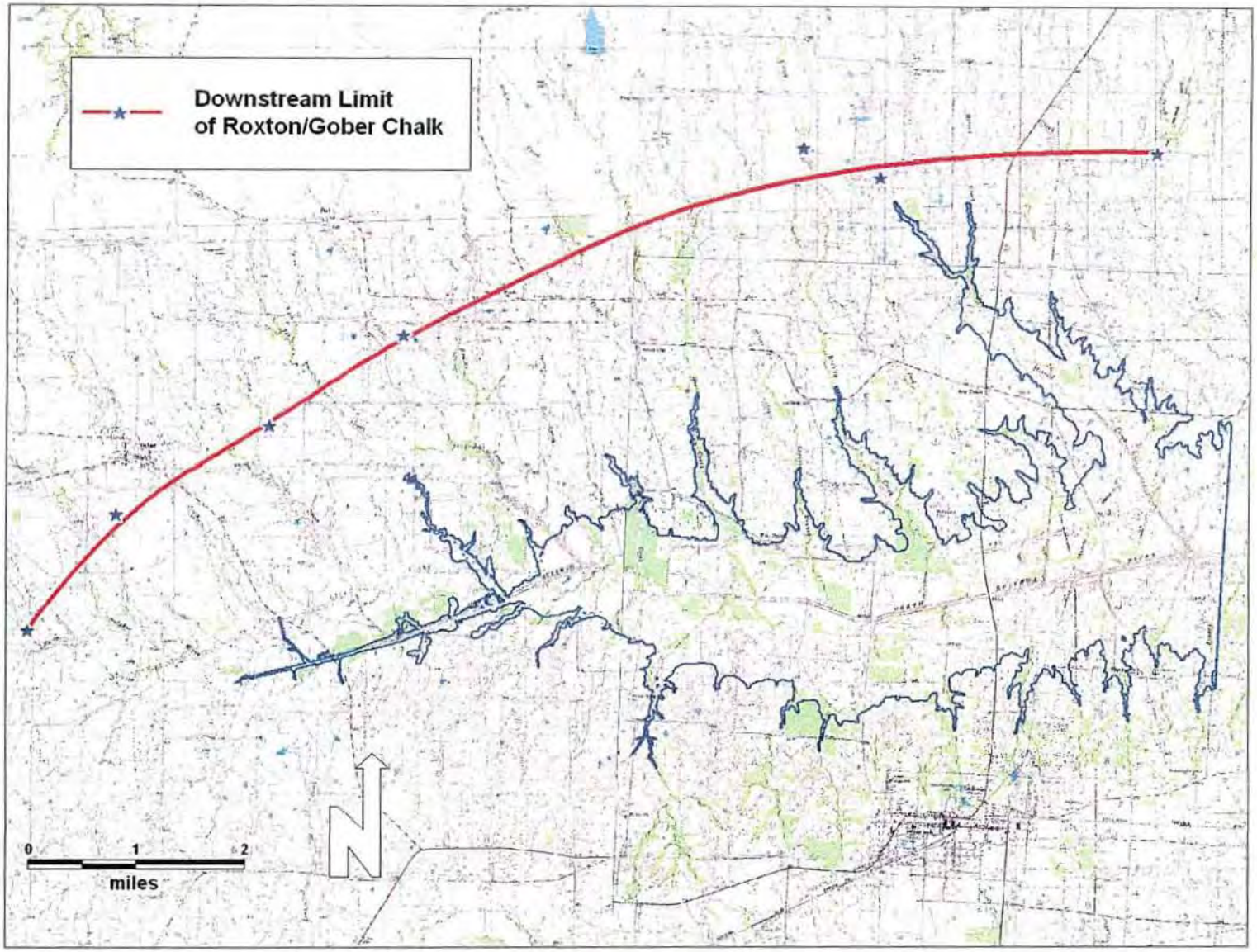

Figure 2.2. Map of the North Sulphur River basin showing the locations of the downstream limits of exposed Roxton/Gober Chalk in the headwaters of the NSR and the north-side tributaries.

weak shale (tensile strength <1 MPa; Crawford, in preparation) may ultimately be controlled by the threshold of motion of a thin mantle of sediment over the bedrock rather than the bedrock hardness (Sklar and Dietrich, 1998; Stock et al., 2005). However, Allen et al. (2002) have measured wetting-drying cycle-driven slaking rates of up to 4 inches per year in the lower bank regions of channels incised into the Taylor Marl, and rates of up to 2 inches per year in the bed. Tinkler and Parish (1998) have documented channel bed erosion rates into shales on the order of 1 inch per year, and have observed that wetting and drying cycles were primarily responsible for fragmenting the exposed shale to a size that could be transported and removed by frequent and moderate high flows. Similar processes have been observed in the bed of the NSR and its tributaries (**Figures A.11 and A.12**), where on average, there are about six wetting and drying cycles per year at the Cooper gage (**Figure 2.3**).

Table 2.1. Lengths of eroding channel between top of conservation pool extent and Roxton/Gober Chalk outcrop.

Channel	Distance to Roxton/Gober Chalk Outcrop (miles)
North Sulphur River	1.8
Allen Creek	1.9
Bear Creek	1.5
Pot Creek	1.3
Brushy Creek	1.1
Pickle Creek	1.0*
Davis Creek	1.0
Leggett Creek	1.0*
Bralley Pool Creek	1.8
Merrill Creek West Branch	0
Merrill Creek East Branch	0.5

*Concrete Box culverts provide grade control downstream of Roxton/Gober Chalk outcrop

Studies of the Quaternary-age alluvial valley fill stratigraphy of the NSR above the Ozan Formation have been conducted by Frye and Leonard (1963), Slaughter and Hoover (1963, 1965) and Rainey (1974), and have been summarized in AR Consultants, Inc. (2005). On average, the alluvial valley fill is about 30 feet thick, but the thickness is variable depending on the underlying relief on the top of the Ozan Formation, and can range from as little as 10 to 32 feet based on field observations (**Figures A.13 and A14**) and the Kleinfelder borings. Tinn clay is the soil unit mapped on the former floodplain of the NSR (NRCS, 2001). Gradation analyses of samples recovered from the floodplain soils indicate that about 90 percent of the soil is smaller than sand (No. 200 sieve) and Atterberg Limits indicate that the soils are classified as high plasticity (CH) and low plasticity (CL) clays (Kleinfelder, 2005). Shallow groundwater is perched on the shale-alluvium contact, and appears to be associated with mass failures of the overlying alluvial materials when it is daylighted in the banks (**Figure A.15**).

2.2. Geomorphology

The NSR originates near the axis of the Preston Anticline and flows east paralleling the general east-northeast strike of the south-southeast dipping Cretaceous-age bedrock (Barnes, 1967).

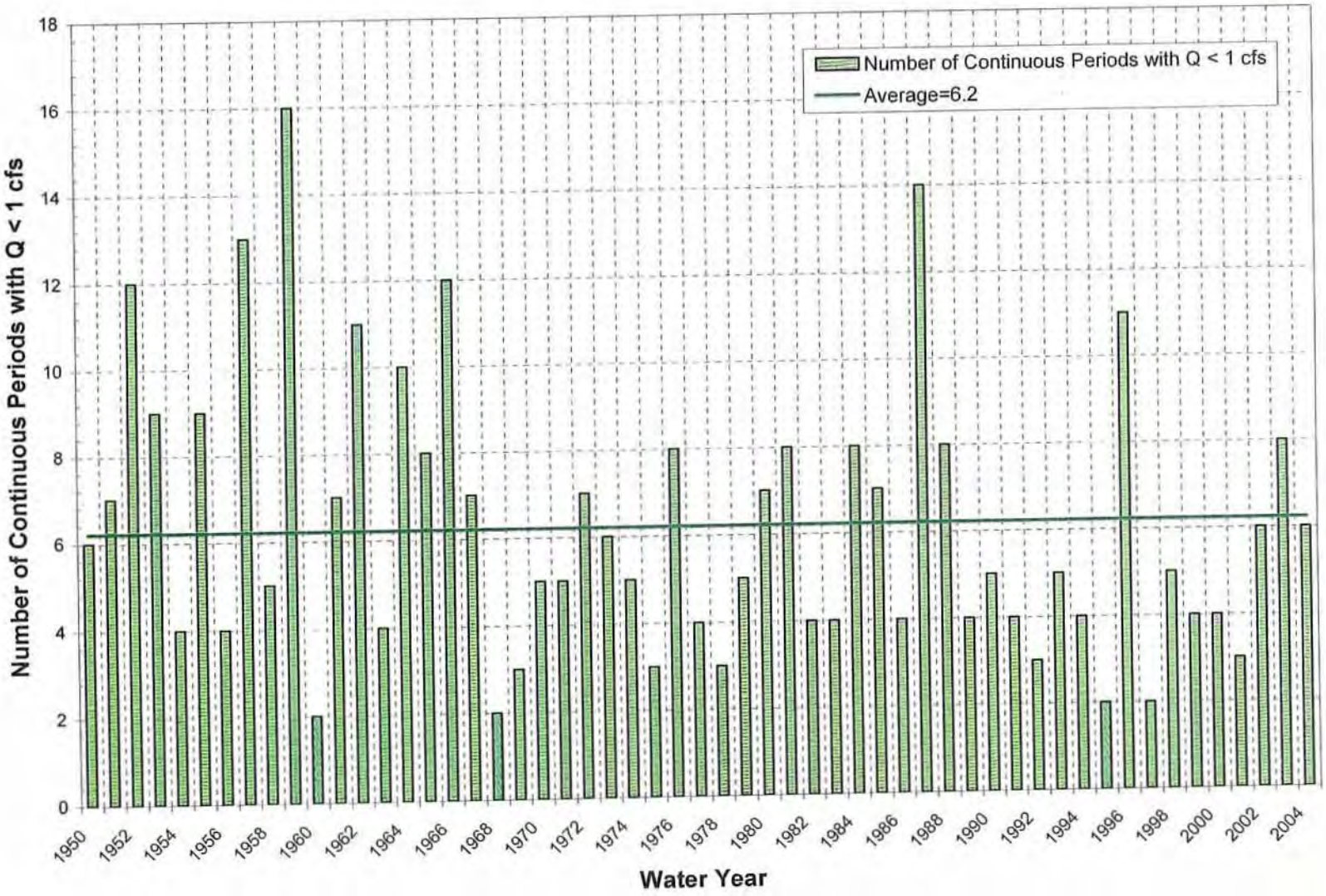

Figure 2.3. Number of continuous periods with flows less than 1 cfs at the USGS gage near Cooper, Texas. On average there are about six wetting and drying cycles per year (Q <1 cfs).

The south-southeast dip of the underlying bedrock is the cause of the asymmetrical valley profile of the NSR. Down-dip preferential erosion has resulted in the south-draining north side tributaries being long and having relatively gentle slopes, while the north-draining south side tributaries are short and steeper (Figure 1.1). Because of the channelization-induced incision, both the north- and south-draining tributaries are currently incised. The pre-channelization floodplains of both the NSR and the incised tributaries are now terraces that are hydrologically disconnected from their channels.

2.2.1. Incised Channel Evolution Models

The dominant characteristic of the present day NSR system is the extent of the incision and the incision-induced widening. In the context of the sediment supply to the system from channel erosion processes, it is necessary to determine whether the system has re-attained equilibrium between the water and sediment supply and the channel morphology 75 years after channelization. Numerous studies of incised channels in alluvial materials in humid regions of the U.S. have shown that following channelization, the channel passes through a consistent, predictable sequence of channel forms with time (Ireland et al., 1939; Schumm et al., 1984; Harvey and Watson, 1986; Simon and Hupp, 1986; Simon, 1989). These systematic temporal adjustments have been collectively referred to as channel evolution, and a number of geomorphic models (Incised Channel Evolution Models—ICEM) have been developed that permit interpretation of past and present channel processes, as well as prediction of future channel processes (Schumm et al., 1984; Simon and Hupp, 1986).

A five-stage ICEM was developed by Schumm et al. (1984), and modified to include the channelized stage by Harvey and Watson (1986). The model describes the systematic evolution of a channelized stream from a state of man-induced disequilibrium (Type II) to a new state of dynamic equilibrium (Type VI) (**Figure 2.4**). The model identifies, quantifies, and integrates four important components of channel evolution: bank stability, the dominant or effective discharge, the hydraulic energy of those discharges and the morphological adjustments of the channel through time and space (Harvey and Watson, 1986; Watson et al., 1988). Through time, the channel incises (Types III and IV), widens as a result of bank failure (Types IV and V), and ultimately aggrades (Type VI), at which point an equilibrium channel that reflects the balance between sediment supply and transport capacity has formed within the over-widened incision into the valley floor. Bank failure occurs when the bank height (h) exceeds the critical bank height (h_c) (Little et al., 1981; Watson et al., 1988). When the banks are steeper slab, or wedge, failures predominate (Type IV), and as the bank angle is reduced deeper seated slump failures predominate (Type V) (Lohnes and Handy, 1968; Harvey and Watson, 1986; Thorne, 1988 and 1999; Simon and Darby, 1999).

Repeat cross-section surveys of an incised channel in northern Mississippi (Schumm et al., 1984), and a computer simulation of the geomorphic evolution of that incised channel (Watson et al., 1986), indicated that total soil loss due to channel erosion (bed and banks) from the 42-square-mile watershed, was on the order of 6.5×10^6 tons over a 15-year period. Initial rates of soil loss were on the order of 0.1×10^6 t/yr (3.7 t/ac/yr), but the maximum rate occurred when the channel was most actively widening and approached 0.5×10^6 t/yr (19 t/ac/yr). Ultimately, channel loss rates diminished to about 0.05×10^6 t/yr (1.9 t/ac/yr) as the channel approached a new state of equilibrium. Simon (1989) showed similar trends with erosion rates eventually returning to less than 2 t/ac/yr. Other studies of incised channels (Simon et al., 1996; Simon and Darby, 1999) have shown that sediment emanating from incised channels can represent up to 80 percent of the total sediment yield from a landscape.

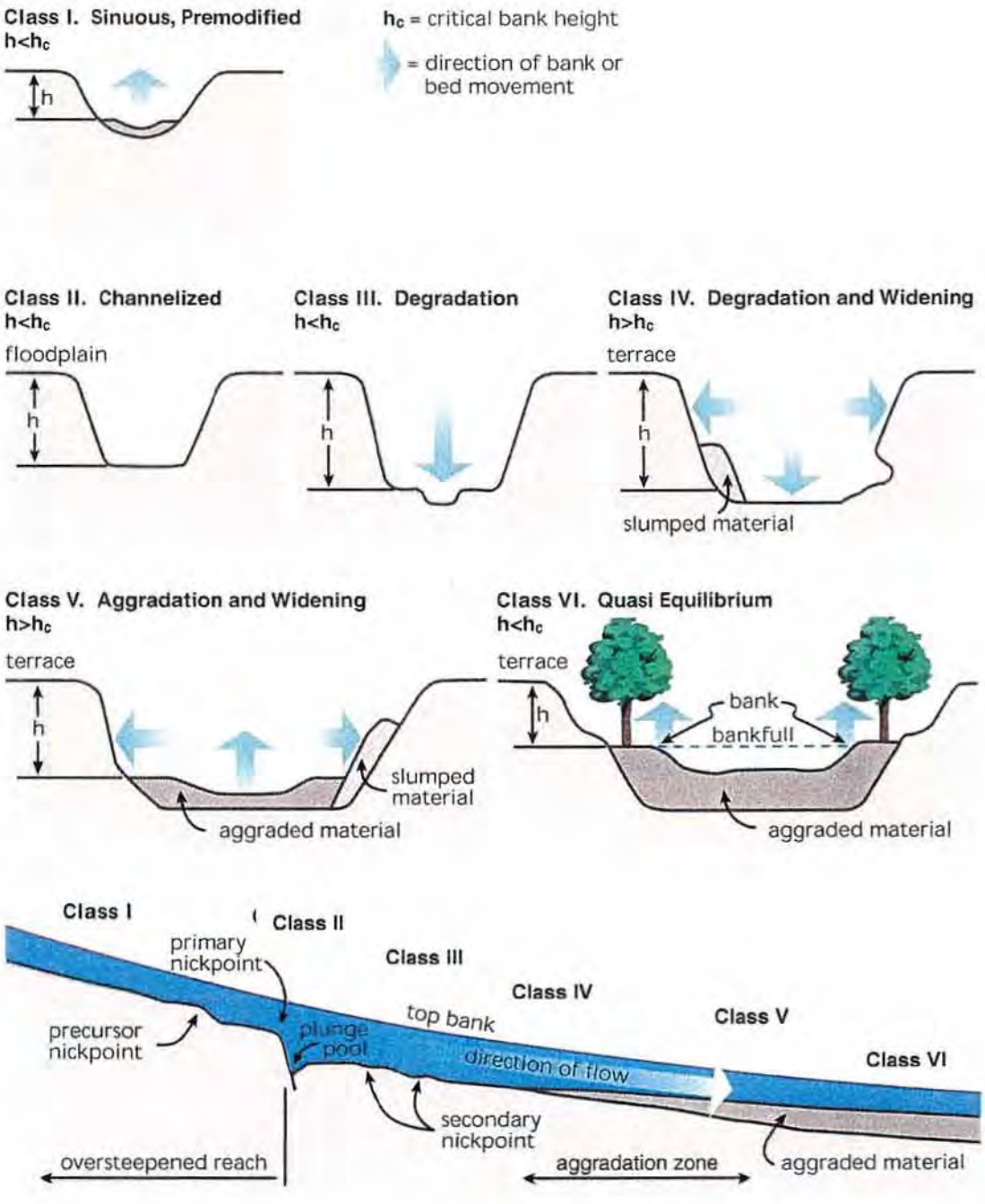

Figure 2.4. Incised channel evolution model (after Schumm et al., 1984).

2.2.2. Channel Evolution in the North Sulphur River

In the context of the current status of the NSR, and sediment yield to the dam site, it is important to know the evolutionary stage of the mainstem and tributaries. In the channelized streams of the humid southeastern U.S., the channel evolution sequence can take about 40 to 50 years (Schumm et al., 1984; Schumm, 1999; Simon, 1989) and over 100 years in the arroyos in the semi-arid southwest (Gellis et al., 1995). Therefore, it could be expected that the NSR, that was channelized about 75 years ago, has completed the evolutionary sequence and might be approaching a new state of equilibrium with the imposed flows and sediment loads. Depending on location, there are indications that this has in fact occurred (**Figure A.16**). However, it is equally apparent that there are sections of the NSR and its tributaries that are still actively widening (**Figure A.17**), and have very little or no sediment accumulation on the bed, which is composed of erodible shale (**Figure A.18**), both conditions which are indicative of ongoing disequilibrium. Similar conditions of apparent disequilibrium (**Figure A.19**), active channel widening (**Figure A.20**) and the presence of shale in the bed and absence of sediment accumulation on the bed can be observed in the tributaries to the NSR. Ongoing degradation below recently replaced bridges across the tributaries also argues for continuing disequilibrium (**Figure A.22**).

The mainstem of the NSR between FM 904 (Sta 00+6) and about 1 mile upstream of SH 68 (the upstream end of the DTM) (Sta 619+66) was subdivided into 10 subreaches, primarily on the basis of the location of the major tributaries (refer to Table 4.1 for subreach boundaries and Figure 2.37 for stationing). Cross sections representing the physical characteristics of the subreaches were developed from the DTM (**Figures 2.5 through 2.18)**, and photographs of the NSR at these locations are provided in Appendix A (**Figures A.23 to A.36**). **Table 2.2** summarizes this subreach information.

Table 2.2. Summary of subreach information for mainstem of North Sulphur River.

Subreach Number	Subreach Description	Cross Section Station (ft)	Figure Number	Photograph Number
1	Upstream of SH 68	604+27	2.5	A.23
2	Allen Creek to Bear Creek	562+44	2.6	A.24
3	Bear Creek to Brushy Creek	530+93	2.7	A.25
3	Bear Creek to Brushy Creek	496+42	2.8	A.26
3	Bear Creek to Brushy Creek	468+60	2.9	A.27
3	Bear Creek to Brushy Creek	453+04	2.10	A.28
4	Brushy Creek to Pickle Creek	390+34	2.11	A.29
5	Pickle Creek to Davis Creek	344+08	2.12	A.30
6	Davis Creek to Leggetts Branch	303+01	2.13	A.31
7	Leggetts Branch to Bralley Pool Creek	273+25	2.14	A.32
7	Leggetts Branch to Bralley Pool Creek	246+13	2.15	A.33
8	Bralley Pool Creek to Merrill Creek	187+60	2.16	A.34
9	Merrill Creek to dam site	88+77	2.17	A.35
10	Dam site to FM 904	32+36	2.18	A.36

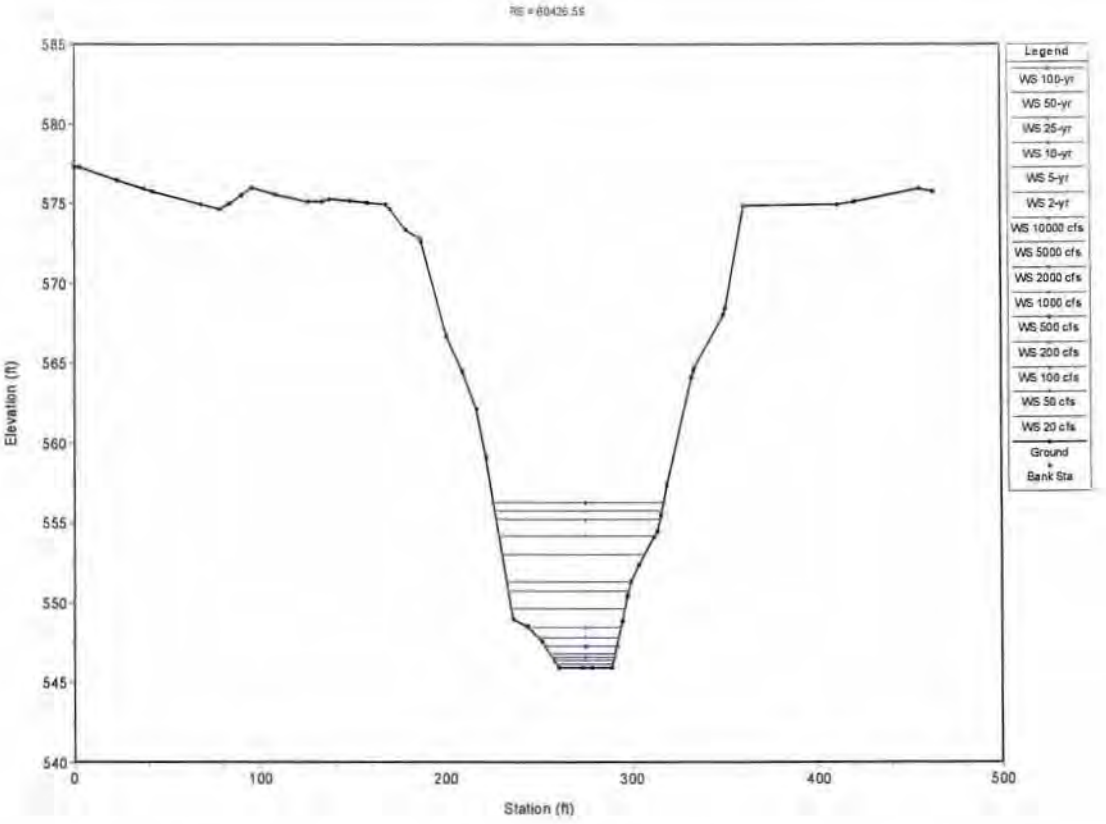

Figure 2.5. Cross section of North Sulphur River in Subreach 1, Sta 604+27.

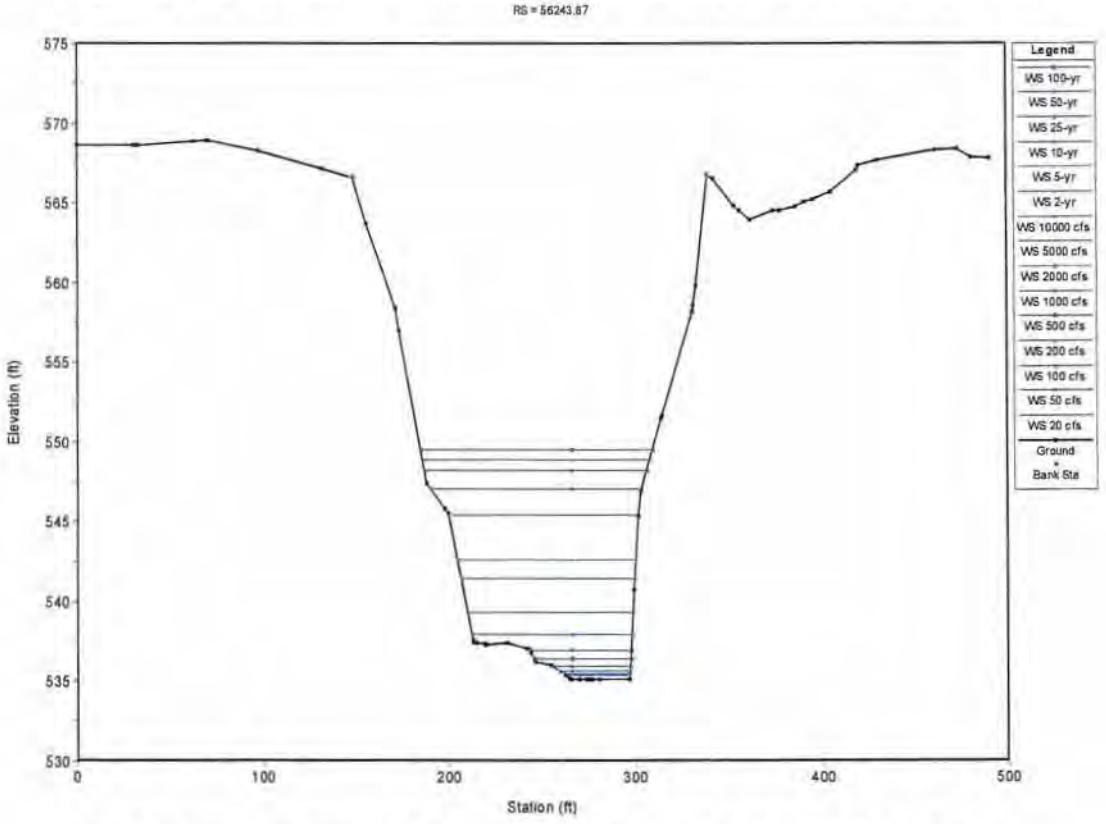

Figure 2.6. Cross section of North Sulphur River in Subreach 2, Sta 562+44.

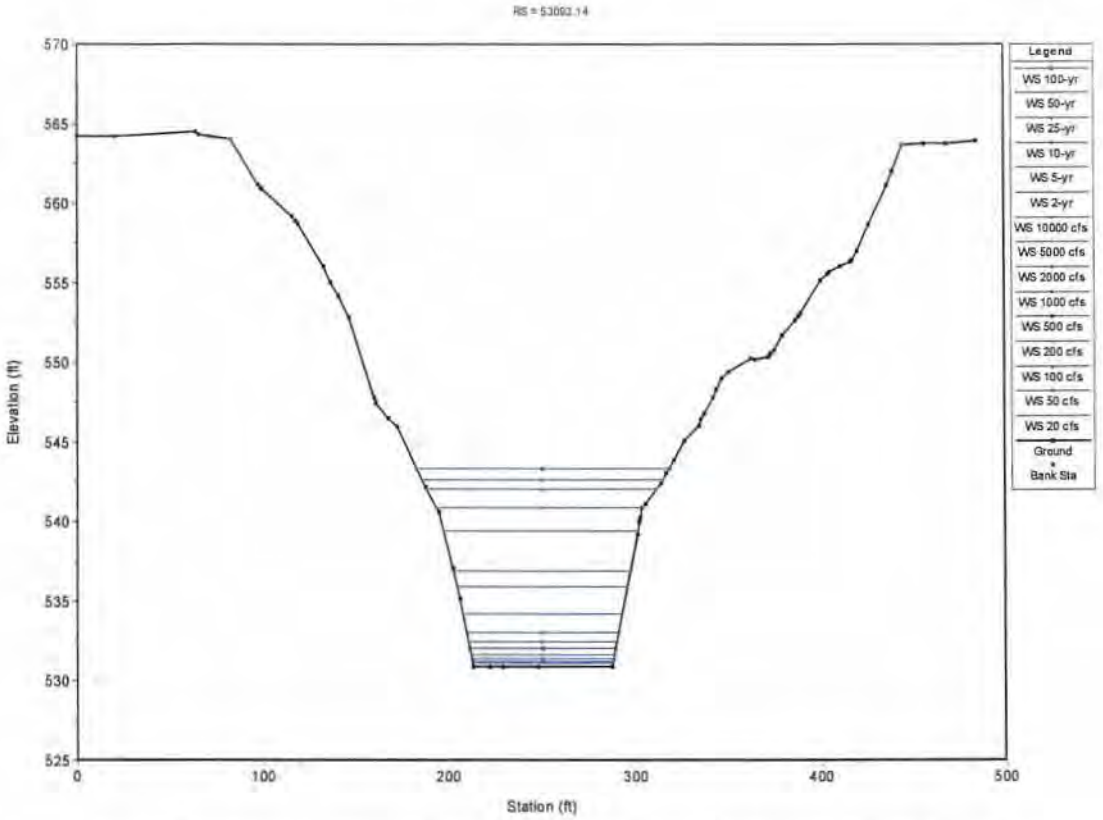

Figure 2.7. Cross section of North Sulphur River in Subreach 3, Sta 530+93.

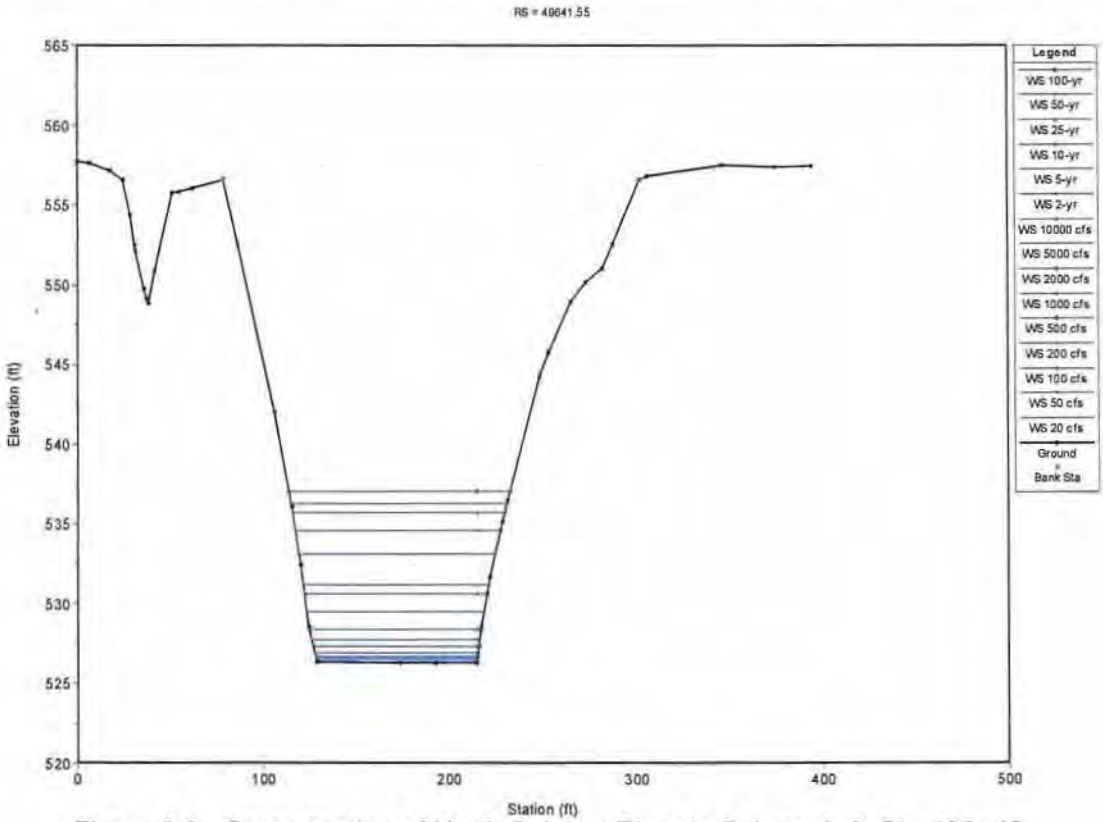

Figure 2.8. Cross section of North Sulphur River in Subreach 3, Sta 496+42.

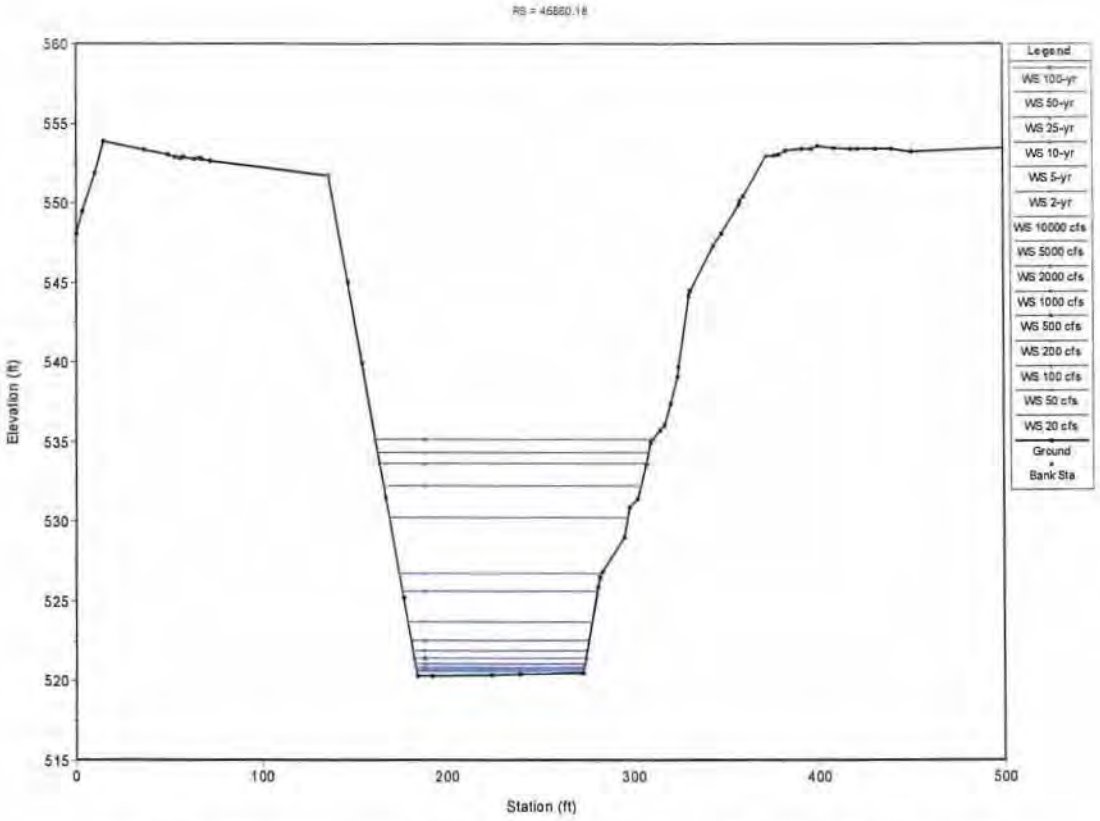

Figure 2.9. Cross section of North Sulphur River in Subreach 3, Sta 468+60.

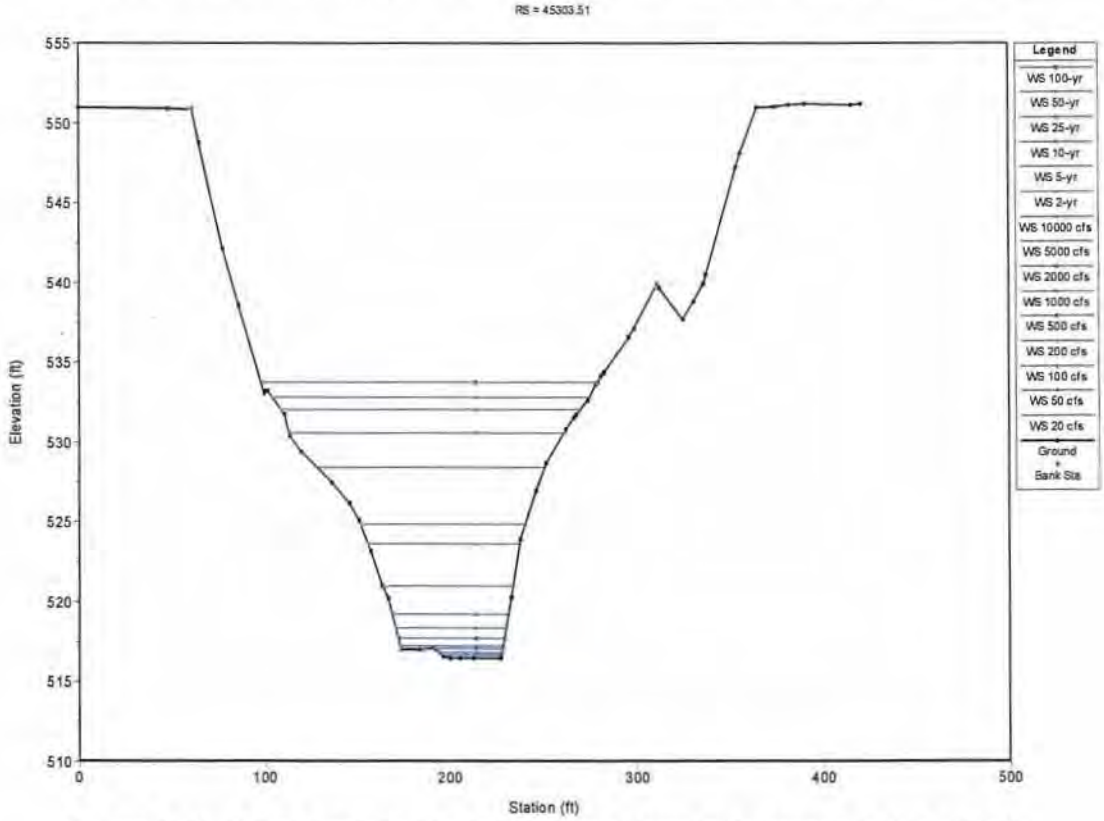

Figure 2.10. Cross section of North Sulphur River in Subreach 3, Sta 453+04.

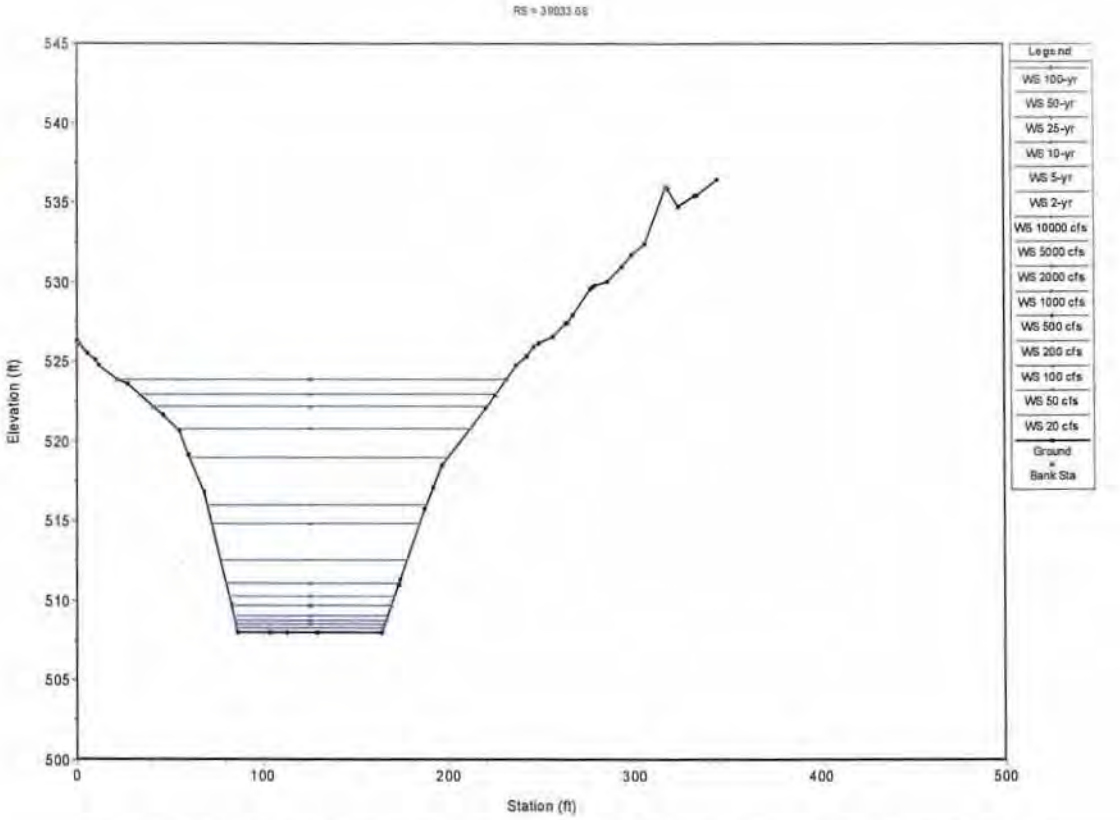

Figure 2.11. Cross section of North Sulphur River in Subreach 4, Sta 390+34.

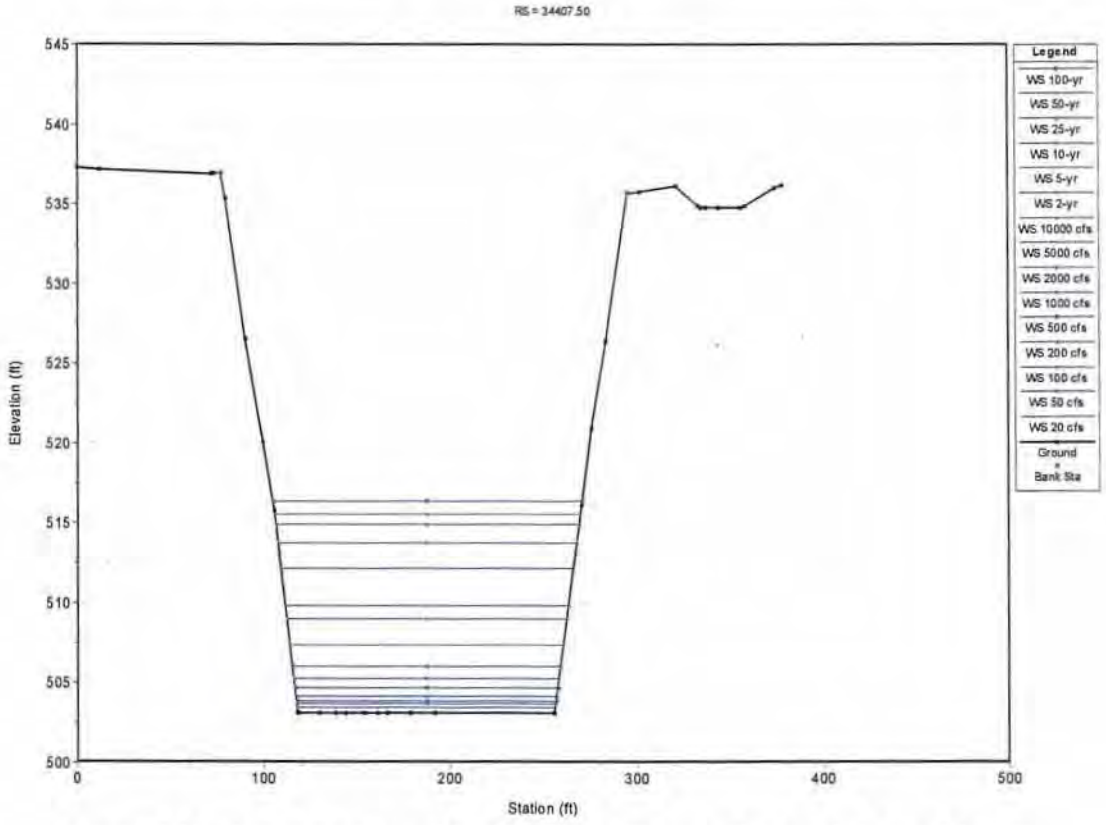

Figure 2.12. Cross section of North Sulphur River in Subreach 5, Sta 344+08.

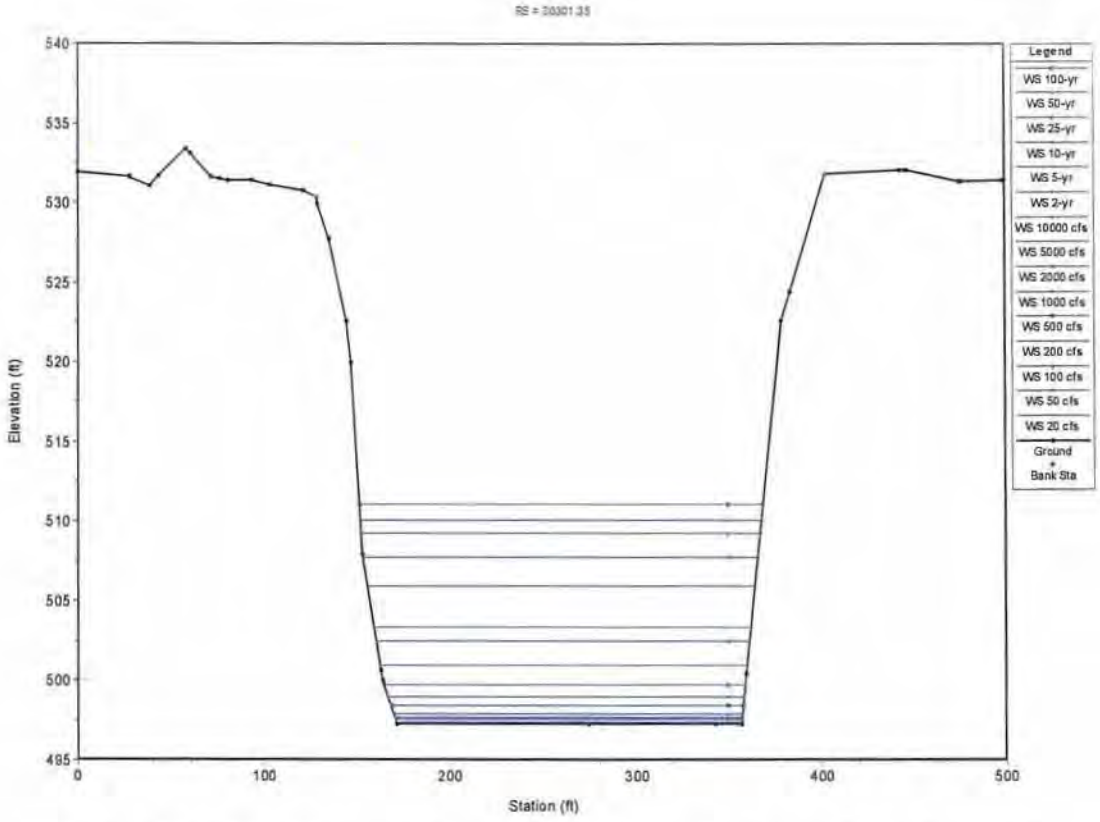

Figure 2.13. Cross section of North Sulphur River in Subreach 6, Sta 303+01.

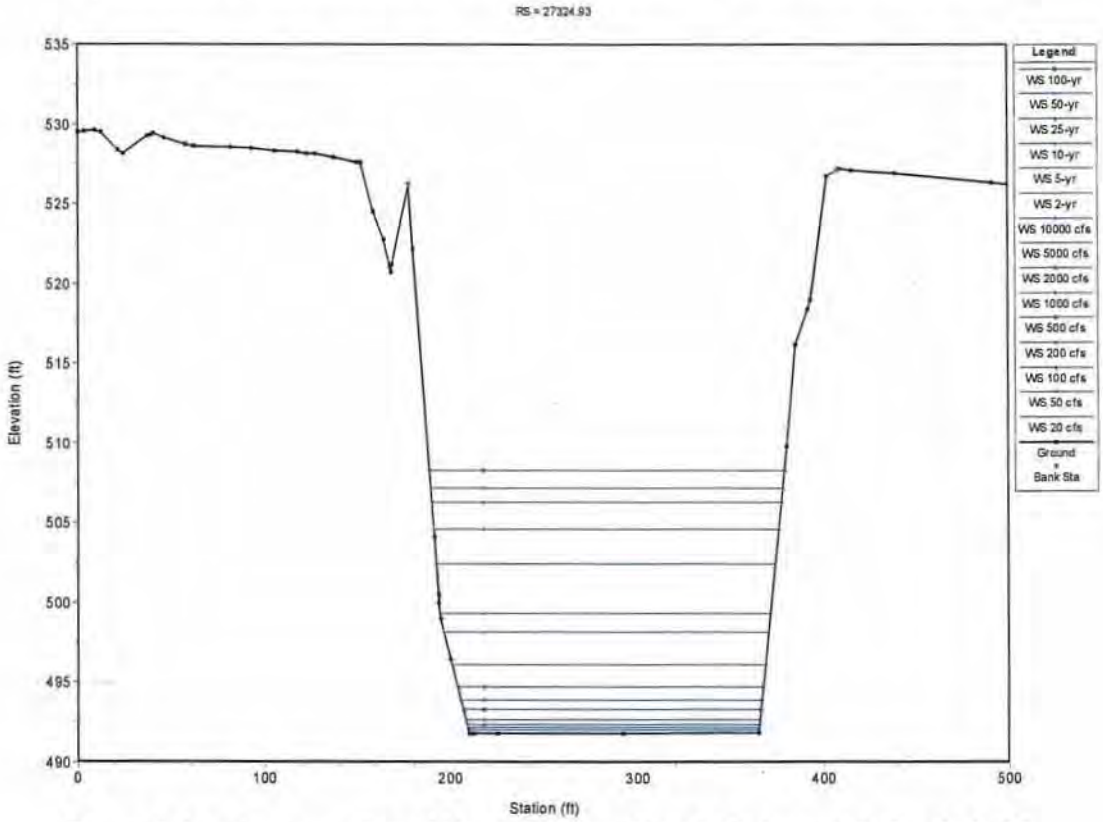

Figure 2.14. Cross section of North Sulphur River in Subreach 7, Sta 273+25.

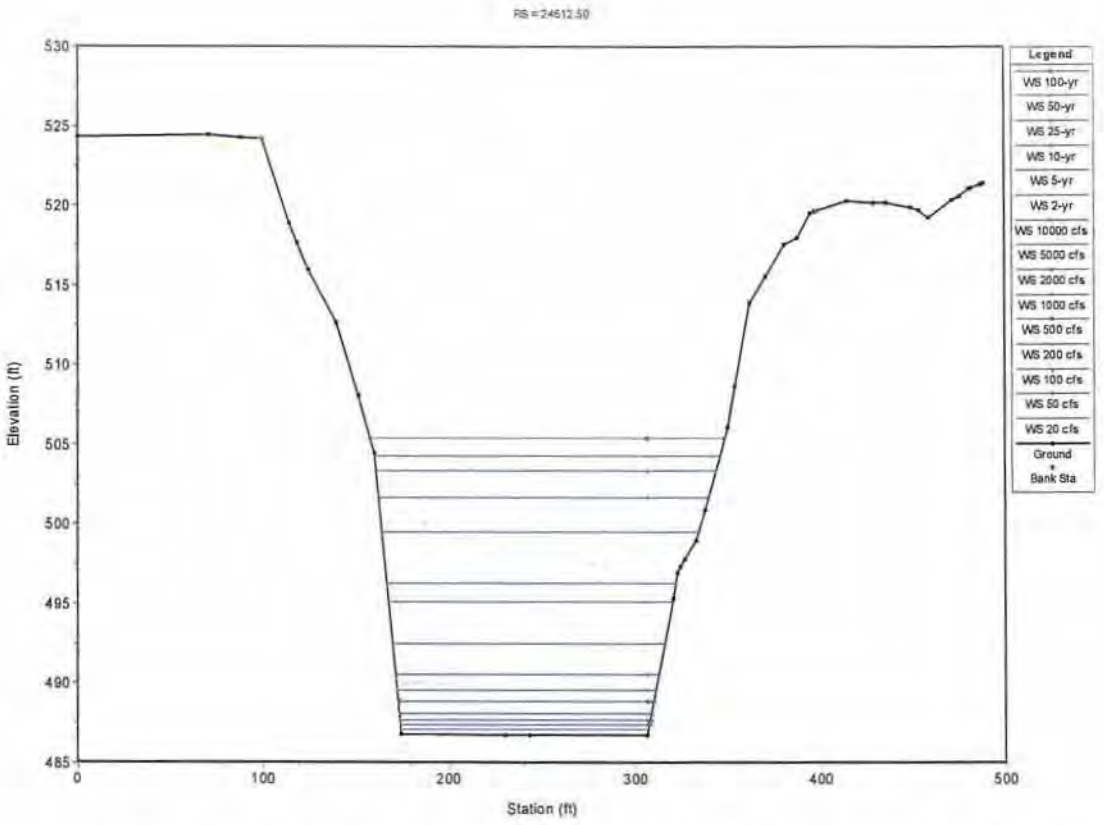

Figure 2.15. Cross section of North Sulphur River in Subreach 7, Sta 246+13.

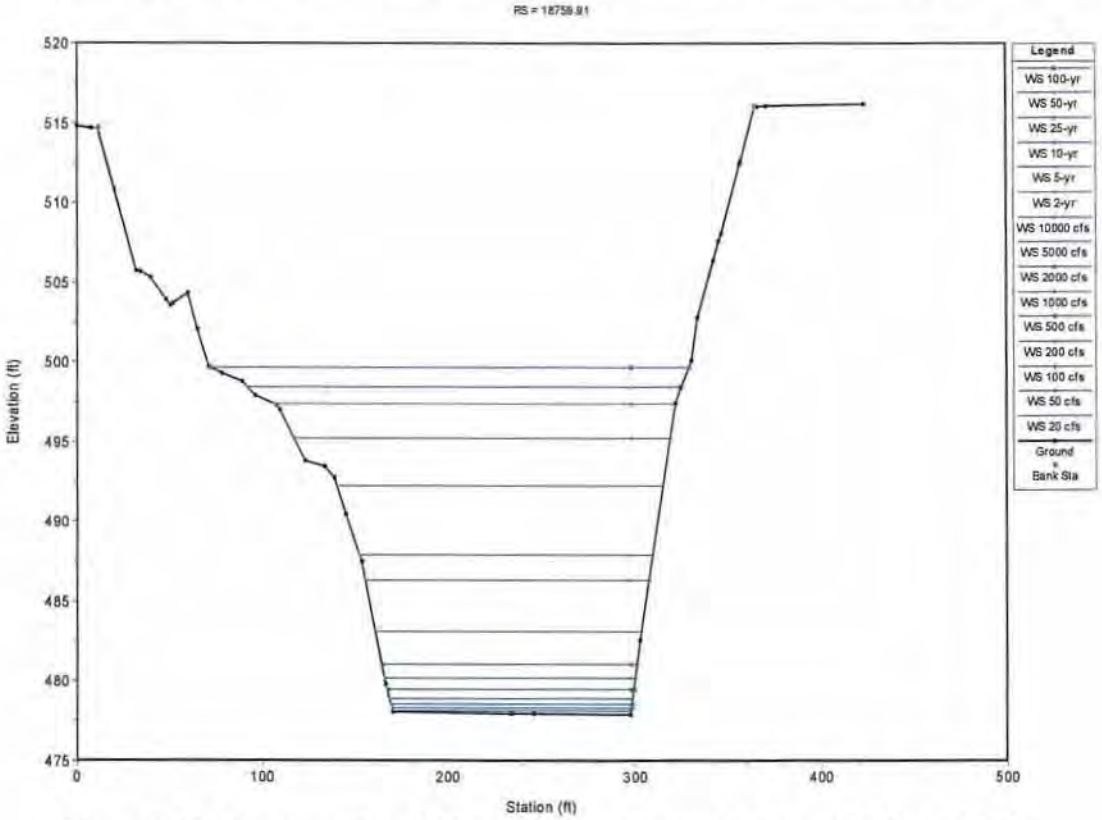

Figure 2.16. Cross section of North Sulphur River in Subreach 8, Sta 187+60.

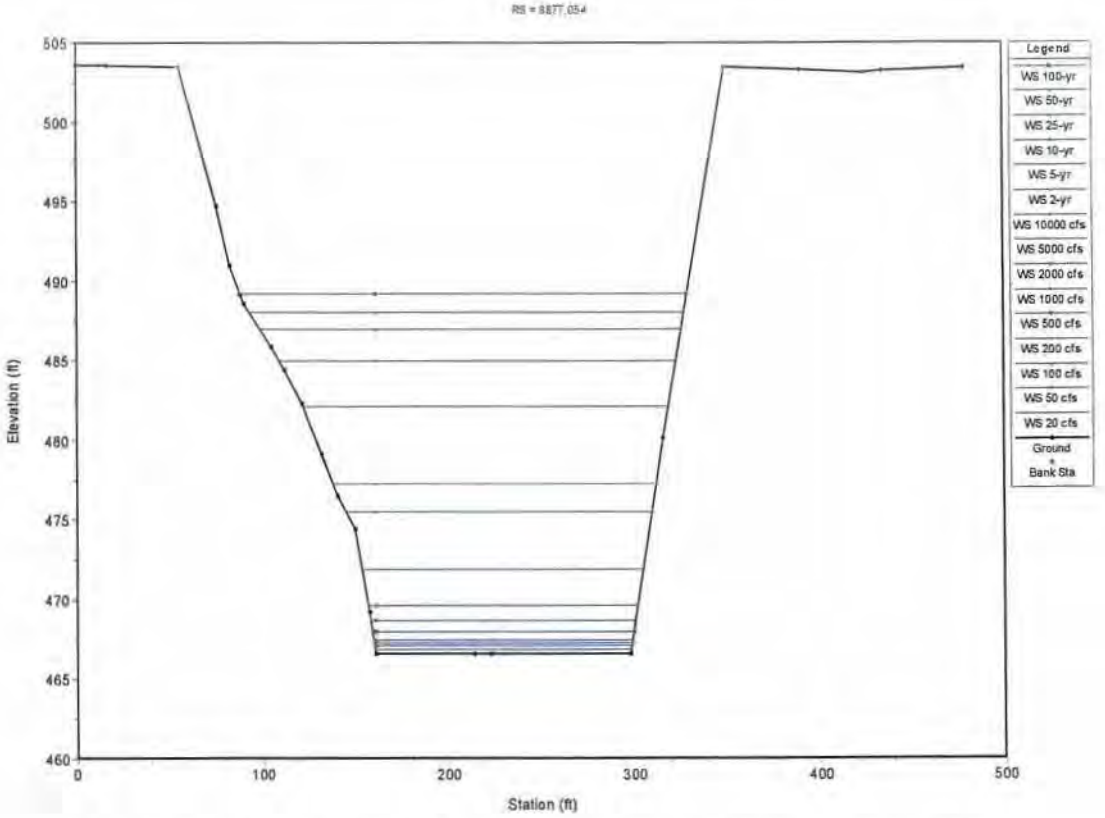

Figure 2.17. Cross section of North Sulphur River in Subreach 9, Sta 88+77.

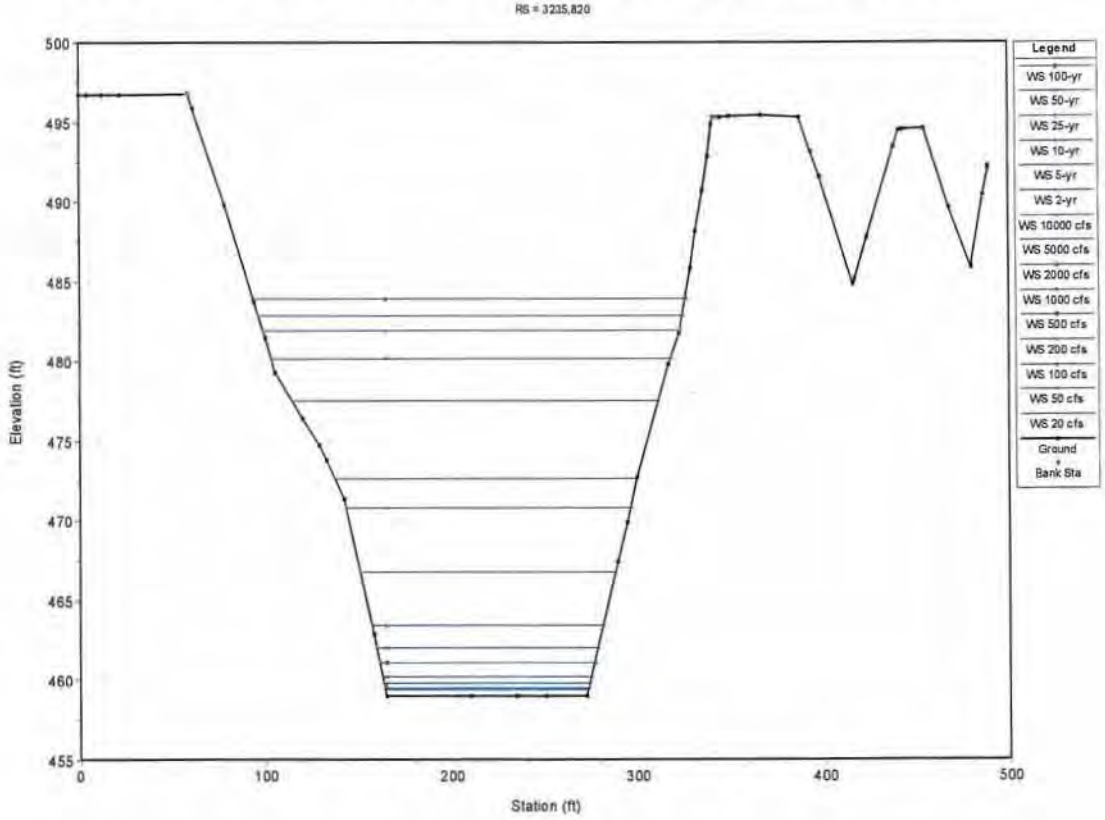

Figure 2.18. Cross section of North Sulphur River in Subreach 10, Sta 32+36.

In Subreach 1 (Figures 2.5 and A.23), the channel has incised at least 10 feet into the shale, and shale forms the lower portion of the banks and the bed. The banks are steep, and weathering of the bed and banks produces a significant amount of gravel-size clasts that are initially transported as bedload, but eventually slake into primarily wash-load-sized material (Tinkler and Parish, 1998; Allen et al., 2002). In Subreach 2 (Figures 2.6 and A.24), the banks are steep, and most of the erosion and channel widening is due to slab failure of the alluvium that overlies the exposed shale (Harvey and Watson, 1986; Thorne, 1988 and, 1999). Subreach 3 (Figures 2.7, 2.8 and A.25, A.26) is characterized by active slab failures of the alluvial fill that maintain a steep bank slope, as well as deeper seated slump failures of the alluvium (Figures 2.9 and A.27). Alternating steeper and flatter bank slopes that create an asymmetrical cross section are characteristic of this subreach (Figure 2.10 and A.28). Subreach 4 (Figures 2.11 and A.29) is characterized by symmetrical cross sections with convex lower slopes and concave upper slopes formed by deep-seated slump failures in the alluvium. The bed of the channel is composed of shale with a veneer of sediment and the banks are composed of displaced, clay-rich alluvium, that is vegetated and root reinforced, and therefore, relatively erosion resistant. Mass failure of both banks, effectively reduces the bottom width of the channel.

Steep banks with slab failures of the alluvium and exposed shale in the lower parts of the banks are characteristic of Subreach 5 (Figures 2.12 and A.30), suggesting that the channel in this subreach has not adjusted as much as in Subreach 4, or that the channel instability has been reactivated by lateral erosion of the mass failed alluvium that had protected the shale from erosion. Lateral erosion of the failed alluvium may be due, in part, to ongoing weathering-driven erosion of the shale in the bed of the channel. Subreach 6 (Figures 2.13, and A.31) has very similar characteristics to Subreach 5, and active channel erosion and widening is ongoing. In Subreach 7, the bank slopes are generally flatter and are indicative of deep seated mass failure of the alluvial fill, but there has been erosion of the toes of the failed banks, and a vertical shale bank that had been buried by the mass failures is now exposed (Figures 2.14, 2.15 and A.32, A.33). Similar conditions are observed in Subreach 8 (Figures 2.16 and A.34), but the degree of erosion of the alluvial toe materials is higher, which might suggests that retreat of the toe is systematic and should progress upstream over time. However, in Subreaches 9 and 10, the toes of the banks are composed of failed alluvium, and there is less sign of toe erosion and retreat (Figures 2.17, 2.18 and A.36, A.36). Therefore, it appears that erosion and retreat of the alluvial material is locally controlled and may be due to the relative erodibility of the shale, which would control the rate of vertical erosion of the bed. Support for the local control of the retreat of the failed alluvial material is provided by variable degrees of failure farther downstream (**Figure A.37**). It is possible that retreat of the failed alluvium (**Figure A.38**), exposure of the shale in the toes of the bank and ongoing degradation into the bed combine to initiate a new cycle of deep seated mass failure of the overlying alluvium (Figure A.15) that results in further widening of the channel top width (**Figure A.39**).

2.2.2.1. North Sulphur River Channel Evolution Model

Field observations permit a channel evolution model (NSRCEM) to be developed for the NSR and its tributaries (**Figure 2.19**), but the model varies significantly from those developed for alluvial streams (Figure 2.4). There is little doubt that following channelization in the late 1920s the NSR incised and widened (Avery, 1974) and followed the typical channel evolution sequence while the channel boundary materials were composed of alluvium (Types I through V). A similar sequence of channel evolution has been observed on Mill Creek, tributary to Chambers Creek in the Blackland Prairie region, but the degradation has yet to expose the underlying shale bedrock (P. Allen, Baylor University, pers. comm., 2006). However, exposure of the shale has added a significant complicating factor to the evolution of

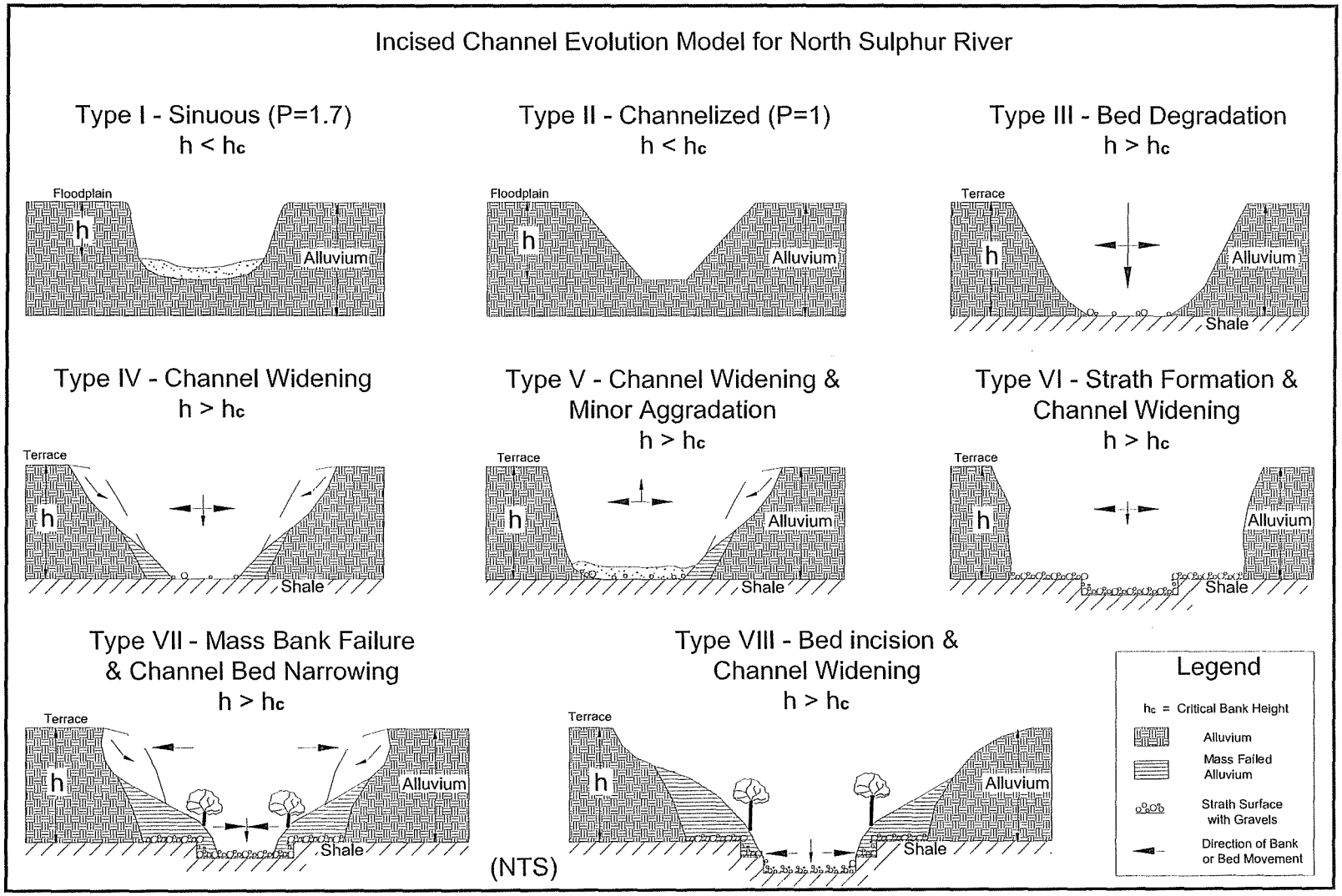

Figure 2.19. Channel evolution model (NSRCEM) for the North Sulphur River.

the channel, to the point where the existing CEMs no longer apply. Ongoing vertical and lateral erosion of the exposed shale in the bed and the banks is dependant primarily on weathering processes that are controlled by wetting and drying cycles (Tinkler and Parish, 1989; Allen et al., 2002) and not hydraulically controlled processes of sediment entrainment and transport. Flow events in the channel remove the weathering products and re-initiate vertical and lateral erosion into the shale. As a rule, lateral erosion rates exceed vertical erosion rates in bedrock and result in the formation of gravel-covered strath surfaces that become terraces when vertical erosion of the bed occurs (Leopold et al., 1964; Schumm, 1977) (Type VI). Deep-seated slump failures of the overlying alluvium bury the strath surfaces (Type VII) and prevent lateral erosion of the shale. Resulting channel narrowing may actually accelerate erosion of the shale exposed in the bed, which in turn leads to undercutting of the erosion-resistant, root-reinforced alluvium, thereby leading to re-exposure of the shale in the toe of the banks and ongoing lateral retreat of the shale (Type VIII). It is likely that over time the incision into the shale will induce further mass failure of the alluvial valley fill and a Type VII condition will be reestablished at a lower bed elevation. The NSRCEM applies equally to the larger tributaries that have degraded into the shale bedrock. Based on the NSRCEM, Subreaches 1 through 3 were classified as Type VI, Subreach 4 was classified as Type VII, Subreaches 5 through 8 were classified as Type VIII, and Subreaches 9 and 10 were classified as Type VII. Similar sequences are present in the larger tributaries.

Based on the current topography of the NSR and the major tributaries as determined from the DTM, and assuming a bulk unit weight of 100 lb/ft^3, approximately 18x10^6 tons of sediment has been eroded upstream of the proposed dam site from the mainstem of the NSR, and a further 10x10^6 tons has been eroded from the major tributaries. Based on the observations of Watson et al. (1986) and Simon (1989), the erosion rates and sediment yields would have varied over time, but on an average annual basis for the period from 1927 to 2005, the channel erosion would have yielded about 3,500 t/sq mi (3.8 t/ac/yr) at the dam site. Suspended-sediment measurements (8 years) at the USGS gaging station on the NSR near Talco, Texas (USGS Gage No. 7343200) showed a maximum annual rate of 2,642 t/sq mi (4.1 t/ac/yr) in 1968 (Texas Dept. of Water Resources, 1979), but this was about 40 years after channelization, and therefore, mostly probably does not reflect the higher sediment loads when the channel was most actively eroding. Currently, the incised channel has the ability to convey in excess of the 100-year flood in-bank (Figures 2.5 through 2.18), the bed of the river is composed of shale, and therefore, the current supply of sediment to the channel is far less than the transport capacity. As a consequence, it is highly unlikely that the NSR will attain a state of equilibrium in the near future. Prevention of further incision and widening of the channels will require significant deposition of sediment on the bed of the river. This can only occur if either the bed-material sediment supply is increased significantly, or the hydraulic capacity is reduced significantly. For example, assuming that sand–sized material would be deposited on the bed of the river, and that velocities less than 2 ft/sec would be required at the 2-year flow to induce deposition of sand on the bed, the effective width of the channel of the NSR would have to increase by an order of magnitude, and shear stresses would have to decrease from between 0.5 and 0.6 lb/ft^2 to less than 0.2 lb/ft^2 (**Figure 2.20**).

2.2.3. Existing Channel Morphology

Existing conditions morphometric characteristics of the mainstem of the NSR and the major tributaries were developed from the DTM. **Figure 2.21** shows the bed and valley floor profiles between FM 904 bridge and the upstream end of the mapping above Allen Creek. The profiles show that on average the channel depth is on the order of 35 feet in the downstream reaches and decreases to about 25 feet in the upstream reaches. The bed slope is about

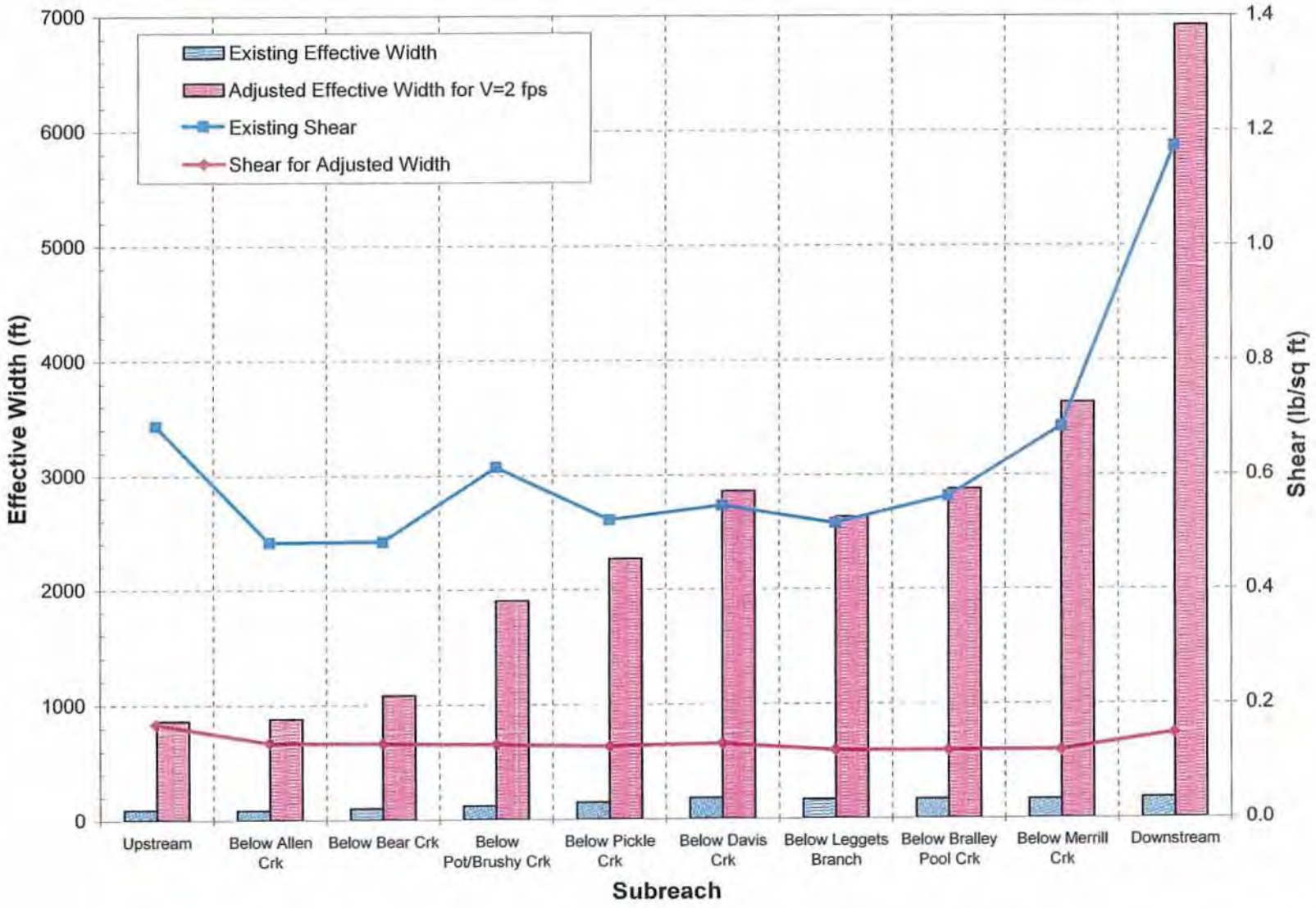

Figure 2.20. Existing and adjusted effective widths and shear stresses for the 10 subreaches of the North Sulphur River at the 2-year peak flow assuming that velocities would have to be < 2 ft/s to induce sediment deposition on the bed.

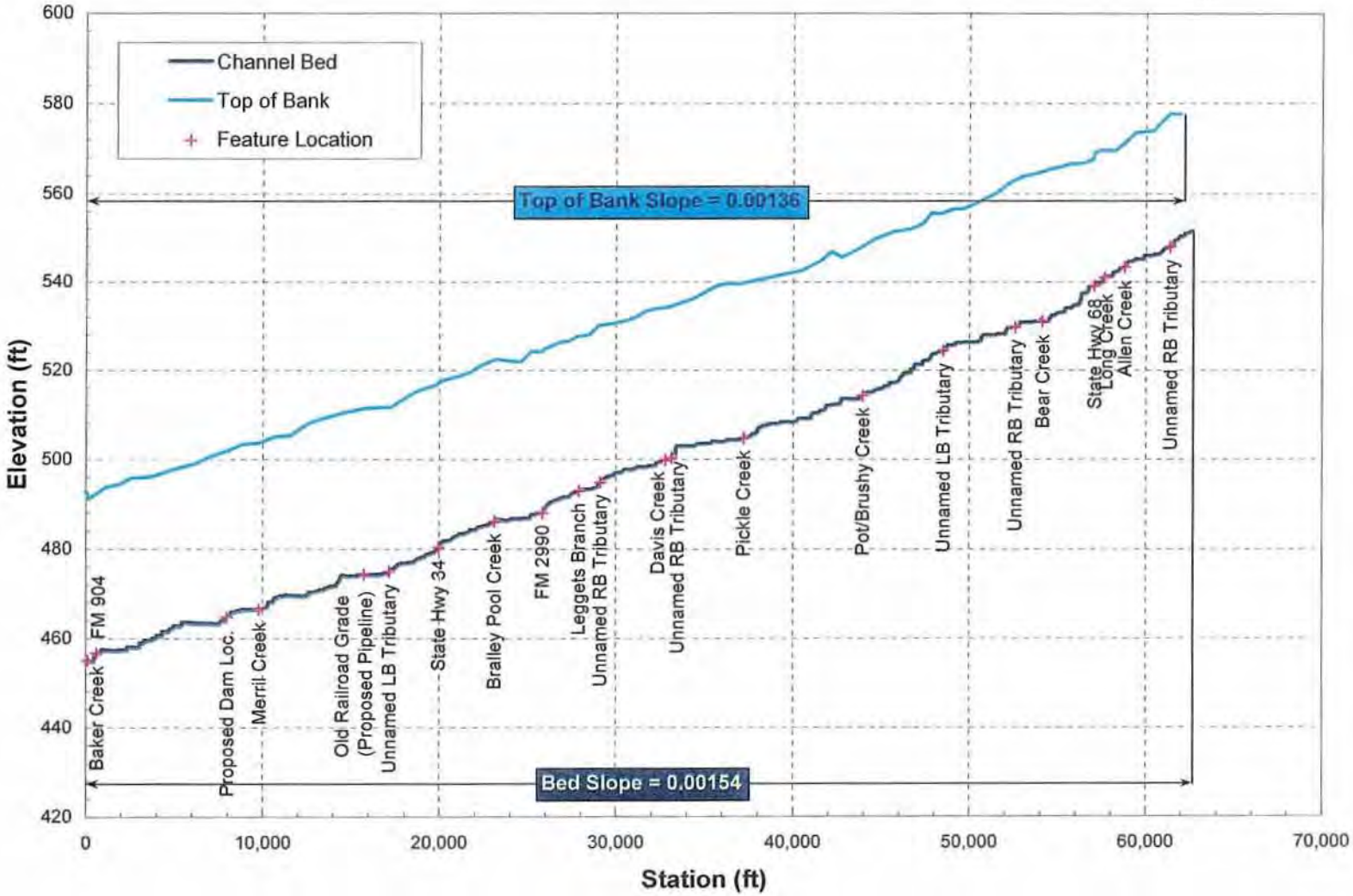

Figure 2.21. Longitudinal profiles of the bed and valley floor of the North Sulphur River between FM 904 Bridge and upstream of Allen Creek.

0.0012 (6.3 ft/mi) between FM 904 and the Brushy Creek confluence (Subreaches 4 through 10) and increases by about 60 percent (0.00195: 10.3 ft/mi) between Brushy Creek and upstream of Allen Creek (Subreaches 3 through 1). The average slope for the valley floor is 0.0014 (7.4 ft/mi) and the average bed slope is 0.0015 (7.9 ft/mi). Channel top widths were identified at cross sections that were used to develop the HEC-RAS model of the NSR (Chapter 4), and were plotted against the distance upstream of the FM 904 bridge (**Figure 2.22**). The data show that in general terms the channel topwidth increases in the downstream direction as would be expected. However, the 5-point moving average shows some interesting patterns. Where the banks tend to be steepest (Subreaches 1, 2, 3, 5, 6) the channel top widths are narrower than where the bank angles are less steep as a result of the deep-seated mass failures (Subreaches 4, 7, 8, 9, 10). This suggests that through time further channel widening should be expected in Subreaches 1, 2, 3, 5 and 6.

Longitudinal profiles of Merrill Creek (**Figure 2.23**), Bralley Pool Creek (**Figure 2.24**), Leggetts Branch (**Figure 2.25**), Davis Creek (**Figure 2.26**), Pickle Creek (**Figure 2.27**), Brushy Creek (**Figure 2.28**), Bear Creek (**Figure 2.29**), Allen Creek (**Figure 2.30**) and Long Creek (**Figure 2.31**) show that all of the tributaries have incised in response to baselevel lowering in the NSR, and channelization of the lower reaches of some of them (Merrill, Bralley Pool, and Davis Creeks). At the mouth of Merrill Creek, the channel depth is about 36 feet, but 4.5 miles upstream (Sta 240+00) the depth has reduced to 22 feet (Figure 2.23). Upstream of the Roxton/Gober Chalk knickpoint, the channel depth is only about 8 feet. Since Merrill Creek is relatively straight, the valley floor slope and the channel slope should be similar, but as can be seen on Figure 2.23 the channel slope is about 2.3 times steeper than the valley slope, and hence further erosion of the bed should be expected. The rate of degradation will depend primarily on the weathering characteristics of the exposed shale. Similar conditions are present in Bralley Pool Creek (Figure 2.24). At the mouth the channel depth is about 36 feet, and it reduces to about 13 feet upstream. Bralley Pool Creek is reasonably sinuous, except in the lower channelized reach, and the channel slope is only about 1.4 times steeper than the valley floor slope, and therefore, some further degradation of the shale bed is to be expected.

A concrete box culvert provides grade control in Leggetts Branch about half a mile upstream of the confluence with NSR (Figure 2.25). Downstream of the box culvert the channel depth is about 35 feet, but upstream it is about 12 feet, which further reduces to about 4 feet upstream of a local bridge crossing. A concrete box culvert is present at the FM 1550 crossing. Provided that the downstream culvert continues to provide grade control, there is little likelihood that there will be significant further degradation of the tributary. Concrete box culverts provide grade control in Davis Creek at the FM 2990 crossing and at the FM 1550 crossing (Figure 2.26). However, before the culverts were emplaced considerable degradation had occurred. At the mouth, the channel depth is about 35 feet, and upstream of FM 2990, it is 22 feet. Further degradation into the shale bed is likely to occur upstream of the FM 2990 crossing. At the mouth, Pickle Creek is about 35 feet deep and this reduces to about 20 feet upstream (Figure 2.27). There is a concrete box culvert at the FM 1550 crossing that provides a measure of grade control for the upstream channel. The presence of a convexity in the bed profile in the downstream portion of the tributary suggests that there will be further degradation into the shale bed in the future.

In common with the other tributaries, the channel depth at the mouth of Brushy Creek is about 35 feet, and the depth reduces in the upstream direction to about 23 feet (Figure 2.28). Further degradation of the shale bed is likely in the future, but the upstream progression of the degradation is likely to be halted by the concrete slab and H-pile grade-control structure at the FM 1550 crossing. The depth of Bear Creek at the confluence with NSR is about 26 feet (Figure 2.29) and this reflects the lesser degree of incision in the mainstem (Figure

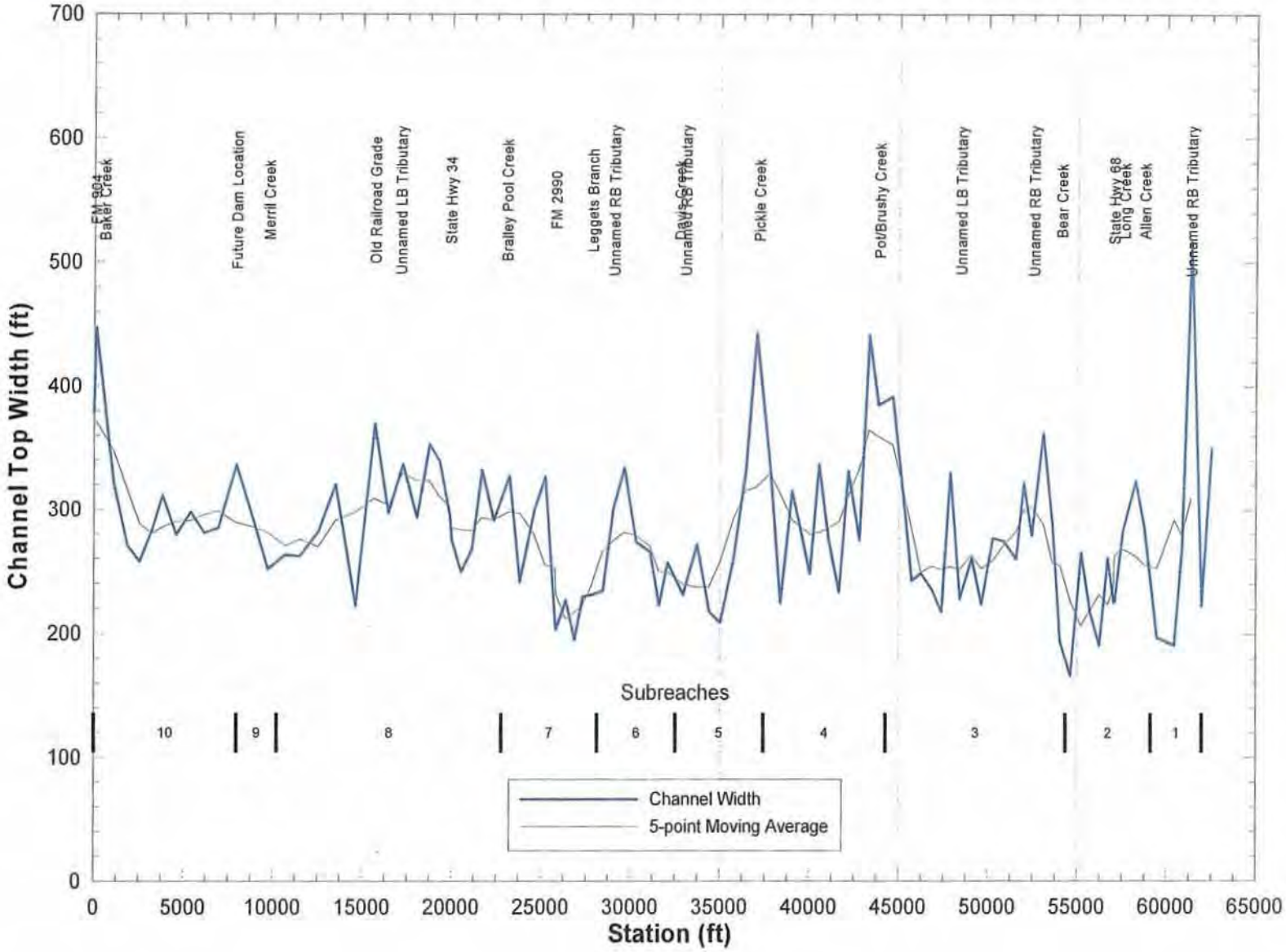

Figure 2.22. Plot of channel top widths along the North Sulphur River between FM 904 Bridge and upstream of Allen Creek.

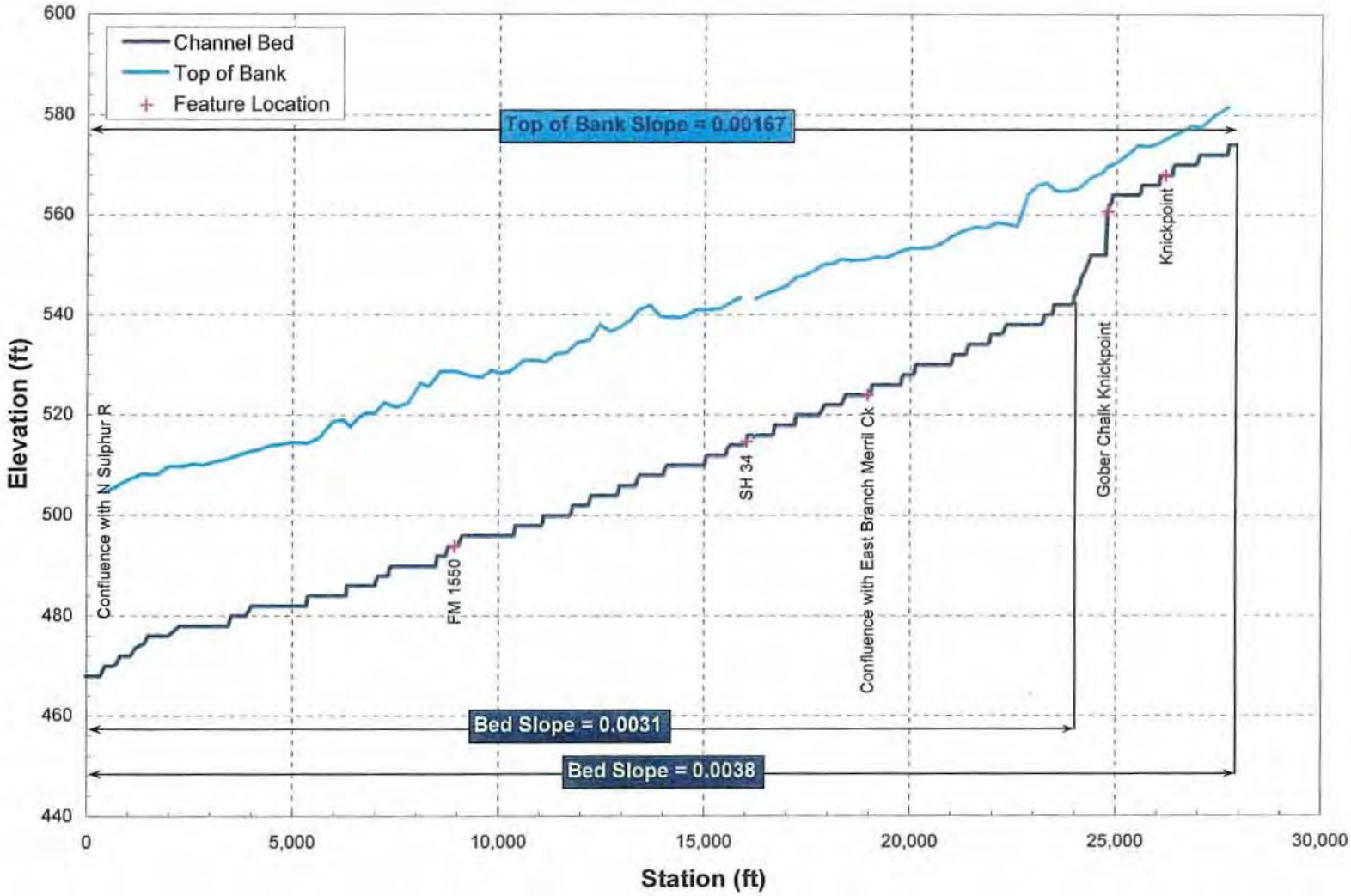

Figure 2.23. Longitudinal profiles of the bed and valley floor of Merrill Creek.

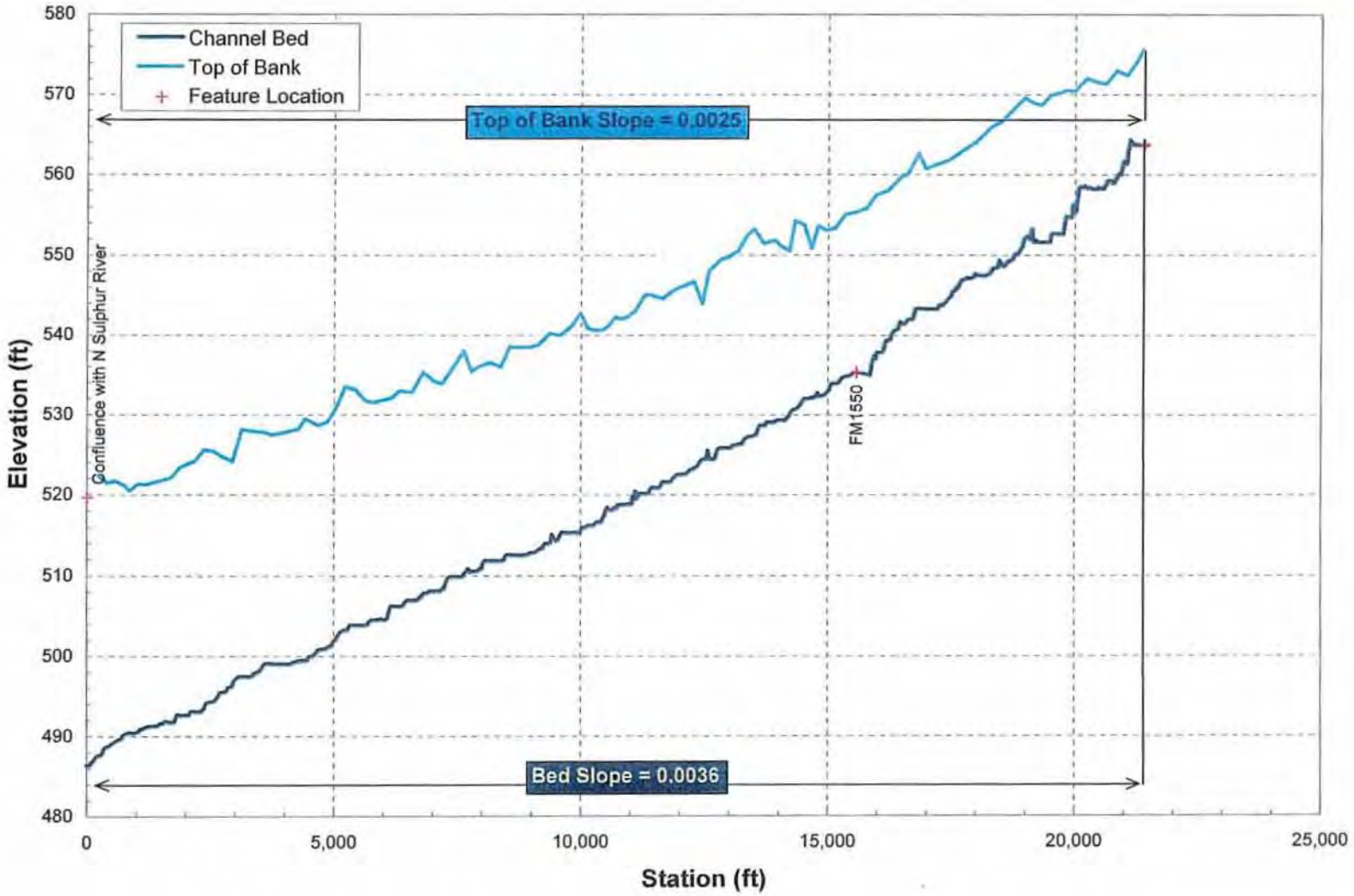

Figure 2.24. Longitudinal profiles of the bed and valley floor of Bralley Pool Creek.

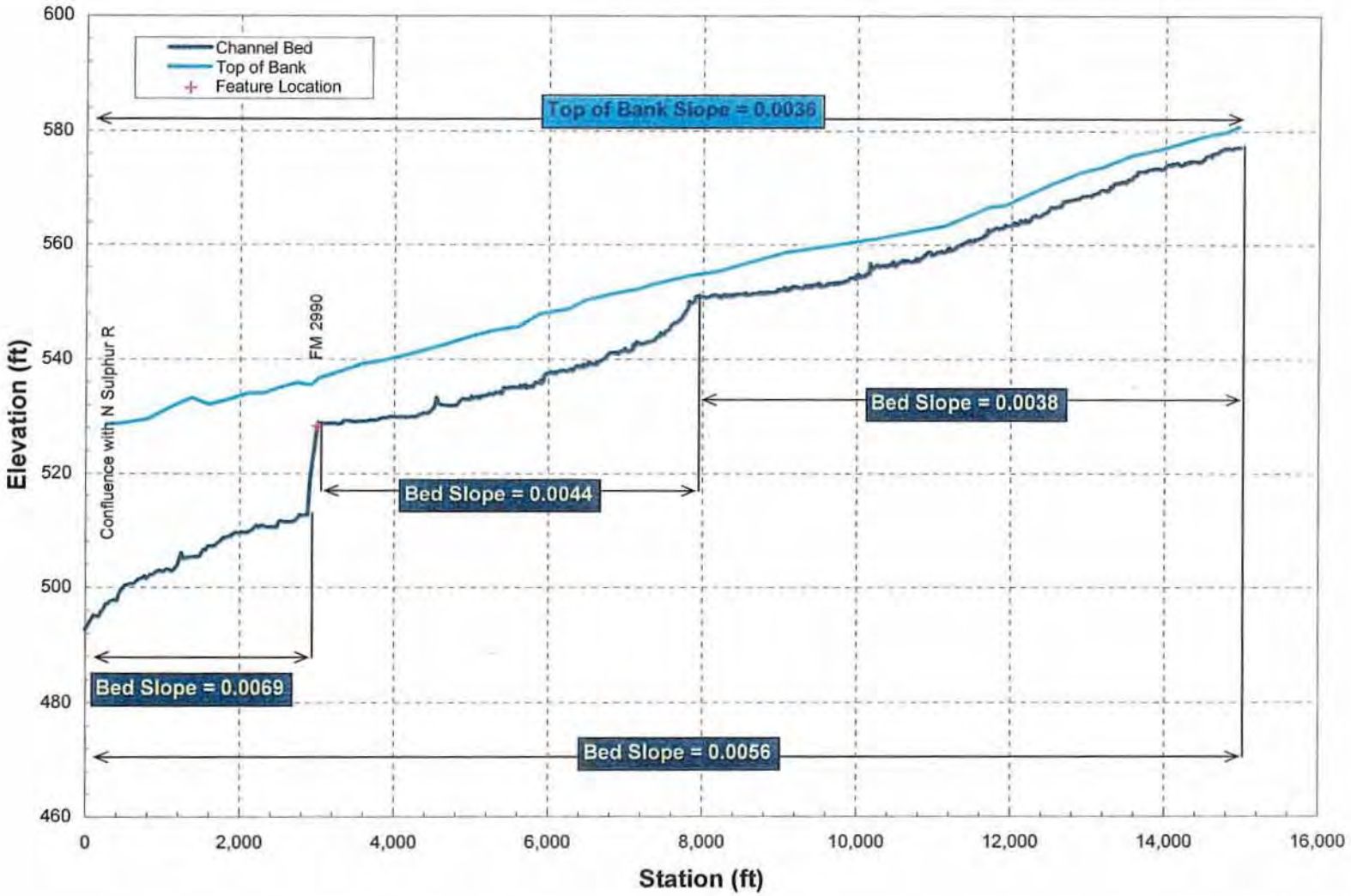

Figure 2.25. Longitudinal profiles of the bed and valley floor of Leggetts Branch.

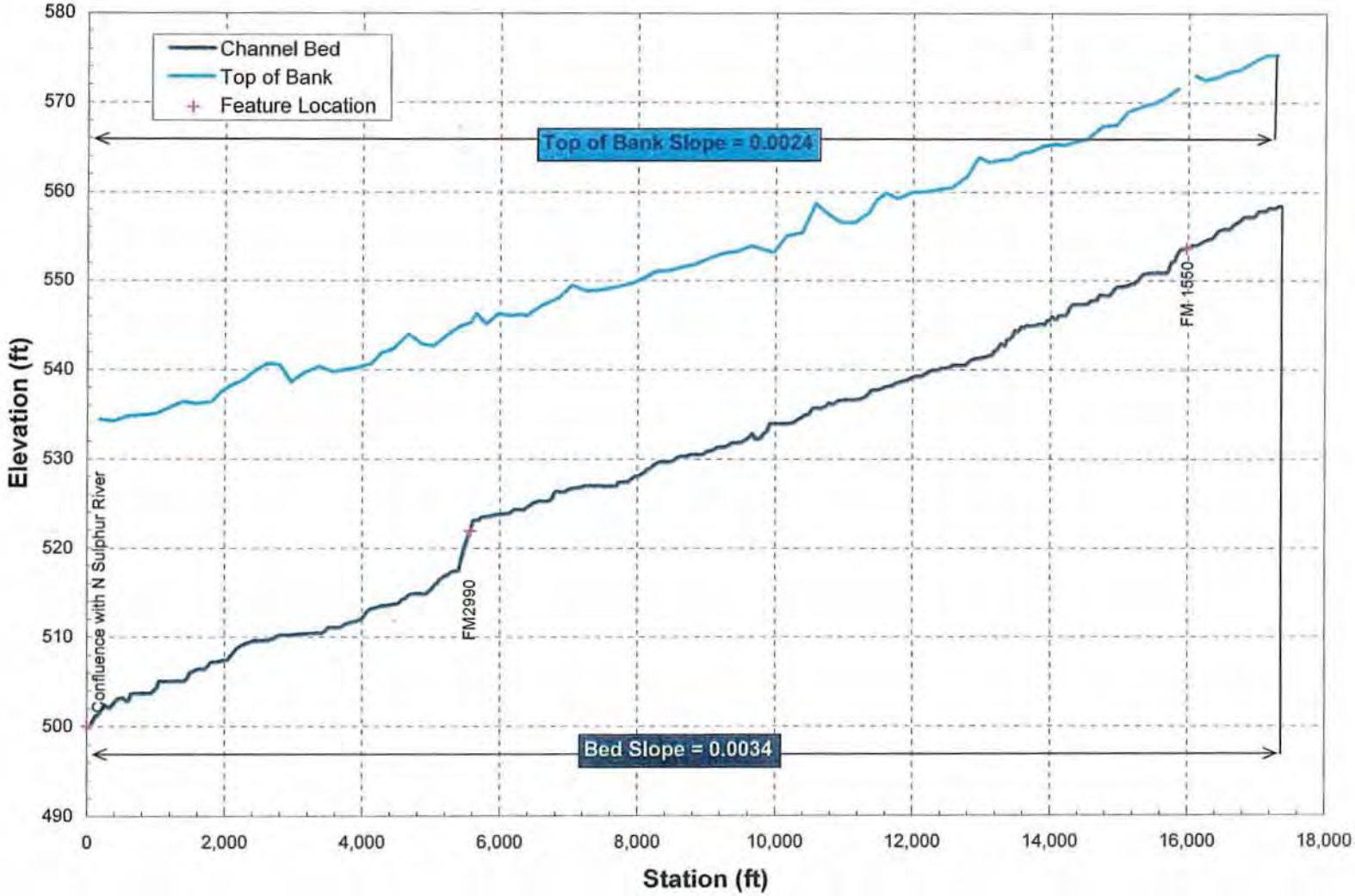

Figure 2.26. Longitudinal profiles of the bed and valley floor of Davis Creek.

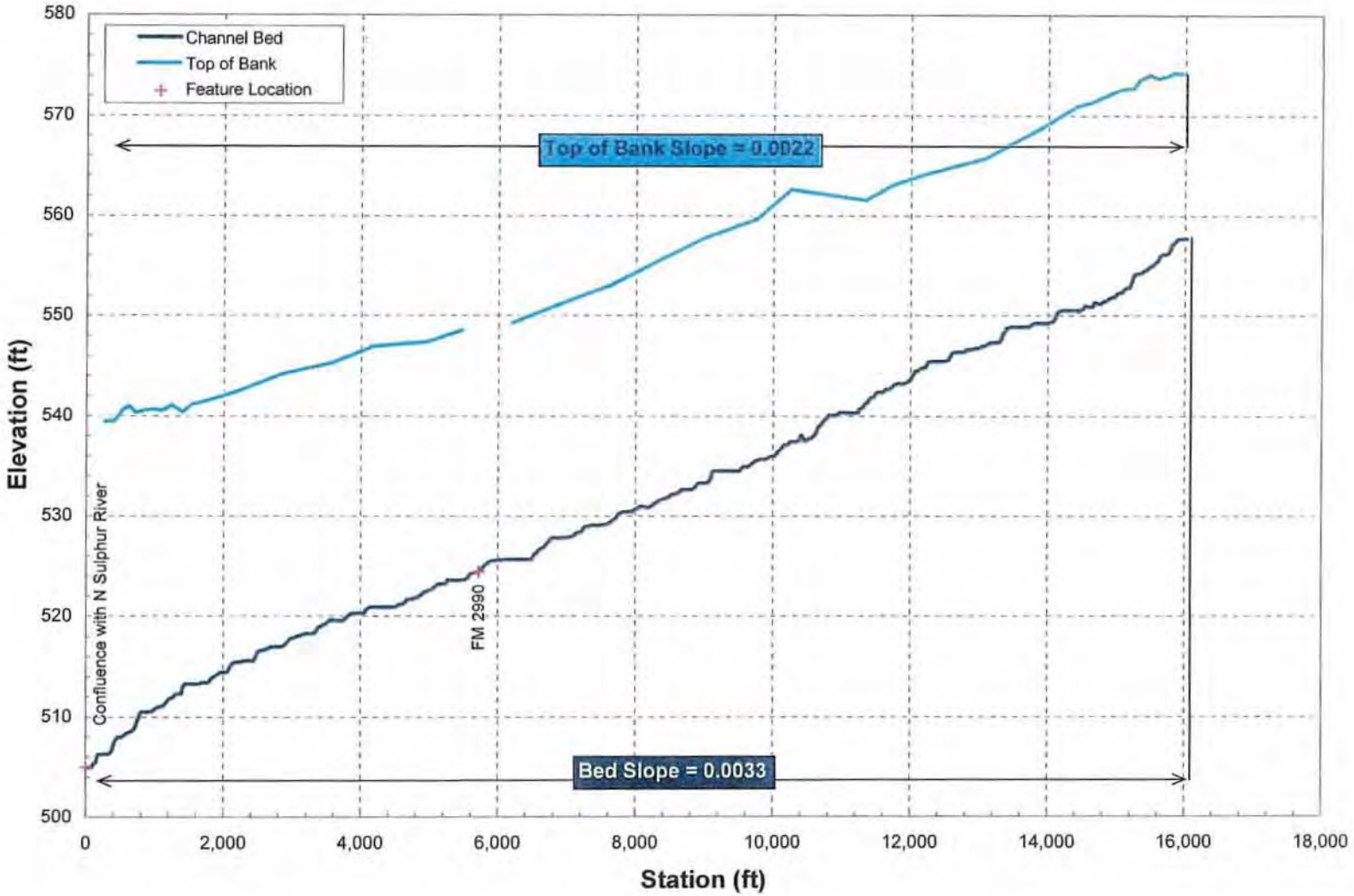

Figure 2.27. Longitudinal profiles of the bed and valley floor Pickle Creek.

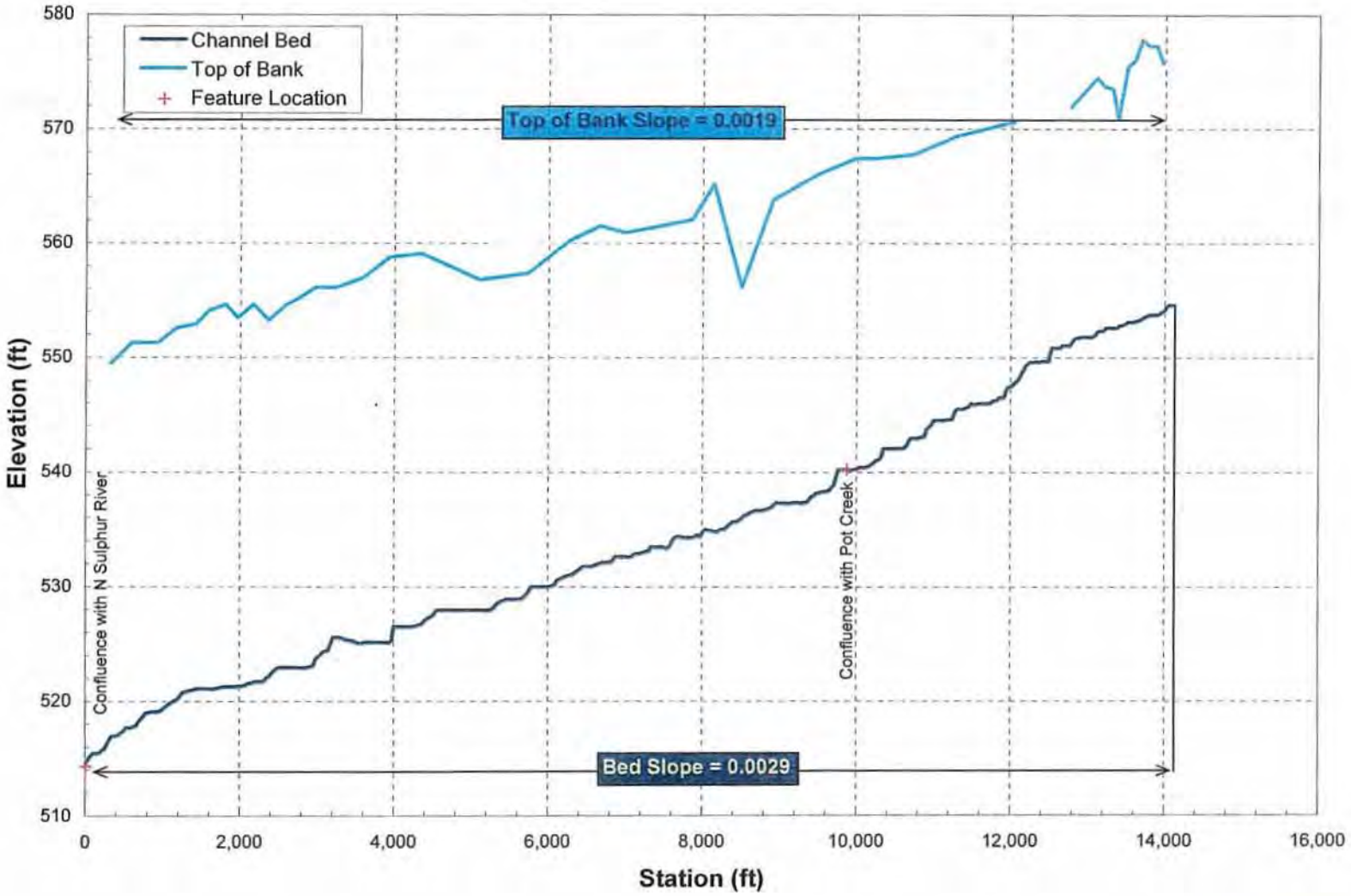

Figure 2.28. Longitudinal profiles of the bed and valley floor of Brushy Creek.

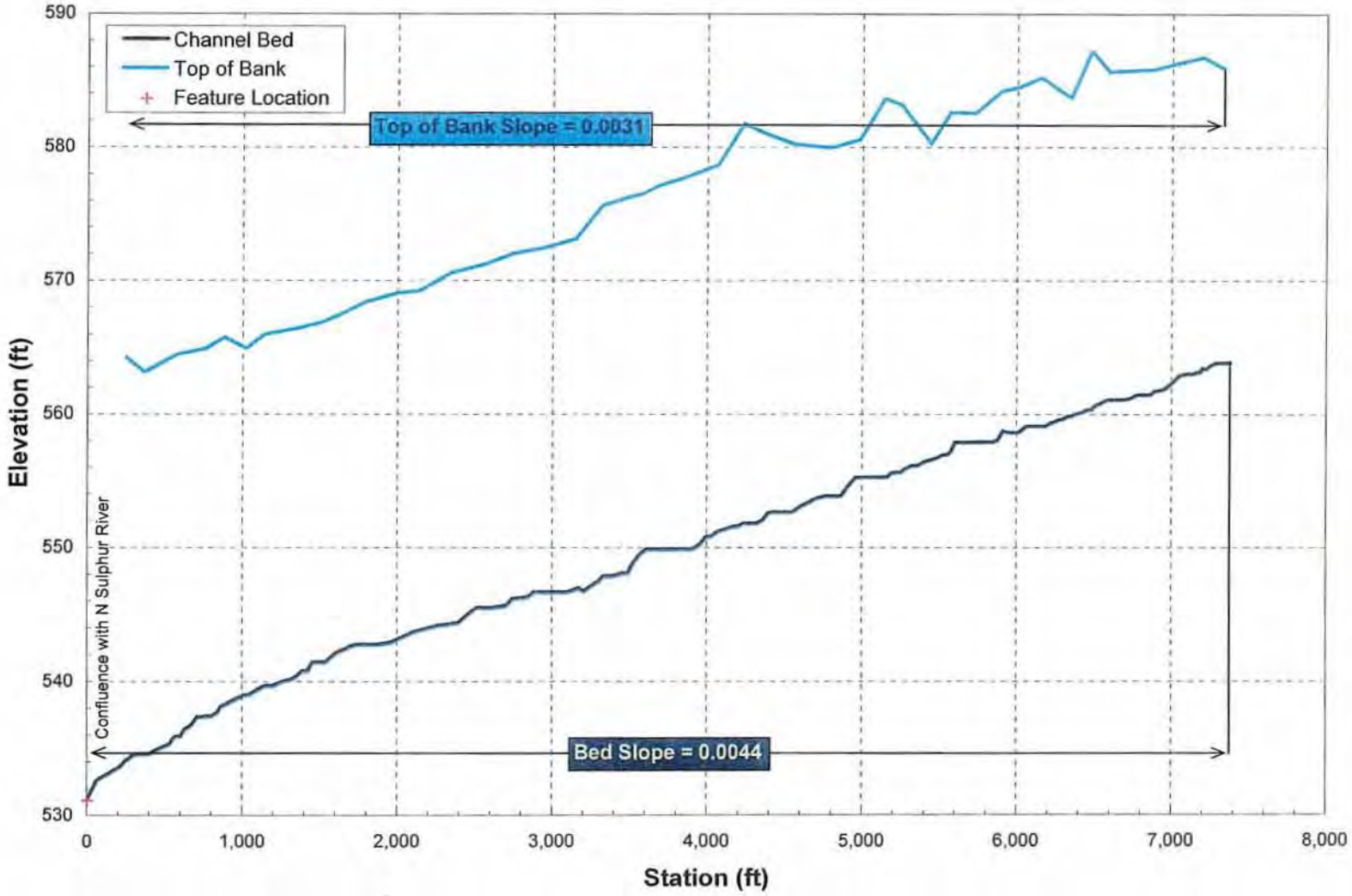

Figure 2.29. Longitudinal profiles of the bed and valley floor Bear Creek.

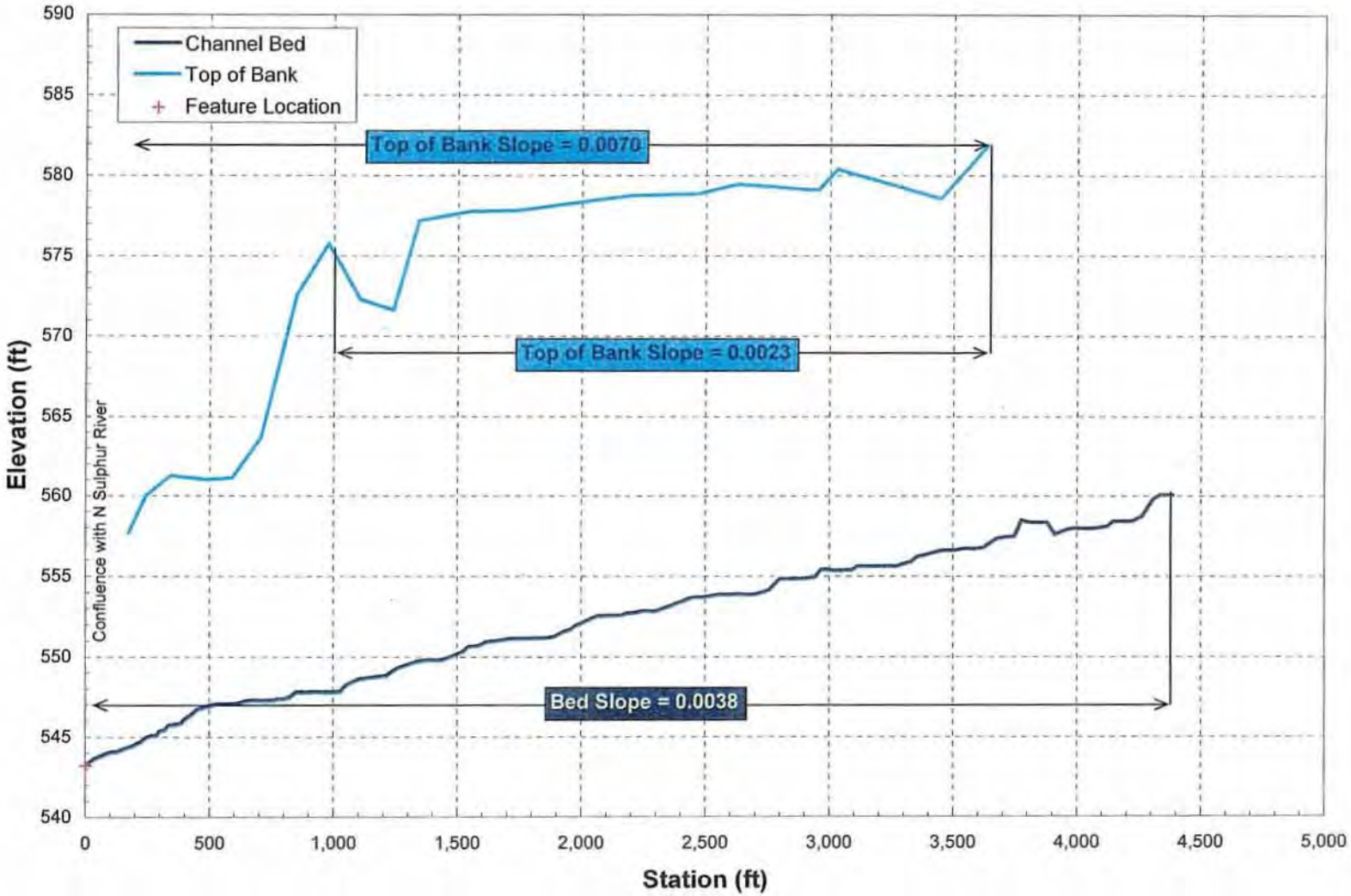

Figure 2.30. Longitudinal profiles of the bed and valley floor of Allen Creek.

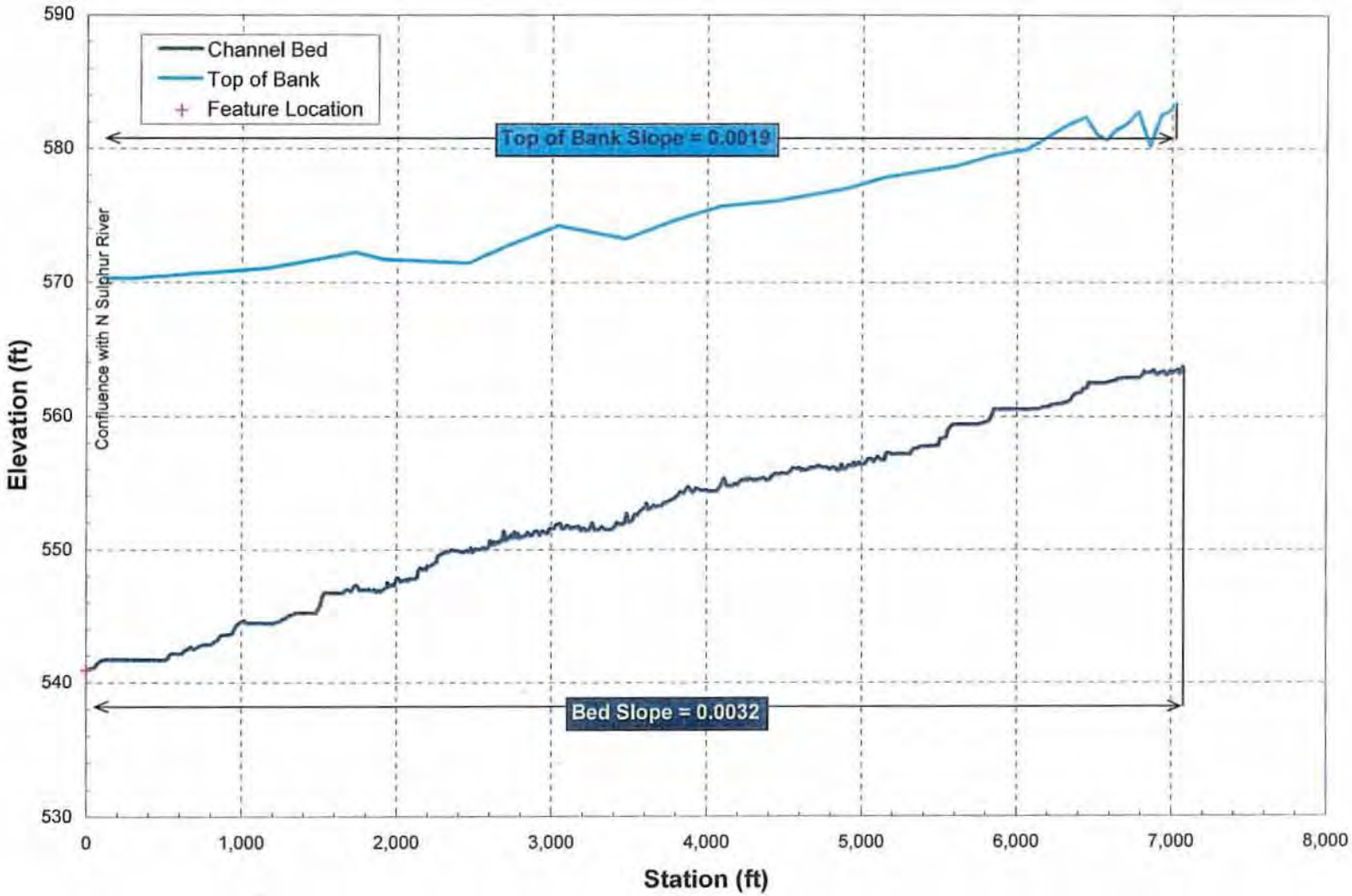

Figure 2.31. Longitudinal profiles of the bed and valley floor of Long Creek.

2.21). Based on the presence of a convexity in the bed profile in the lower reaches, it is highly likely that there will be further incision into the shale bed. At its mouth, Allen Creek is only 15 feet deep which reflects the local depth of the NSR, but the depth increases to about 25 feet farther upstream (Figure 2.30). As the NSR continues to degrade, Allen Creek will also degrade in the future. No grade controls were observed downstream of the Roxton/Gober Chalk outcrop (Figure 2.2) in this tributary. Long Creek is the largest tributary draining the south side of the NSR valley, and it has responded to the lowered baselevel in a similar fashion (Figure 2.31). At the mouth, the channel is about 30 feet deep and this reduces to about 20 feet farther upstream. SCS floodwater retarding structures have been built in the upper reaches of this channel.

In summary, all of the tributaries to the NSR have incised through the valley fill alluvium, and the bed and lower portions of the banks are composed of shale. The inevitable ongoing erosion of the shale in both the bed and banks is primarily the result of weathering processes, and the rate of erosion is governed by the number of wetting and drying cycles. Slab failure of the alluvial materials above the exposed shale does deliver alluvial sediment to the channels, but as failures progress, the upper bank angle becomes flatter, and therefore, more stable since the erosion of the shale toe occurs at a much lower rate. Consequently, through time, the sediment delivery from the alluvial fill declines and the major source of sediment is the weathering of the exposed shale in the bed and banks of the channel. In the lower reaches of the larger tributaries, deep-seated mass failures of the alluvial sediments increase the channel top with, but also bury the exposed shale in the toes of the banks and provide an appearance of stability in a similar manner to the mainstem. As shown in the NSRCEM (Figure 2.19), a mass failure of the alluvial field temporarily protects the exposed shale in the toe of the bank with cohesive and vegetated material, thereby accelerating the bed erosion. In time, the deepened channel causes lateral erosion of the mass-failed toe material and re-exposure of the shale.

2.2.4. Channel Incision Rates

Two sources of information were obtained to evaluate incision rates on the NSR and the tributaries, repeat surveys at bridges and stage-discharge data at the USGS gage at Cooper (USGS Gage No. 07343000). Bridge profiles were obtained by CP&Y for State Highway 34, FM 2990 and FM 904 on the NSR, State Highway 34 and FM 1550 on Merrill Creek, FM 1550 on Bralley Pool Creek, and FM 1550 on Baker Creek. The USGS 9207 summary gaging forms that provide measured stage-discharge data for a range of flows were also obtained for the period from 1950 to the present.

Bridge profiles for the FM 2990 crossing of the NSR (**Figure 2.32**) and the State Highway crossing of Merrill Creek (**Figure 2.33**) provide good examples of historic incision at these structures. Between 1967 and 1985, the bed of the NSR at FM 2990 degraded by about 5 feet at a rate of about 3.3 in./yr (**Figure A.40**). In the following 17 years (1985-2002), there was little if any degradation based on a comparison of the 1985 profile and the cross section derived from the 2002 DTM. However, since the nominal accuracy of the DTM is 1 foot (one-half contour interval), it is possible that there has been up to 1 foot of erosion at this bridge (0.7 in./yr). Review of the 1969 aerial photography (1:20,000), suggests that shale was present in the bed in 1969, and therefore, the erosion rates of up to 3.3 in./yr are consistent with measured rates in shale in other channels in northeast Texas (Allen et al., 2002).

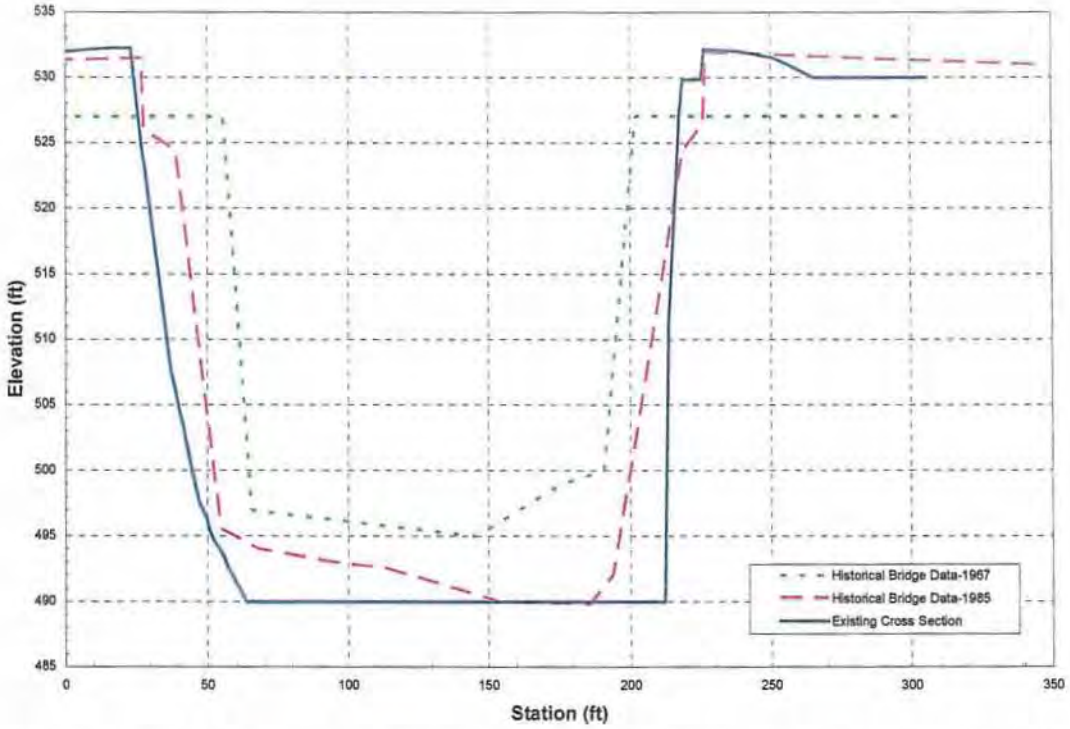

Figure 2.32. Bridge cross-section profiles for the FM 2990 crossing of the North Sulphur River.

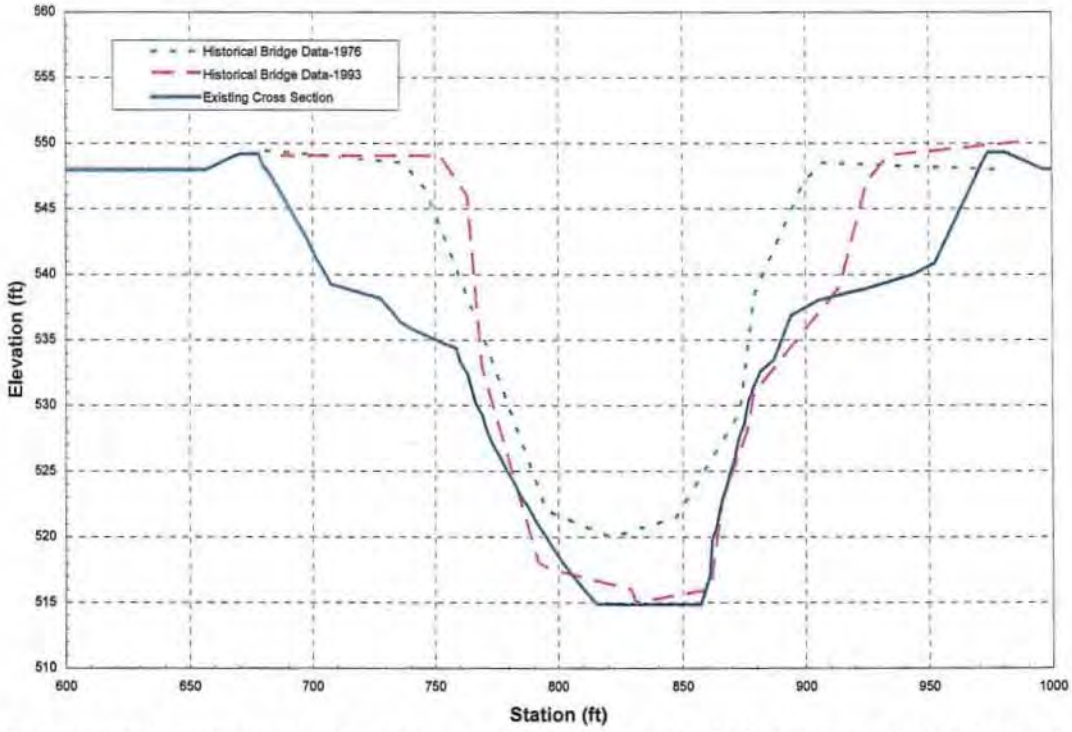

Figure 2.33. Bridge cross-section profiles for the FM 1550 crossing of Merrill Creek.

The bridge profiles at the State Highway 34 crossing of Merrill Creek (Figure 2.33) indicate that Merrill Creek degraded by about 5 feet between 1976 and 1993 at a rate of about 3.5 in./yr. Between 1993 and 2002 there appears to have been little erosion, but it could have been as high as 1.3 in./yr if it is assumed that 1 foot of degradation took place. Both values are consistent with reported values of erosion into the shale (Allen et al., 2002). **Figure 2.34** summarizes the bridge survey data for the seven bridges investigated. With the exception of the FM 1550 bridge at Merrill Creek, rates of incision into the shale average 2 to 3 in./yr, which is very consistent with measured rates in other channels in northeast Texas (Allen et al., 2002). These rates of incision can be expected to occur in the future for as long as the shale is exposed to weathering and slaking processes.

Stage-discharge rating curves were developed from the USGS 9207 summary gaging forms for the Cooper gage for seven periods between 1950 and the present (**Figure 2.35**). The data show that the channel at the gage aggraded between 1950 and 1979, which is consistent with a much higher sediment load from the upstream eroding channels of the NSR and the tributaries (Schumm et al., 1984; Harvey and Watson, 1986; Watson et al., 1986; Simon, 1989). Review of the 1979 aerial photography (1:40,000) suggested that there were a large number of depositional bars on the bed of the NSR at that time. Analysis of the stage-discharge rating curves for flows below 1,000 cfs from 1971 to the present (**Figure 2.36**) indicate that the channel began to degrade after 1985. Degradation rates were about 1.5 in/yr between 1986 and 1993, 1.4 in./yr between 1993 and 1999, and 1 in./yr between 2000 and the present (2005). The bed of the river at the gage is composed of shale (**Figure A.41**), and it is reasonable to conclude that at least the 2000–2005 degradation represents erosion of the shale. Degradation at the gage since 1985 is consistent with a reduced sediment supply due to channel evolution upstream, and the general observation from both helicopter and ground reconnaissance, that there is little sediment stored in the bed of the NSR from its confluence with the South Sulphur River to the headwaters. The bed of the NSR from the confluence with the South Sulphur River to the headwaters downstream of the Roxton/Gober Chalk outcrop is primarily composed of shale with a veneer of alluvial sediment at some locations, generally the mouths of larger tributaries.

2.2.5. Sediment Sources and Bed-material Gradations

Sediment delivery to the NSR is from both watershed and channel erosion sources. Because most of the soils in the watershed are clays and clay loams (NRCS, 2001), the bulk of the sediment supplied to the channels is in the form of wash load that contributes little to channel processes, but is an important component of the annual sediment load. Channel sources include slab (Figure A.13) and slump (**Figure A.42**) failures of the valley fill alluvium, and a variety of shale-related sources. Plucking of the shale in both the bed (Figure A.7) and the banks (**Figure A.43**) produces gravel-cobble sized shale clasts (Figures A.11 and A.12) that are initially transported as bed material. In situ weathering of the shale in the bed tends to produce gravel- and finer-sized clasts (Figure A.10) that are readily transported at the onset of flow in the channel, and probably contribute to the very high initial sediment concentrations (100,000 ppm) reported for similar channels in northeast Texas (Allen et al., 2002). Weathering (**Figure A.44**) and mass failure (Figure A.8) of shale exposed in the banks also produces gravel- and cobble-sized shale clasts that are initially transported as bed material, but eventually slake (Figure A.6) and are transported as part of the wash load. Most of the larger, non-shale, clasts observed in the channel are derived from sandstone and limestone stringers exposed by erosion of the shale (**Figure A.45**), or from poorly cemented, weathered gravels interbedded in the exposed shale (**Figure A.46**). Low-density chalk sands and gravels are derived from the Roxton/

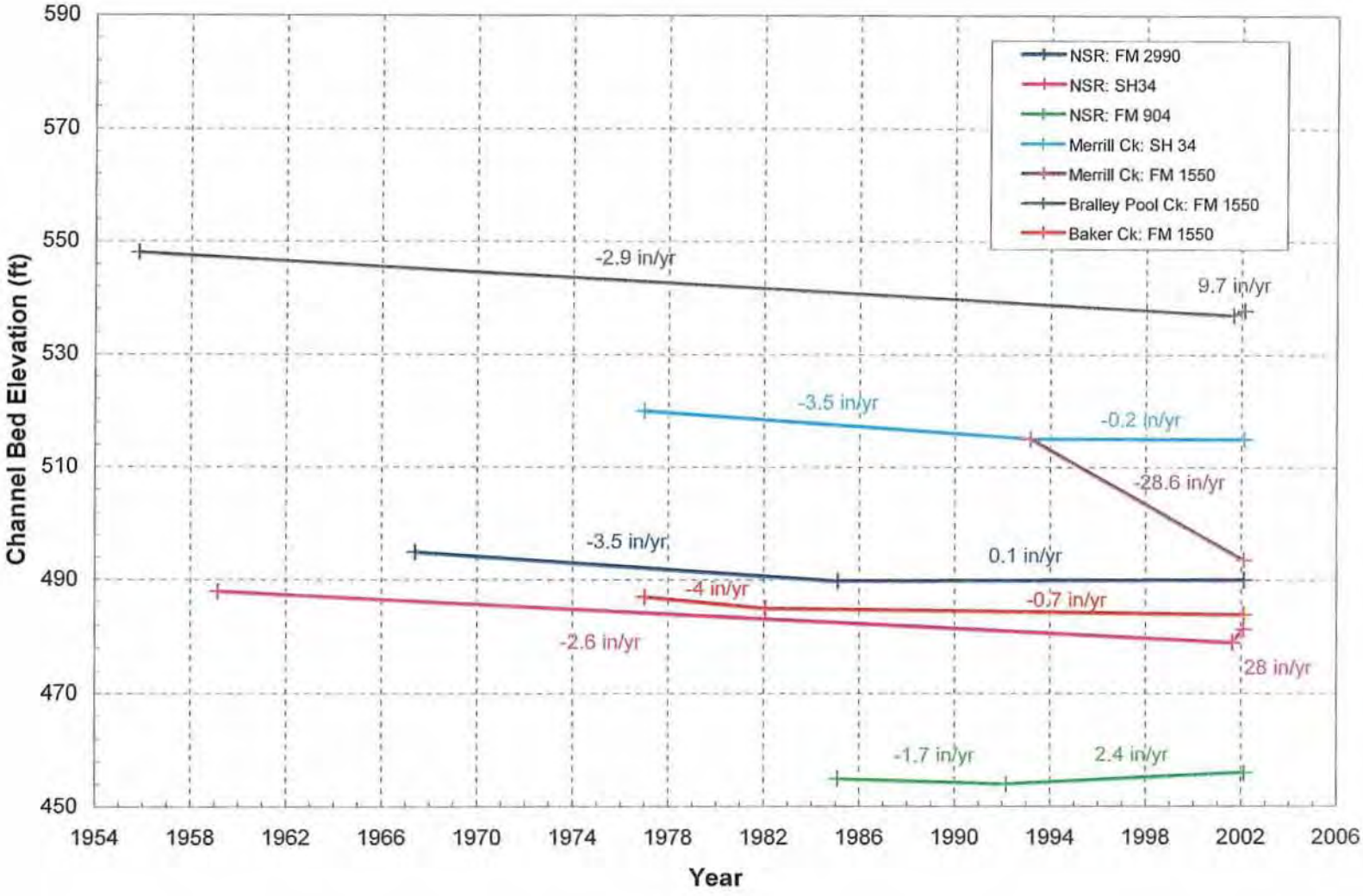

Figure 2.34. Bed degradation rates at the seven evaluated bridges in the upper North Sulphur River basin.

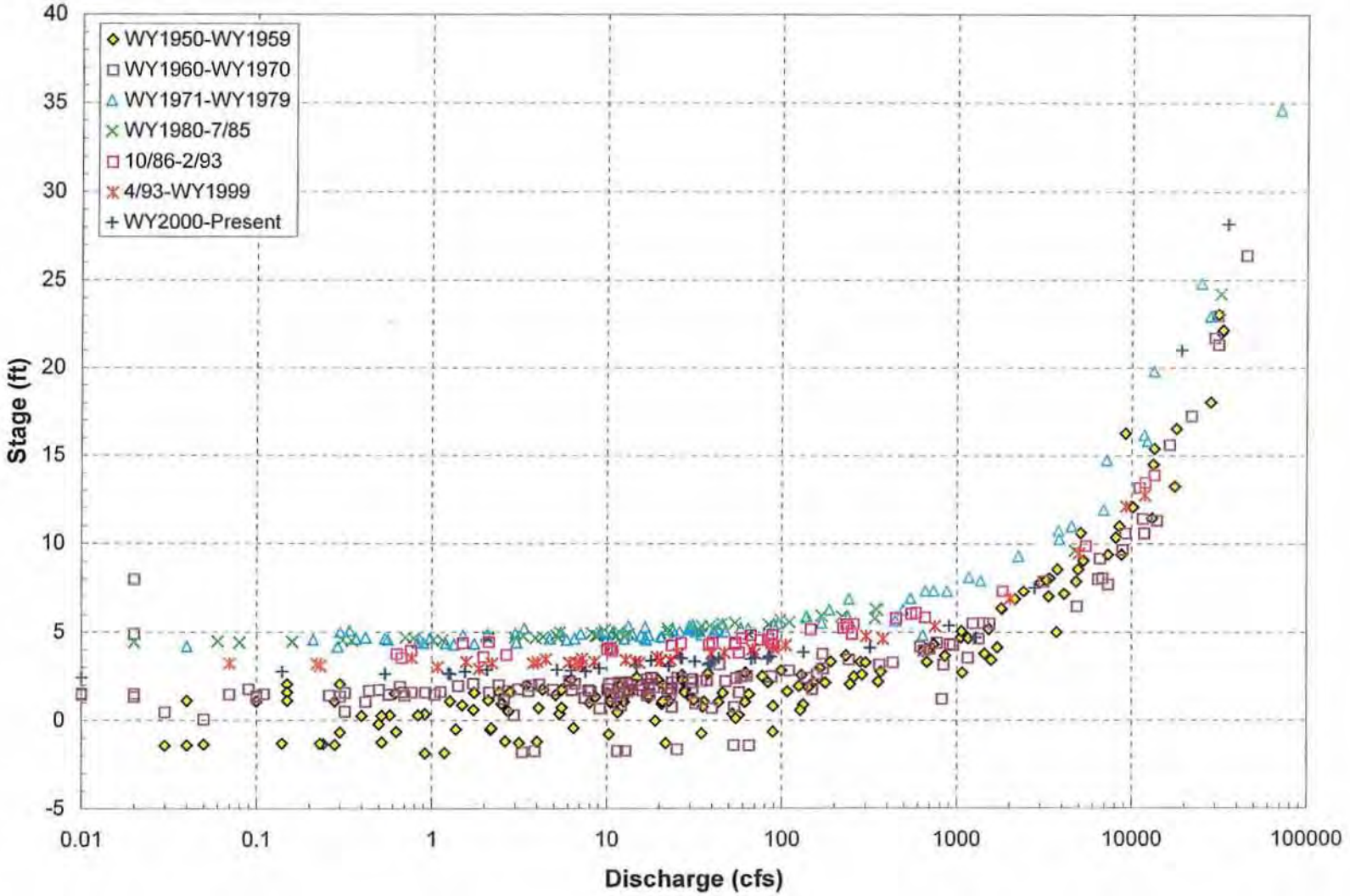

Figure 2.35. Stage-discharge rating curves from 1950 to 2005 for the USGS gage on the North Sulphur River, near Cooper, Texas (USGS Gage No. 07343000).

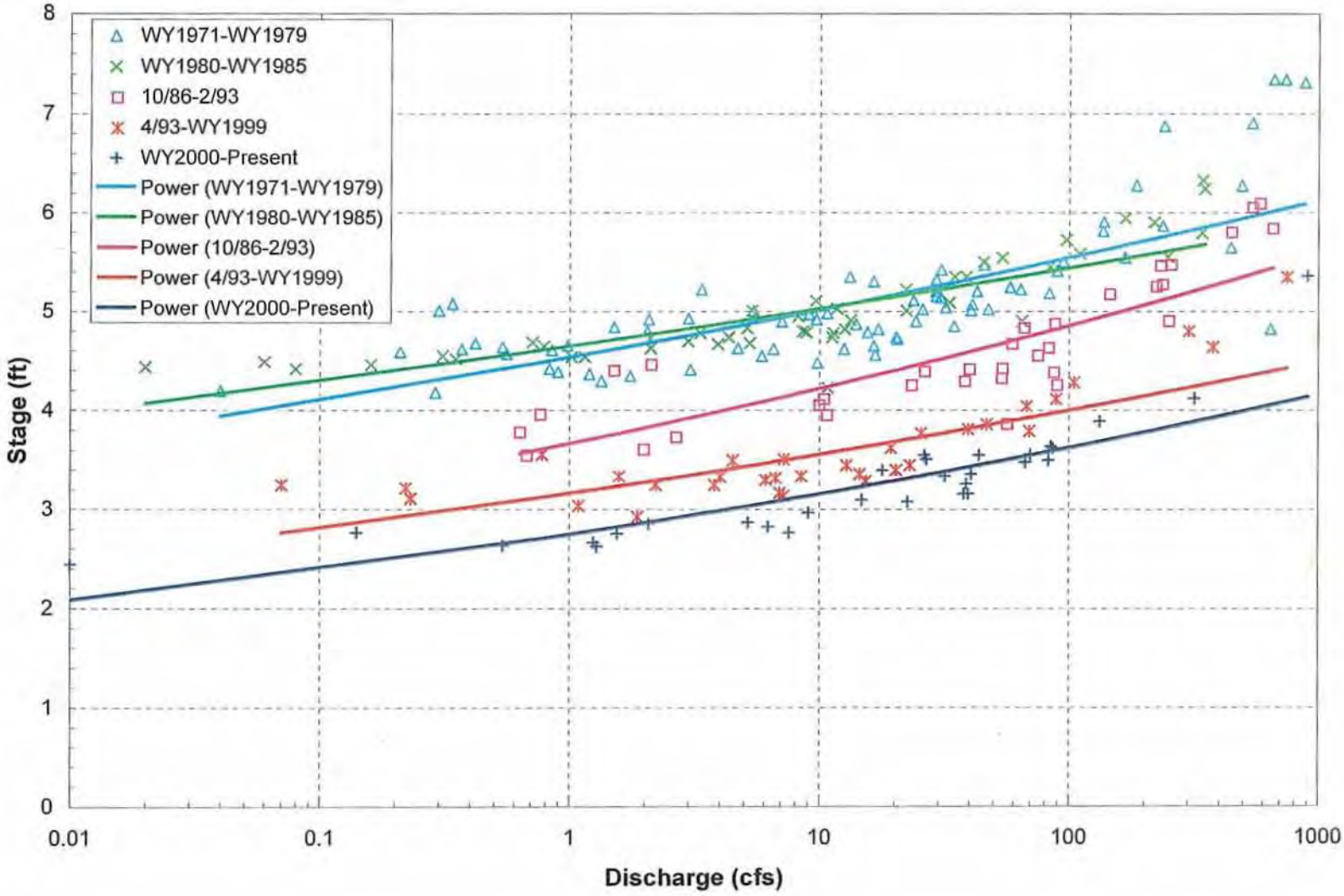

Figure 2.36. Stage-discharge rating curves from 1971 to 2005 for the USGS gage on the North Sulphur River, near Cooper, Texas (USGS Gage No. 07343000).

Gober Chalk (Figure A.4). Shale clasts in the coarse sand to fine gravel range are transported as bed material in dune-like features (**Figure A.47**).

During the two field visits to the NSR and its tributaries a number of bed-material samples were collected (**Figure 2.37**). Field observations indicated that in the upstream areas of the NSR as well as the tributaries, the bed material was predominantly composed of shale clasts (**Figure A.48**). Farther downstream at the Bralley Pool Creek confluence, the bed material contains less shale pieces and more non-shale material as a result of downstream transport, weathering and slaking of the shale clasts (**Figure A.49**). At the FM 904 bridge, the bed material is primarily composed of non-shale clasts (**Figure A.50**).

Samples collected in the NSR and the tributaries were provided to the Kleinfelder soils laboratory in McKinney, Texas. Dry and slaked gradations were developed for each of the samples (Appendix B). Dry (dry-sieved field samples) gradations for the NSR bed-material samples are shown on **Figure 2.38**. The median (D_{50}) sizes of the samples range from 1.7 to 3.7 mm (coarse sand to fine gravel), and the D_{84} sizes range from 4.5 to 13.2 mm (fine to medium gravel). Silt-clay contents (<0.075 mm) are less then 5 percent of the samples. Wet (slaked) gradations for the same bed-material samples are shown on **Figure 2.39**. Median sizes range from <0.075 to 2.0 mm and the D_{84} sizes range from <0.075 to 4.7 mm. Silt-clay contents range from 10 to 90 percent of the samples. Comparison of the dry and wet gradations for sample NSR4 (**Figure 2.40**) demonstrates the effects of slaking on the size distribution of the materials available for transport, and confirms the necessity of taking the transformation of bed material into bed material and wash load into account in any computation of sediment transport. The dry D_{50} is 2.7 mm (fine gravel), the wet D_{50} is 0.7 mm (coarse sand) and the silt-clay content increases from 4 to 45 percent.

Dry- and wet-sieved gradation curves for the tributary samples (Baker, Merrill, and Bralley Pool Creeks) are shown in **Figure 2.41**. Dry-sieved D_{50} values range from 2.5 to 3.7 mm, and wet-sieved values range from <0.075 to 1.5 mm. Silt-clay contents for the dry-sieved samples are about 3 percent, and range from 24 to 66 percent for the wet-sieved samples.

The transformation of the slaked bed material from silt-clay dominated in the upstream reaches to non-shale sand-sized material in the downstream reaches is summarized in **Figure 2.42**. In the upstream reach (NSR2) the silt-clay content is greater than 80 percent. At the Bralley Pool confluence (NSR0), the silt-clay content reduces to about 30 percent, at the FM 904 bridge (NSR8) it is about 12 percent, and at the USGS gage near Cooper (NSR1), it is reduced to about 10 percent. Conversely, the non-shale component varies from less than 20 percent upstream to about 90 percent downstream.

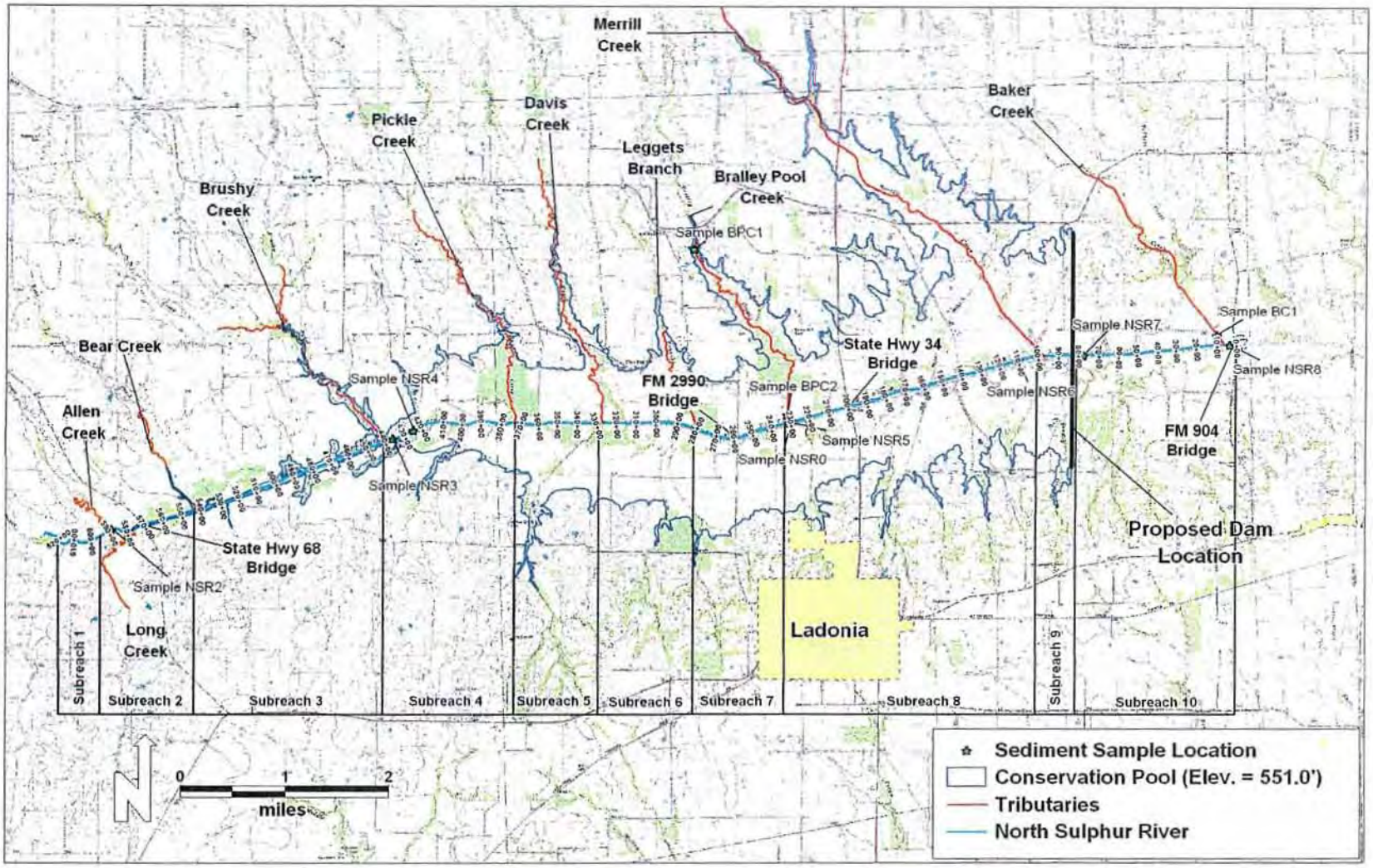

Figure 2.37. Map showing the locations of the bed-material samples in the North Sulphur River and the tributaries.

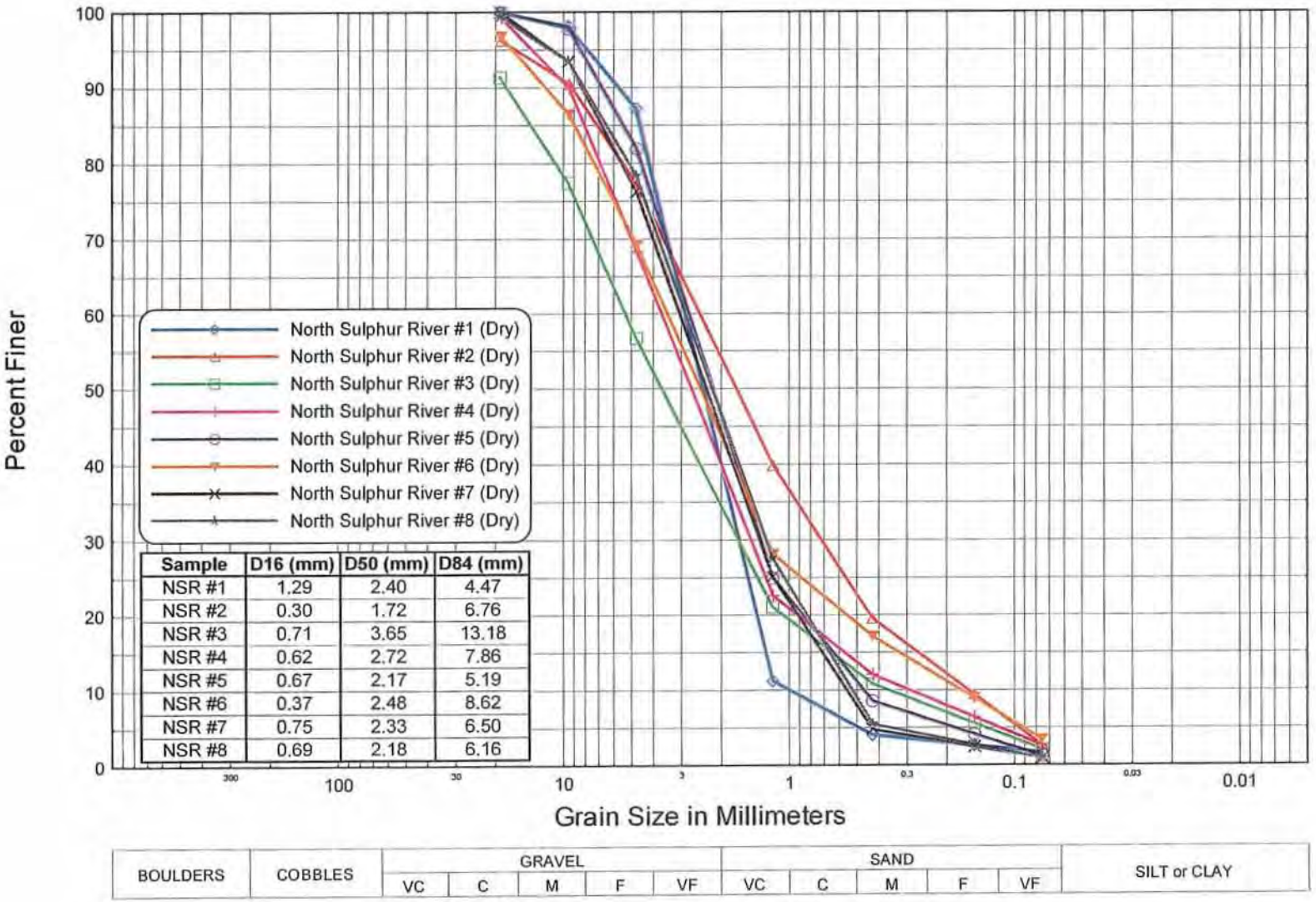

Sample	D16 (mm)	D50 (mm)	D84 (mm)
NSR #1	1.29	2.40	4.47
NSR #2	0.30	1.72	6.76
NSR #3	0.71	3.65	13.18
NSR #4	0.62	2.72	7.86
NSR #5	0.67	2.17	5.19
NSR #6	0.37	2.48	8.62
NSR #7	0.75	2.33	6.50
NSR #8	0.69	2.18	6.16

Figure 2.38. Dry-sieved gradation curves for the bed-material samples collected in the North Sulphur River.

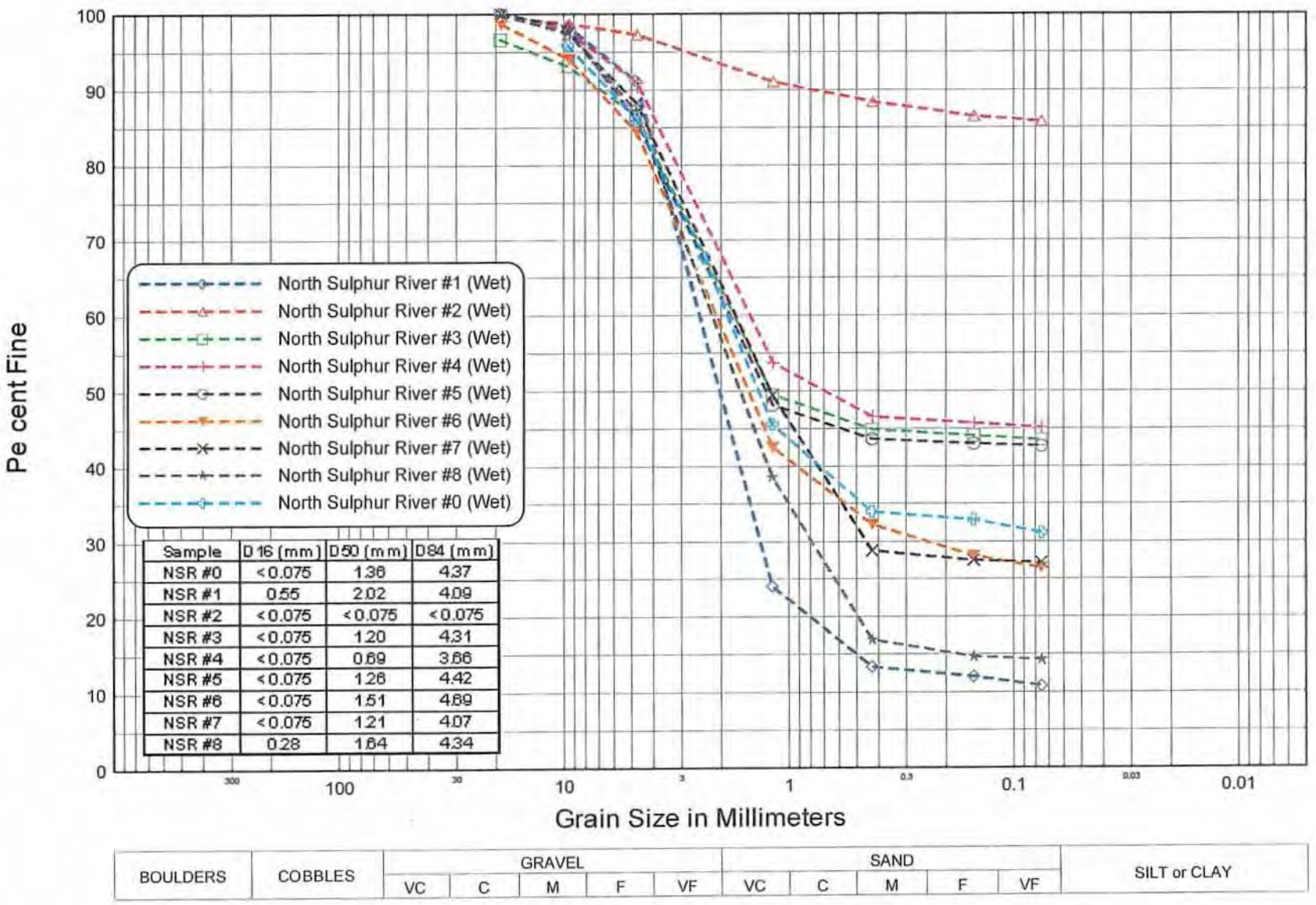

Sample	D16 (mm)	D50 (mm)	D84 (mm)
NSR #0	<0.075	1.36	4.37
NSR #1	0.55	2.02	4.09
NSR #2	<0.075	<0.075	<0.075
NSR #3	<0.075	1.20	4.31
NSR #4	<0.075	0.69	3.66
NSR #5	<0.075	1.26	4.42
NSR #6	<0.075	1.51	4.69
NSR #7	<0.075	1.21	4.07
NSR #8	0.28	1.64	4.34

Figure 2.39. Wet-sieved gradations for the bed-material samples collected in the North Sulphur River.

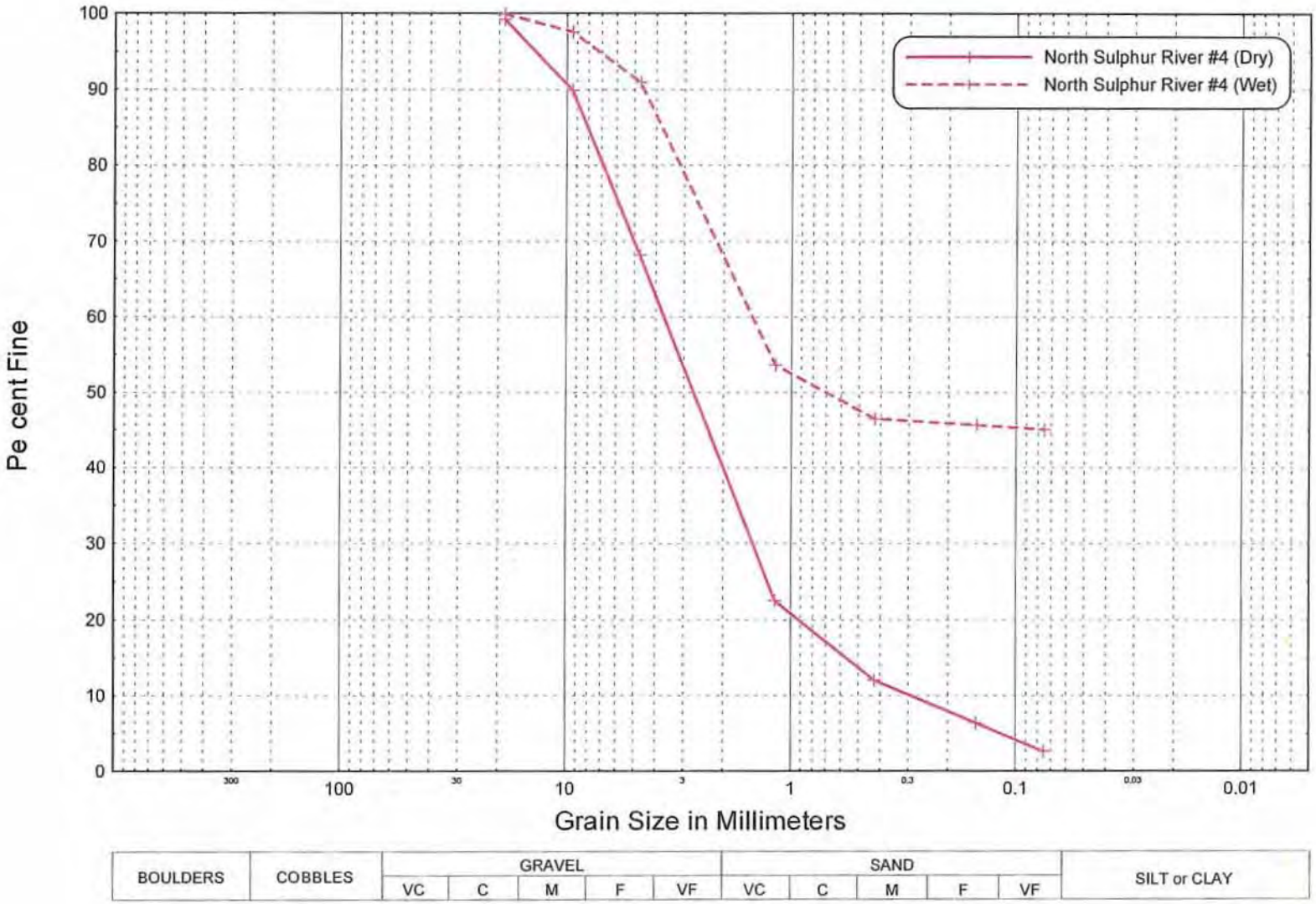

Figure 2.40. Comparison of dry- and wet-sieved gradations for sample NSR4 located about 1,500 feet downstream of the Brushy Creek confluence.

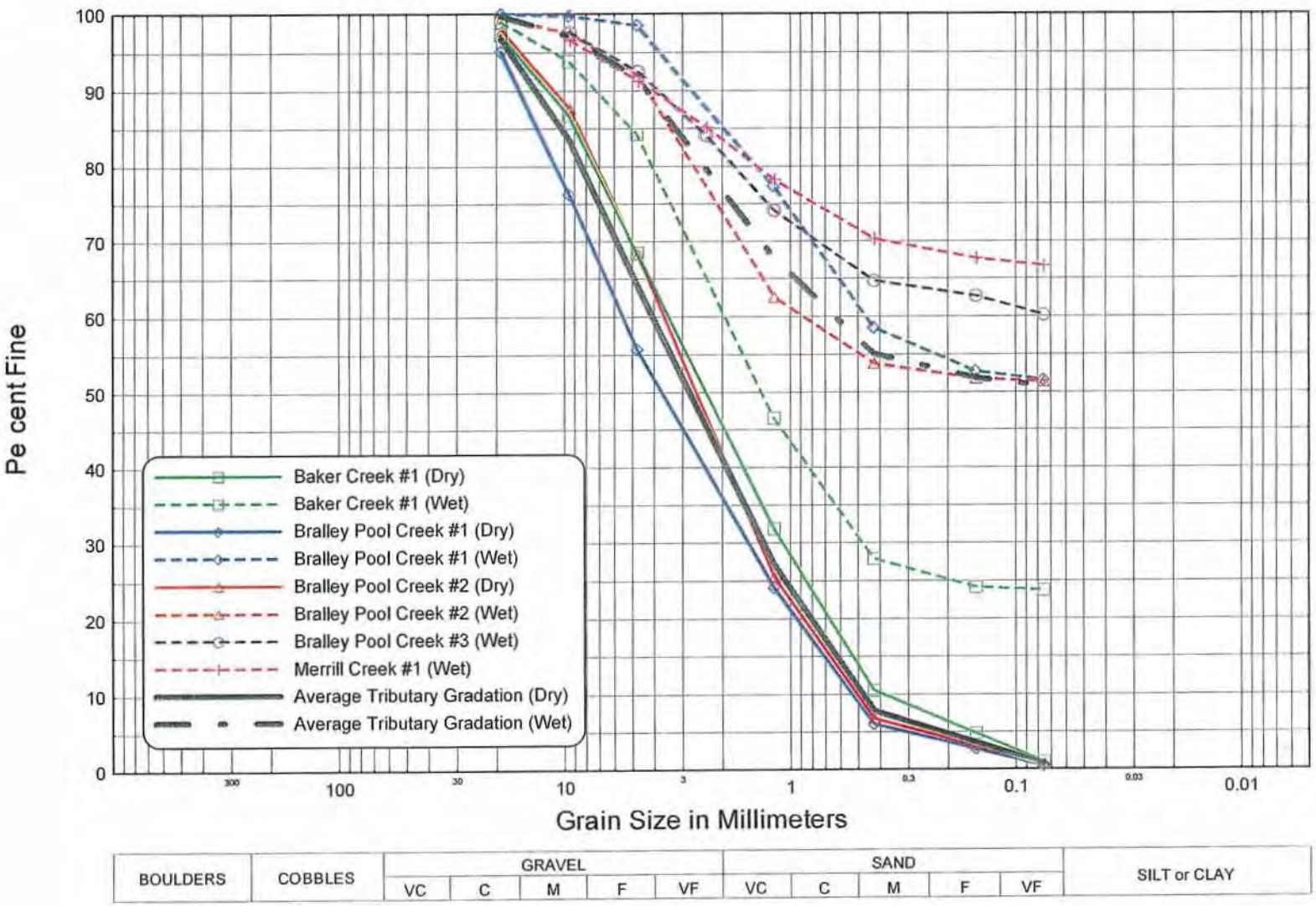

Figure 2.41. Dry- and wet-sieved gradation curves for the tributary samples.

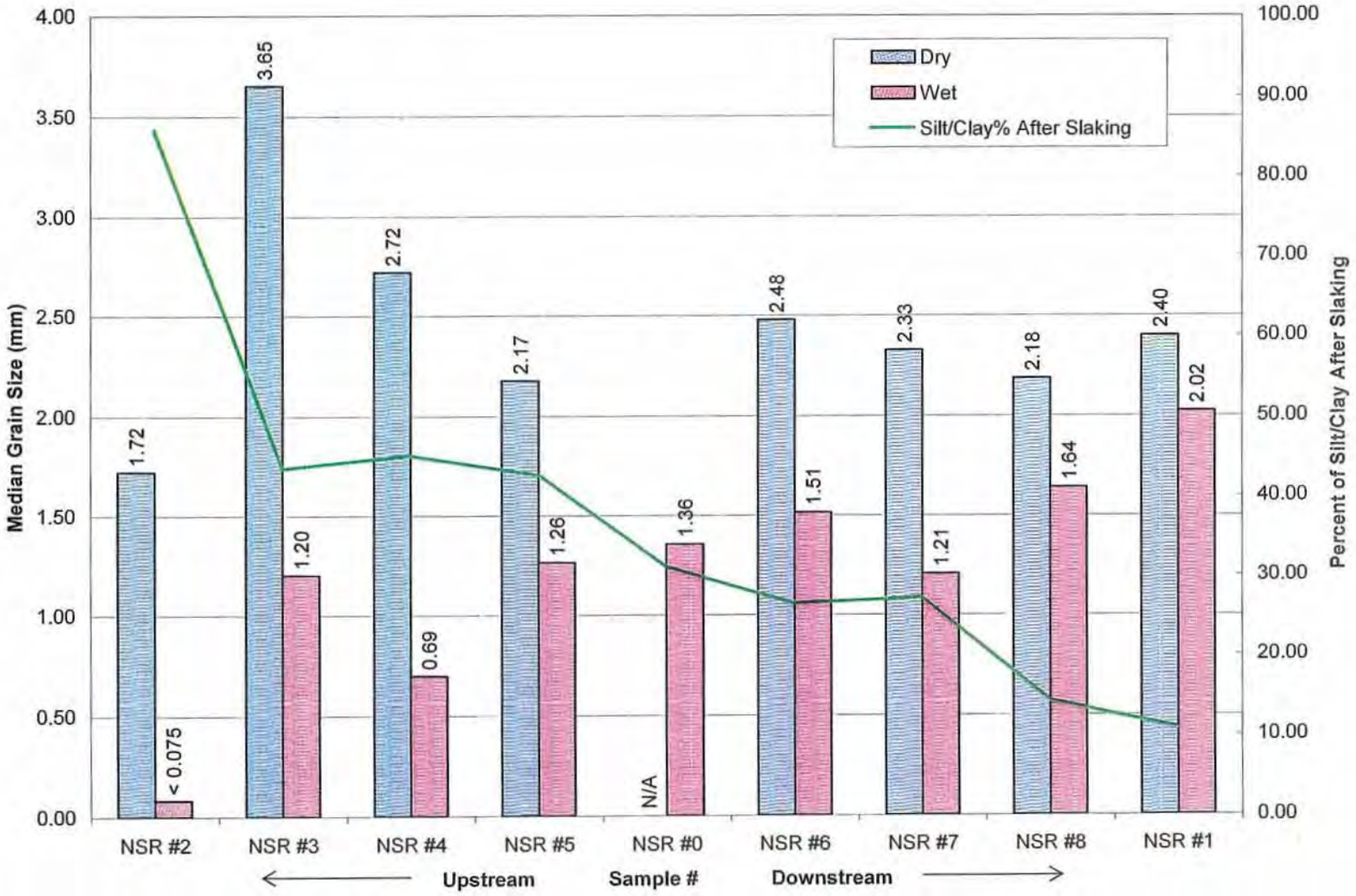

Figure 2.42. Changes in the median sizes of the dry- and wet-sieved bed-material samples of the North Sulphur River as well as the silt-clay content of the samples following slaking arranged from upstream to downstream.

3. HYDROLOGY

An evaluation of the hydrologic data and information in the vicinity of the proposed Lake Ralph Hall project was conducted to evaluate the existing hydrologic conditions in the NSR watershed. The evaluation included a review of the measured flow data, regional regression relationships, and previously-developed hydrologic models (HEC-1; RJ Brandes Co., 2004), development of revised hydrologic models (HEC-1), and an analysis of the peak flood frequencies and flow durations. The results of the hydrologic analysis were used to conduct the hydraulic and sediment-transport analyses.

3.1. USGS Gage near Cooper, Texas

Measured flow data were obtained for the USGS North Sulphur River near Cooper, Texas, gage (USGS Gage No. 07343000), which is located about 19.5 river miles downstream from the proposed dam site and has a drainage area of about 276 square miles. Available data at the gage include mean daily flow and peak flood data that extend from Water Year (WY) 1950 to WY2004. Mean daily flow-duration and peak flood-frequency analyses were performed at the gage to provide a basis of reference for the hydrologic analysis at the proposed dam location.

3.1.1. Annual Flow Volume and Mean Daily Flow-duration Analysis

Annual water volumes were computed for the period of record using the measured mean daily flows (**Figure 3.1**), and indicate that the annual volume ranges from 25,200 to 397,000 ac-ft, with an average volume of about 191,000 ac-ft. The mean daily flow-duration curve (**Figure 3.2**) indicates that the median flow is 12 cfs, that the flow exceeds 1.0 cfs 75 percent of the time, exceeds 316 cfs 10 percent of the time, and exceeds 5,830 cfs about 1 percent of the time.

3.1.2. Peak Flood Frequency Analysis

Measured flood peaks during the gage period of record have ranged from 5,600 cfs in 1996 to 90,600 cfs in 1972 (**Figure 3.3**). Using these flood peaks, a flood-frequency curve was developed using the U.S. Army Corps of Engineers HEC-FFA computer program (USACE, 1992), which is based on the procedures outlined in Water Resource Council (WRC) Bulletin 17B (WRC, 1981) with a generalized skew coefficient of -0.28 (**Figure 3.4**). At the Cooper gage, the computed frequency curve indicates that the 2-year peak flow is about 34,800 cfs, the 10-year peak flow is about 60,700 cfs, and the 100-year peak flow is about 84,100 cfs (**Table 3.1**).

3.1.3. Annual Flow Frequency

Because the NSR is an ephemeral stream, an evaluation of the number of times per year that the river is dry was carried out to assess the effects of wetting and drying on slaking of the shale bed and banks, and the breakdown of the bed material (discussed in Chapter 2). The evaluation was conducted by determining the number of times that a specified flow rate of <1 cfs occurred at the gage each year in the period of record. The results from the analysis indicate that, on average, about six periods occur throughout the year when the flow is less than 1 cfs (Figure 2.3), and, therefore, the bed is essentially dry. Since the location of the proposed dam has a significantly smaller drainage area, it is likely that the very low discharges measured at the gage are representative of conditions within the project reach as well.

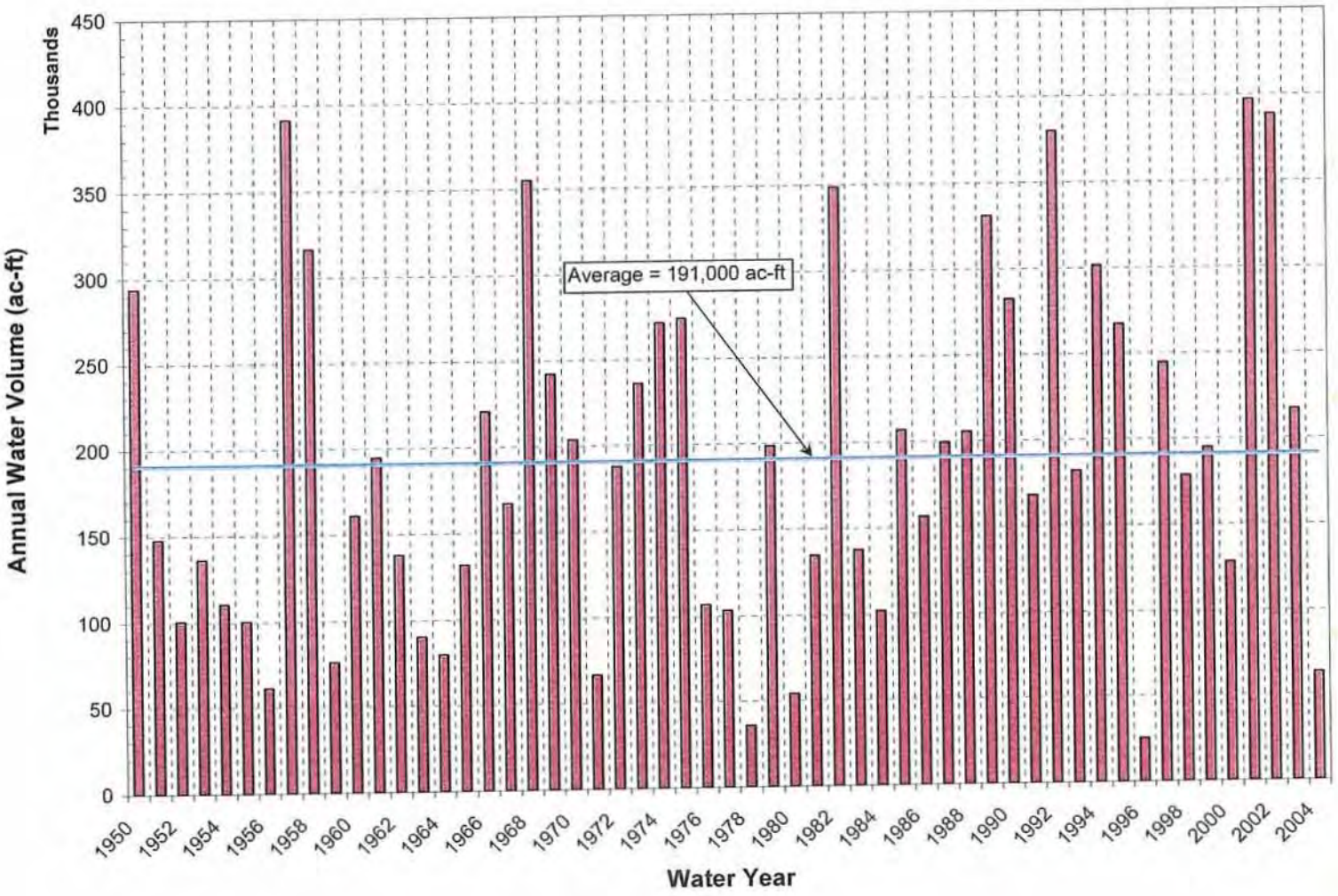

Figure 3.1. Mean annual flow volumes between 1950 and 2004 at the North Sulphur River near Cooper, Texas, gage.

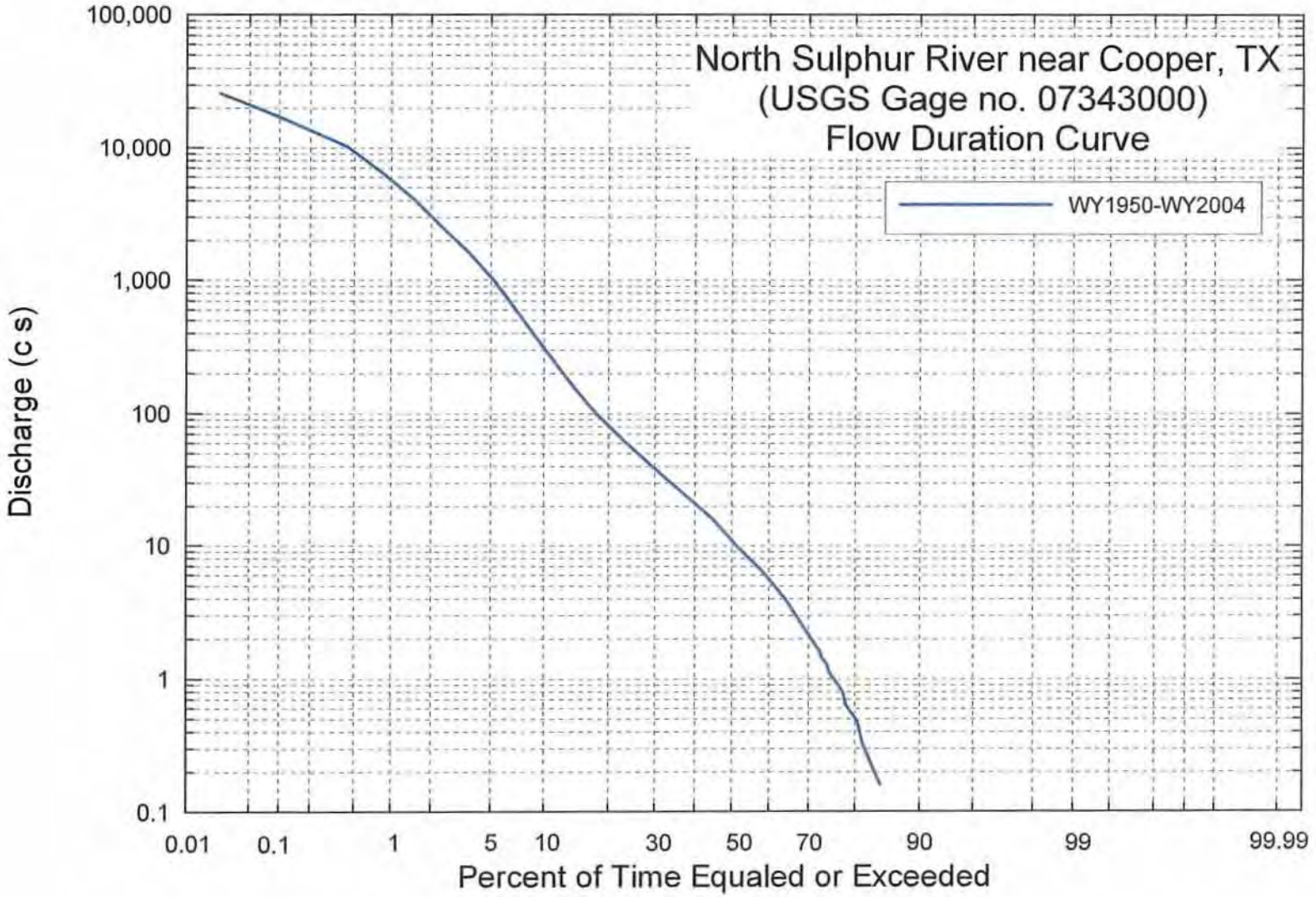

Figure 3.2. Computed flow-duration curve at the North Sulphur River near Cooper, Texas, gage.

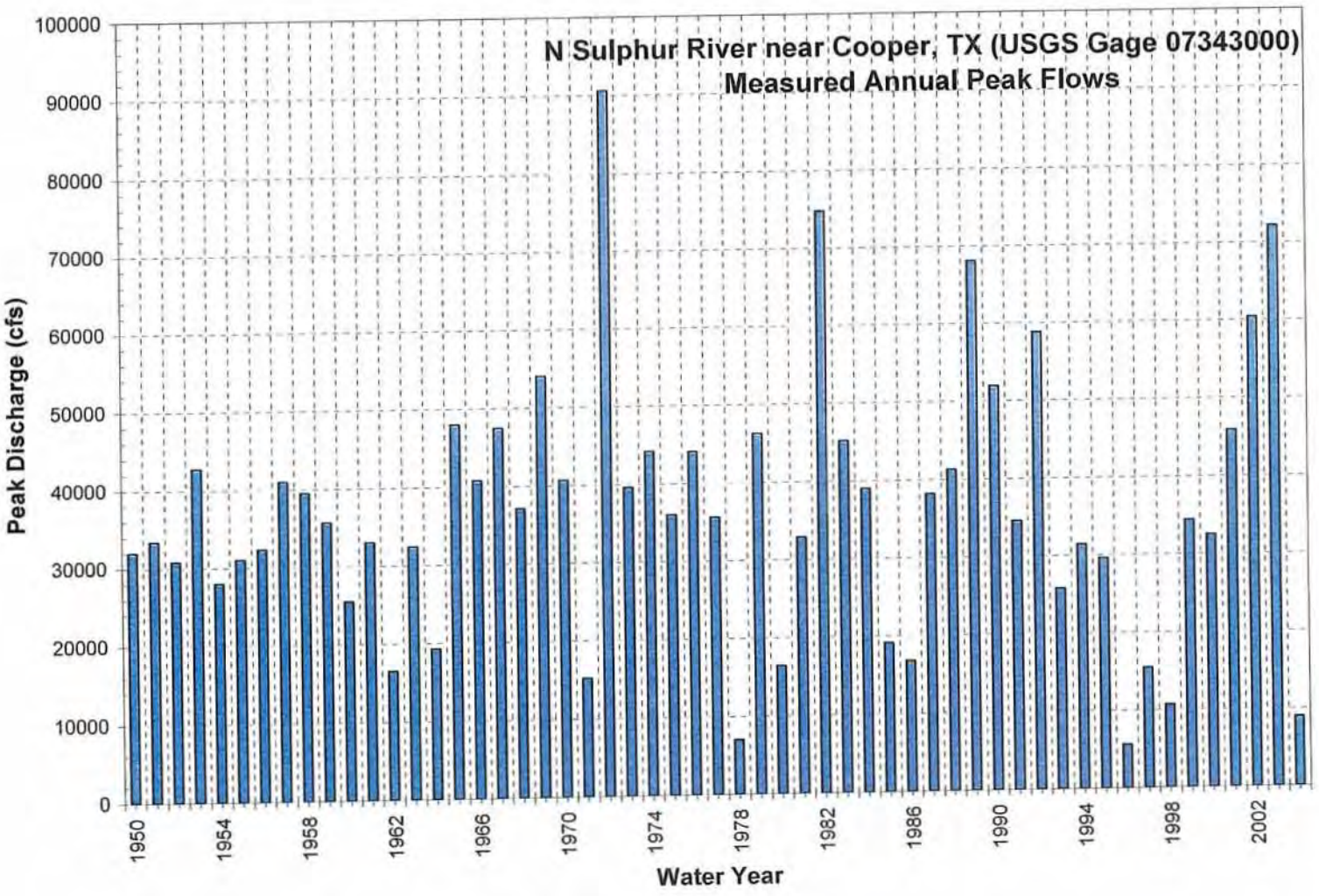

Figure 3.3. Measured annual peak flows (1950-2004) at the North Sulphur River near Cooper, Texas, gage.

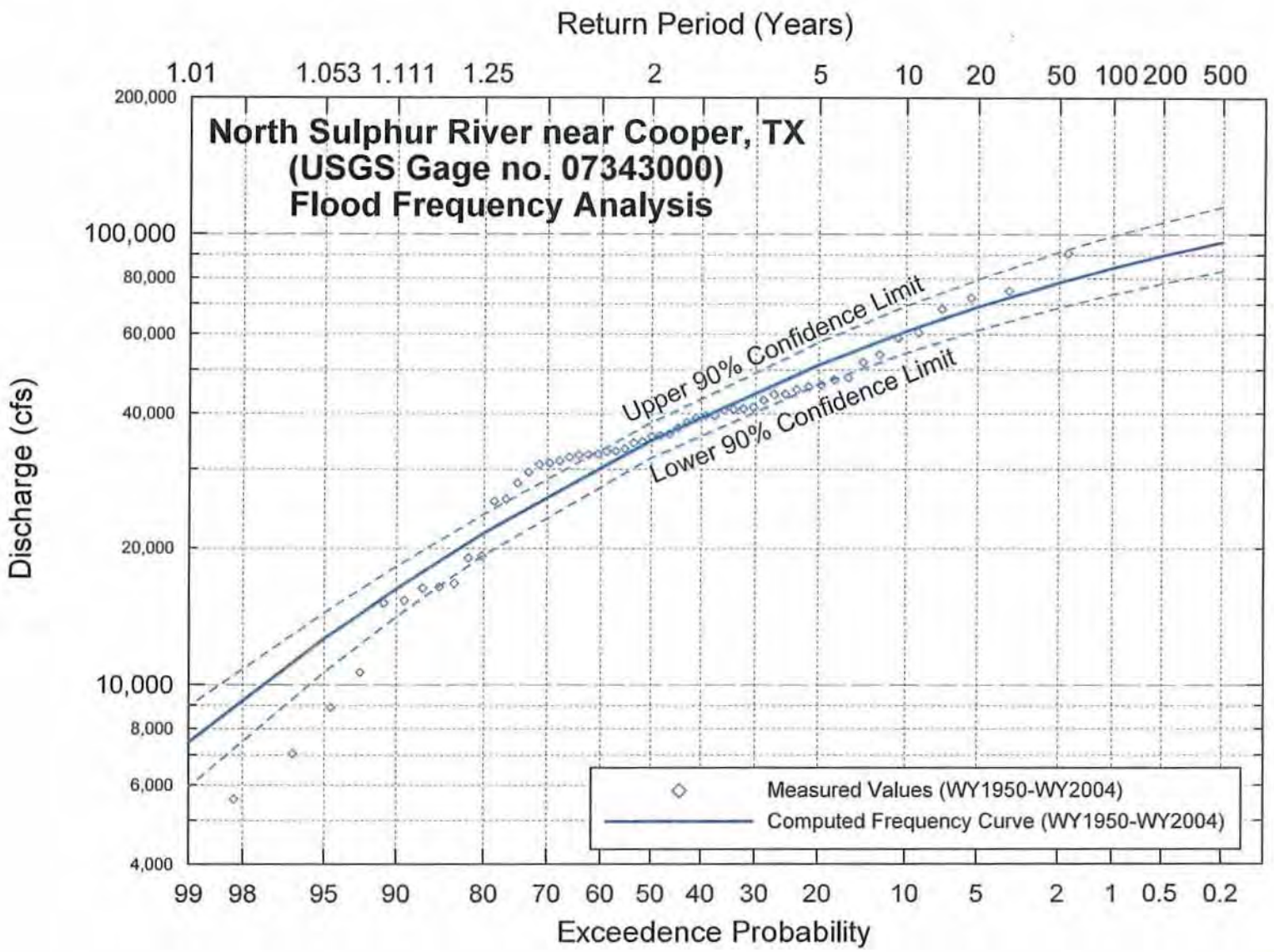

Figure 3.4. Computed peak flow-frequency curve at the North Sulphur River near Cooper, Texas, gage.

Table 3.1. Summary of results from the flood-frequency analysis at the Cooper gage.		
Flow (cfs)	Return Interval (yrs)	Exceedence Percent
21,700	1.25	80
27,300	1.5	66.7
34,800	2	50
51,200	5	20
60,700	10	10
68,800	20	5
78,000	50	2
84,100	100	1

3.2. Hydrology at the Proposed Dam Site

The contributing drainage basin at the proposed dam is about 100 square miles, significantly less than the drainage basin area at the USGS gage. It was, therefore, necessary to evaluate the peak flow frequency and annual flow volumes at the dam location to provide input to the hydraulic model and sediment-transport analysis of annual sediment yield to the dam site.

3.2.1. Regional Regressional Relationships

A series of regional regression equations for estimation of peak streamflow frequency for ungaged natural basins in Texas was developed by Asquith and Slade (1997). The regression equations are based on measured peak flow data (up to 1993) and estimated frequency curves for 559 stations in Texas with natural (unregulated and rural) basins. The State of Texas was subdivided into 11 separate regions, and equations were developed for the 2-, 5-, 10-, 25-, 50-, and 100-year events in each of the regions based on the drainage area, the stream slope, and a basin area shape factor.

The Lake Ralph Hall dam is located in Region 7, and the equations for this region for basins with drainage areas greater than 32 square miles are:

$$Q_2 = 129\ A^{0.578}\ SL^{0.364} \quad (3.1)$$

$$Q_5 = 133\ A^{0.605}\ SL^{.578} \quad (3.2)$$

$$Q_{10} = 178\ A^{0.644}\ SL^{0.699}\ SH^{-0.239} \quad (3.3)$$

$$Q_{25} = 219\ A^{0.651}\ SL^{0.776}\ SH^{-0.267} \quad (3.4)$$

$$Q_{50} = 261\ A^{0.653}\ SL^{0.817}\ SH^{-0.291} \quad (3.5)$$

$$Q_{100} = 313\ A^{0.654}\ SL^{0.849}\ SH^{-0.316} \quad (3.6)$$

where $Q_2, Q_5, Q_{10}, Q_{25}, Q_{50}, Q_{100}$ = the peak flows for the 2-, 5-, 10-, 25-, 50-, and 100-year events,

A = the contributing drainage area in square miles,

SL = the stream slope in feet per mile, and

SH = the basin shape factor (ratio of length of longest stream channel in basin squared to contributing drainage area).

The Cooper gage site is located in Region 10, and the regression equations for basins with drainage areas greater than 32 square miles are given by:

$$Q_2=16.9\ A^{0.798}\ SL^{0.777} \quad (3.7)$$

$$Q_5=33.0\ A^{0.790}\ SL^{.795} \quad (3.8)$$

$$Q_{10}=51.3\ A^{0.775}\ SL^{0.785} \quad (3.9)$$

$$Q_{25}=87.9A^{0.752}\ SL^{0.760} \quad (3.10$$

$$Q_{50}=129A^{0.733}\ SL^{0.735} \quad (3.11)$$

$$Q_{100}=187\ A^{0.713}\ SL^{0.708} \quad (3.12)$$

Using the Region 10 equations and the measured area, slope, and basin shape factors for the contributing basin to the USGS gage results in significant underestimation of peak values (**Figure 3.5**), and the regression equations were therefore not used to estimate the peak flow values at the Lake Ralph Hall dam site. The reason for the underestimation of peak flows using the regression equations is not clear, but could be a result of local climate and soil conditions (Harmel et al., 2006), and the incised nature of the channels that affect the time of concentration and thus increase the flood peaks.

3.2.2. Hydrologic (HEC-1) Models

3.2.2.1. RJ Brandes Company Model

The magnitude and duration of flood flows of various recurrence intervals in the vicinity of the proposed dam were previously evaluated by RJ Brandes Company (RJ Brandes Co., 2004) to design the dam and spillway. The evaluation was carried out using the Corps of Engineers HEC-1 computer software (USACE, 1990). HEC-1 simulates the surface runoff response of a river basin to precipitation by representing the basin as a system of interconnected hydrologic and hydraulic components. The precipitation-runoff response of the watershed is simulated by performing mathematical computations for four hydrologic and hydraulic processes:

a) Precipitation
b) Infiltration/interception
c) Transformation of precipitation excess to subbasin outflow
d) Hydrograph routing

The RJ Brandes Co. model for existing conditions used three subwatersheds and two connecting stream channels for the 100-square-mile basin that contributes runoff to the proposed dam location. Precipitation input was based on the 24-hour rainfall duration as prescribed in the U.S. Weather Bureau's Technical Paper Number 40 (Hershfield, 1961). As described in the Brandes report (RJ Brandes Co., 2004), no area reduction factor was applied to the precipitation depths, which likely results in higher than actual rainfall intensities, and therefore, the model results would be expected to be conservatively high. The infiltration (movement of water into the soil) and interception (surface storage in topographic depressions and vegetation) of the precipitation were simulated using Soil Conservation Service (SCS, U.S. Department of Agriculture) curve numbers, which are empirical parameters that describe the

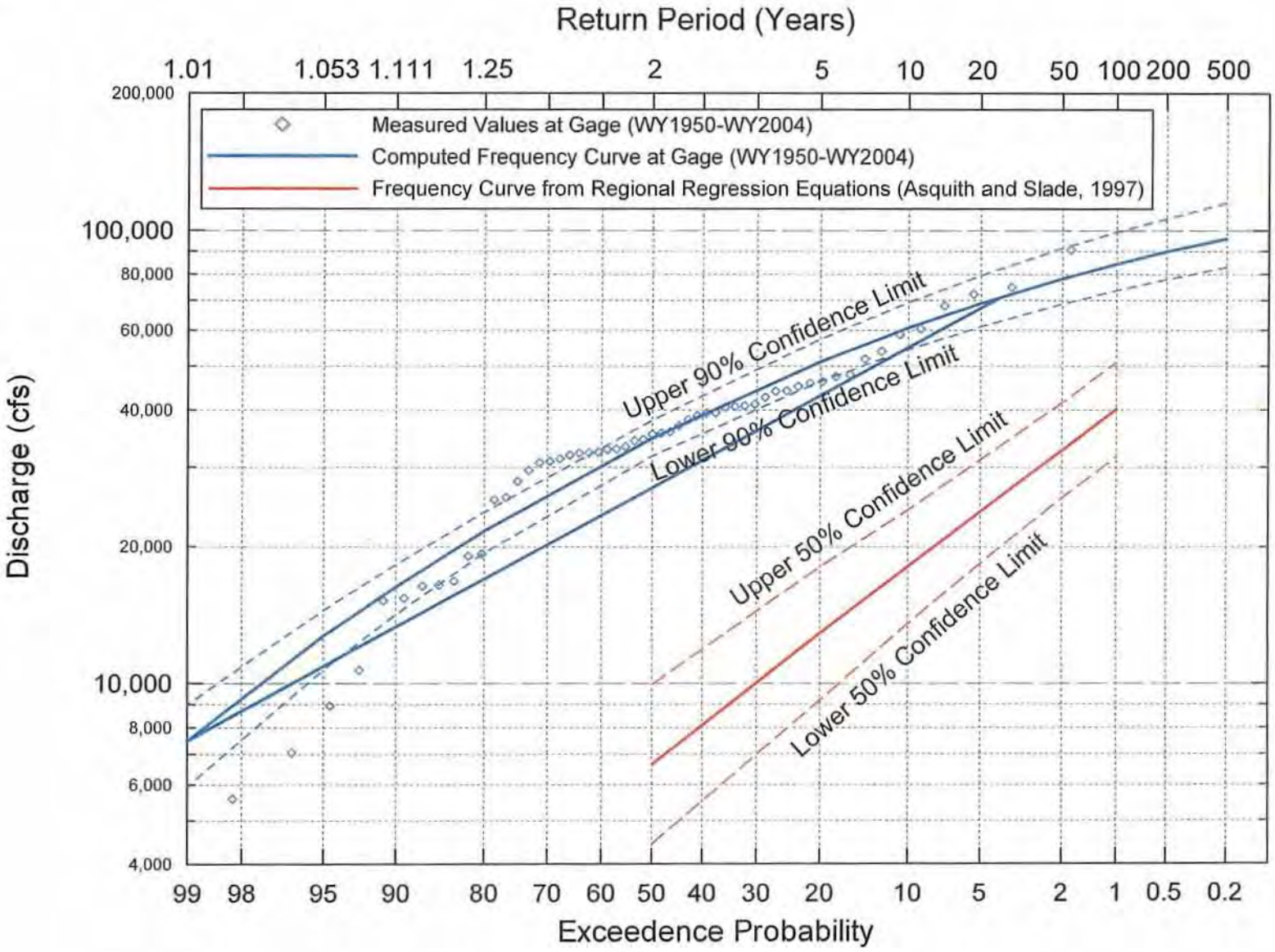

Figure 3.5. Computed frequency curves at the Cooper gage using the measured peak flow values (HEC-FFA) and using the regional regression equations for Region 10 (Asquith and Slade, 1997).

drainage characteristics of soil based on typical soil cover, land-use and antecedent runoff conditions (ARC). A curve number of 70 was assigned to each of the three subbasins in this model based on normal antecedent runoff conditions and soil types and conditions throughout the watershed. The Snyder unit hydrograph method was used to transform the excess rainfall (i.e., precipitation remaining after infiltration and interception) to subbasin flow. The lag time (the time between the center of mass of rainfall excess and the peak of the unit hydrograph at the point of interest) was developed using procedures outlined in SCS Technical Release 55 (NRCS, 1986), and ranged from 1.14 to 3.44 for the three subbasins, while a Snyder peaking coefficient of 0.55 was used for the entire watershed, consistent with Corps of Engineers studies for nearby lakes located in the Sulphur River Basin (Lakes Jim Chapman and Wright Patman) (RJ Brandes Co., 2004). The computed subbasin hydrographs were routed through the connections and main channels using the Modified Puls method using a volume-discharge rating curve that was based on results from a one-dimensional (1-D) hydraulic step-backwater model.

The Brandes model indicates that the peak of the 100-year event at the location of the proposed dam under existing conditions is about 36,300 cfs. A modified model was developed for with-dam conditions that included a fourth subbasin that represented the reservoir surface area and modified basin parameters to account for the effects of the reservoir. The model indicated that the 100-year peak flow would increase to about 46,200 cfs due to the increased flow that result from rainfall falling directly onto the reservoir.

3.2.3. Modified HEC-1 Models for Contributing Watershed to Proposed Dam Site

Since the RJ Brandes Co. HEC-1 model was developed primarily to evaluate the 100-year event and the Probable Maximum Storm (PMS) to design the dam and spillways, a separate series of models were developed for this study for the more frequent storms. Precipitation input to the models was based on the 24-hour duration rainfall depths for the 2- through 100-year events (Hershfield, 1961). Consistent with the RJ Brandes Co. model, no area reduction factor was applied to the precipitation-duration input with the expectation that the models will predict conservatively high results. Except for the SCS curve numbers, all input and basin parameters used in the Brandes models were adopted for the additional models. To determine the appropriate SCS curve numbers, an evaluation of the antecedent runoff conditions was carried out using daily precipitation data from the National Weather Surface (NWS, National Oceanic and Atmospheric Administration) weather station gage at Honey Grove, Texas (Figure 1.1). Assessment of the number of days with heavy rainfall (i.e., greater than 0.1 inches) that precede the measured peak at the USGS gage (**Figure 3.6**) indicates that heavy rainfall typically occurs for about two days prior to the flood peak, which suggests that wet antecedent runoff conditions should be considered in the rainfall-runoff calculations for the more frequent events. The assessment also indicated a slight trend toward more normal antecedent runoff conditions for the less frequent events. Selected curve numbers for the revised models, therefore, ranged from 85 for the 2-year event to 72 for the 100-year event.

The frequency curve that was developed from the computed peaks at the proposed dam location (**Figure 3.7**) is generally parallel to the computed frequency curve at the USGS gage near Cooper, Texas, and is similar to the curve that is based on the unit discharge (discharge per unit area of basin) at the dam location using an area exponent of 0.8. (An area exponent of 0.8 was selected based on previous experience with rivers in the Southwest.) A summary of the computed peak flows at the location of the dam is provided in **Table 3.2**. The frequency curves that were developed using the regional regression equations and from the HEC-1 models with normal antecedent runoff conditions significantly underpredict the peak discharges, especially at the more frequent events.

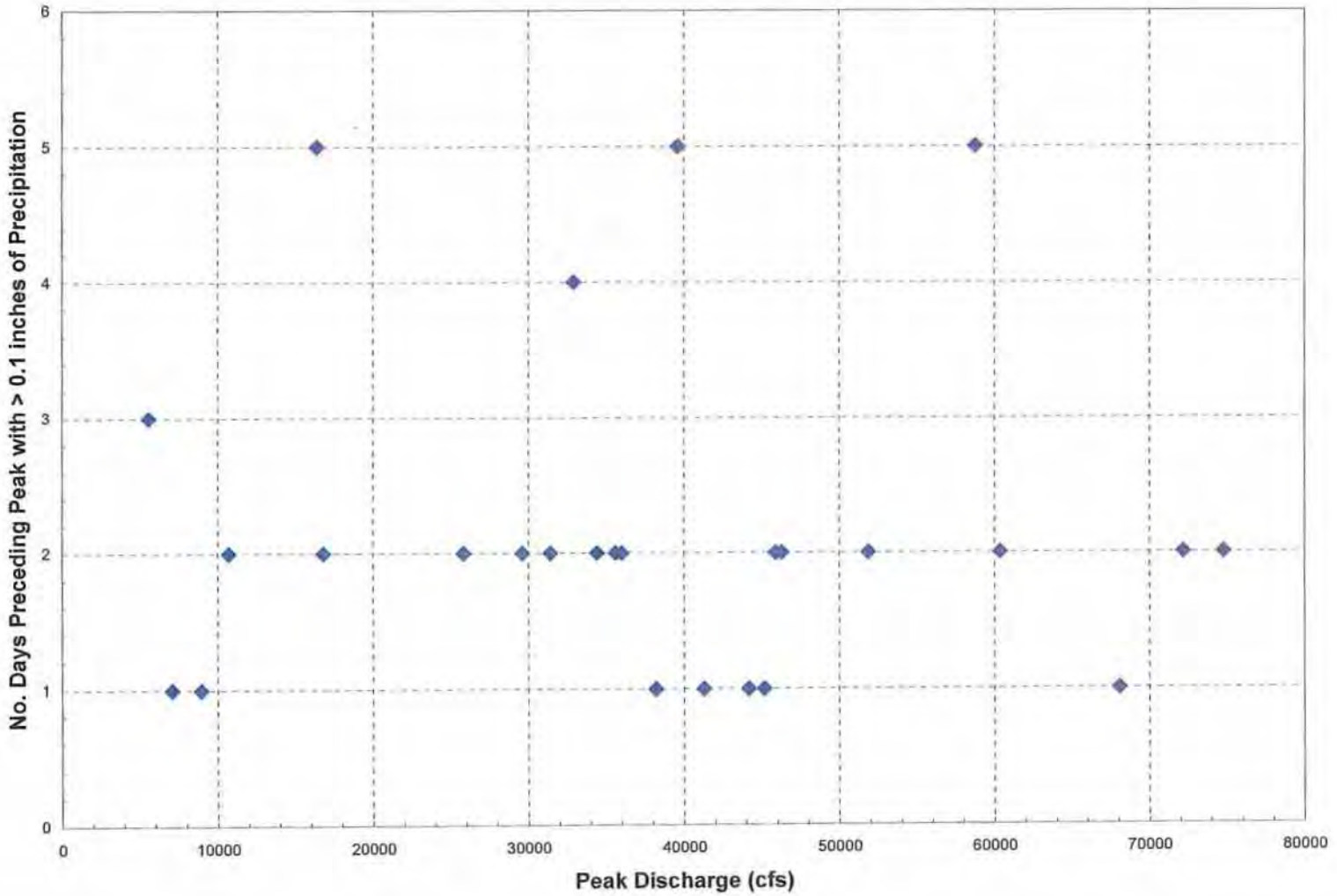

Figure 3.6. Number of days preceding measured peak discharges at the USGS gage near Cooper with rainfall exceeding 0.1 inches at the Honey Grove weather station.

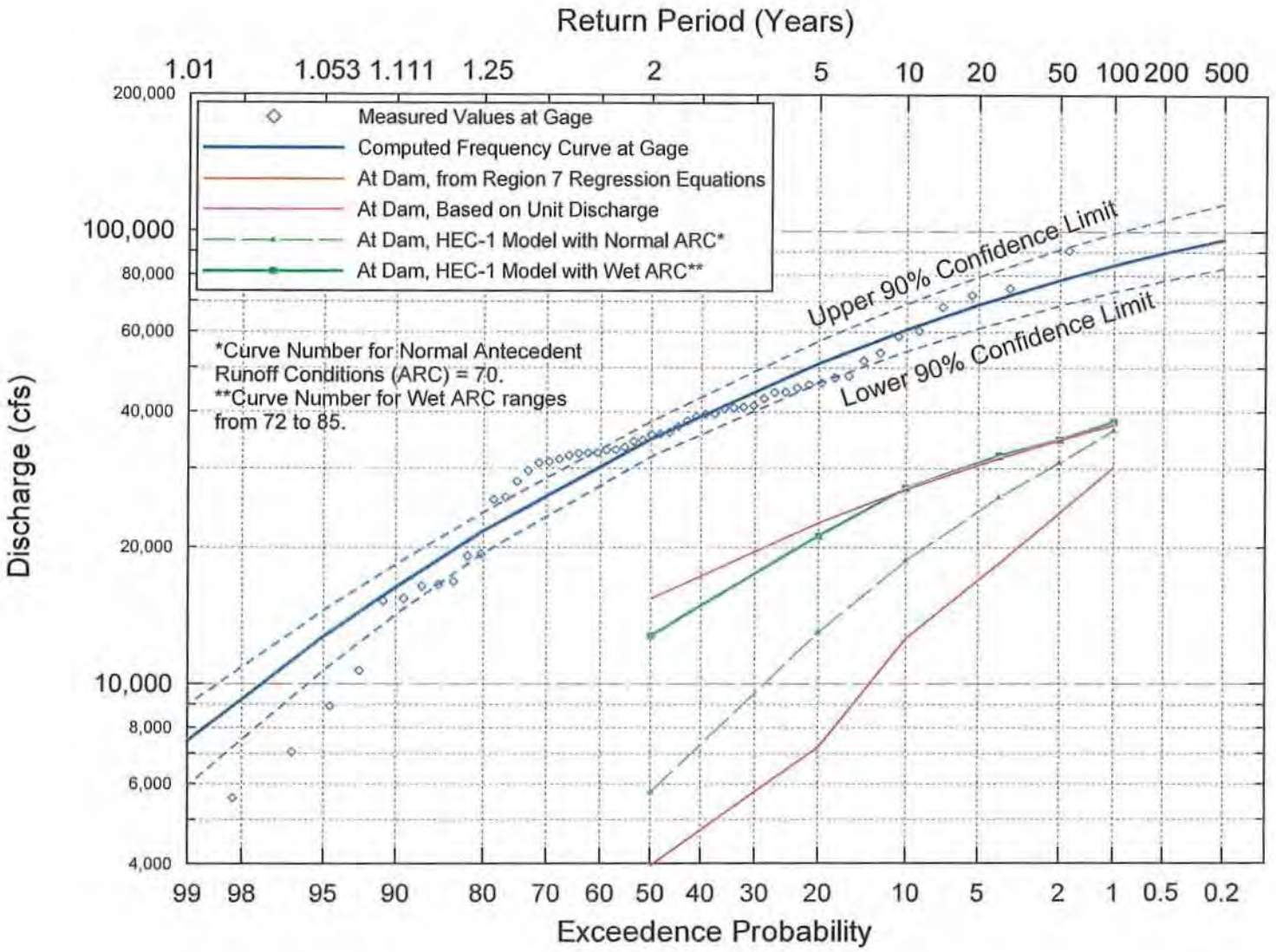

Figure 3.7. Flood-frequency curves based on the computed peak discharges from the MEI HEC-1 models (using wet antecedent runoff conditions), from the HEC-1 models using normal antecedent runoff conditions, from the regional regression equations, and based on the unit discharge at the Cooper gage location. Also shown is the computed frequency curve at the USGS gage near Cooper, Texas.

Table 3.2. Summary of computed peak flows at the proposed dam from the HEC-1 model with wet antecedent runoff conditions (ARC).		
Flow (cfs)	Return Interval (yrs)	Exceedence Percent
12,700	2	50
21,100	5	20
27,000	10	10
31,900	25	4
34,600	50	2
37,900	100	1

3.2.4. HEC-1 Models for Tributary Basins

HEC-1 models were developed for each of the nine larger tributaries located upstream of the dam. These include Merrill Creek, Bralley Pool Creek, Leggets Branch, Davis Creek, Pickle Creek. Brushy Creek, Bear Creek, Long Creek, and Allen Creek. An additional model was developed for Baker Creek to evaluate a representative tributary below the proposed dam site. A model for Pot Creek (tributary to Brushy Creek) was developed to complete the Brushy Creek model. Basin areas were computed using a USGS Digital Elevation Model (DEM), (September 2001), and included up to seven subbasins for the overall tributary basins (**Figure 3.8**). (Basin parameters are summarized in Table 5.1.) Precipitation input and the SCS curve numbers for wet antecedent runoff conditions that were developed for the overall basin were applied to the tributary models. The lag time was developed using procedures outlined in SCS Technical Release 55 (NRCS, 1986) and information from the hydraulic models that were developed for each of the tributaries (Chapter 4). Computed lag times ranged from 0.84 hours in the smallest subbasin to 2.5 hours in the largest subbasin. Consistent with the overall reservoir model, a Snyder peaking coefficient of 0.55 was used for the each of the subbasins, and the computed subbasin hydrographs were routed through the connections and main channels using the Modified Puls method with a volume-discharge rating curve that was developed from the hydraulic models (Chapter 4).

Because the primary tributaries do not include all of the subbasins that contribute water and sediment to the proposed dam location (Figure 3.8), data from the tributary models were used to develop regression equations that relate peak discharge or storm runoff volume to contributing drainage area (**Figures 3.9 and 3.10**). The regression equations are believed to adequately relate peak flow and runoff volume to drainage area because the square of the Pearson product moment correlation coefficient (R^2 value) ranges from 0.97 to 0.98 for the peak flow equations, and range from 0.99 to nearly 1.00 for the storage volume equations. The regression equations were used to estimate the peak flow and runoff volume from the tributary basins that were not specifically modeled under existing conditions, and for all of the tributaries under with-dam conditions.

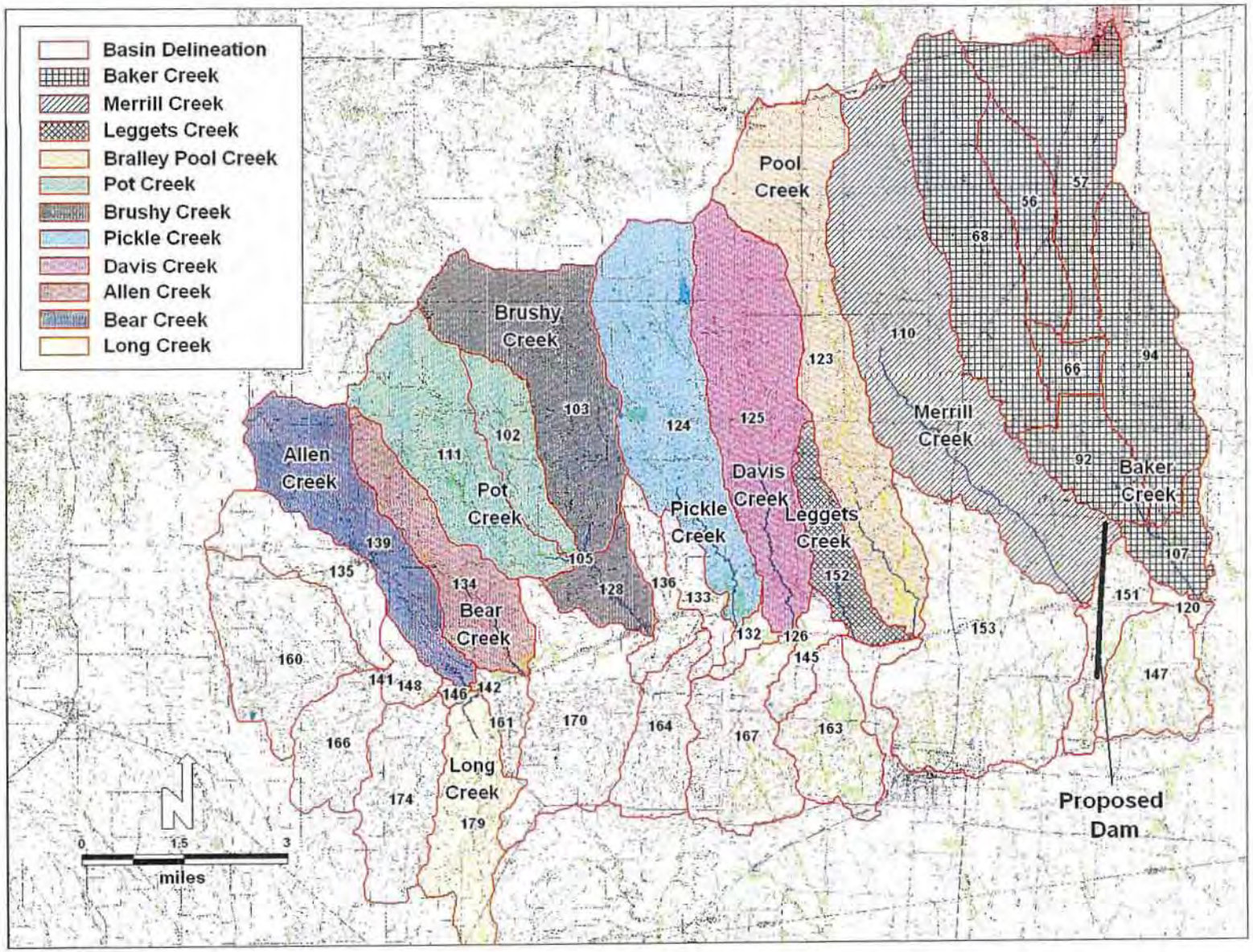

Figure 3.8. Delineated subbasins for the contributing watershed to the proposed Lake Ralph Hall dam site near Ladonia, Texas, and the primary tributary basins that were modeled using HEC-1.

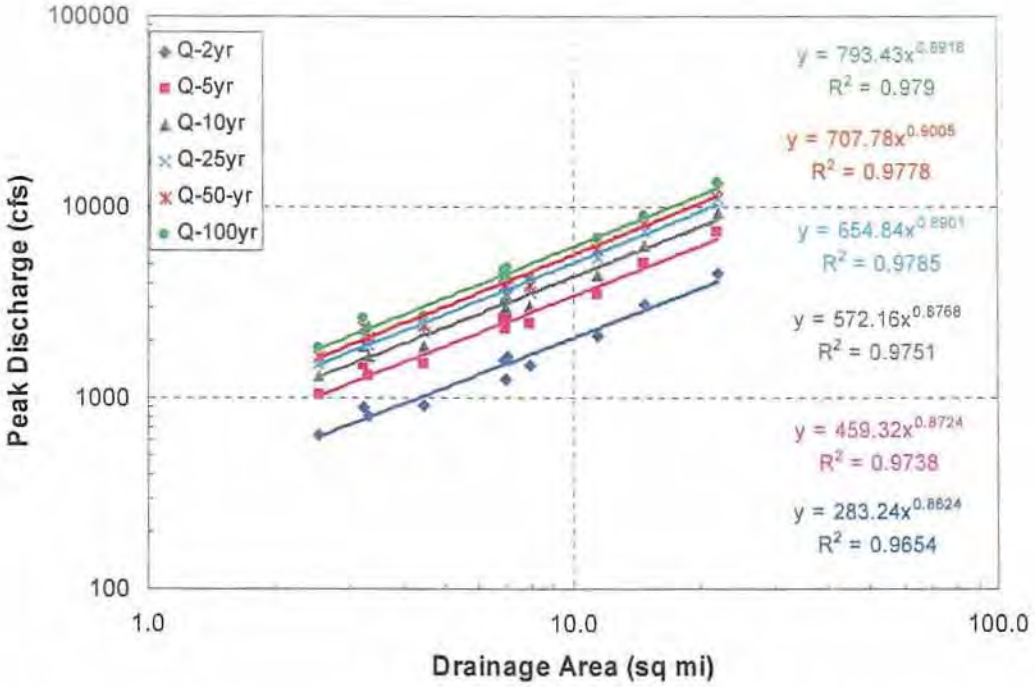

Figure 3.9. Computed peak discharges from the HEC-1 models for the primary tributaries as a function of contributing drainage area, and the resulting regression equations.

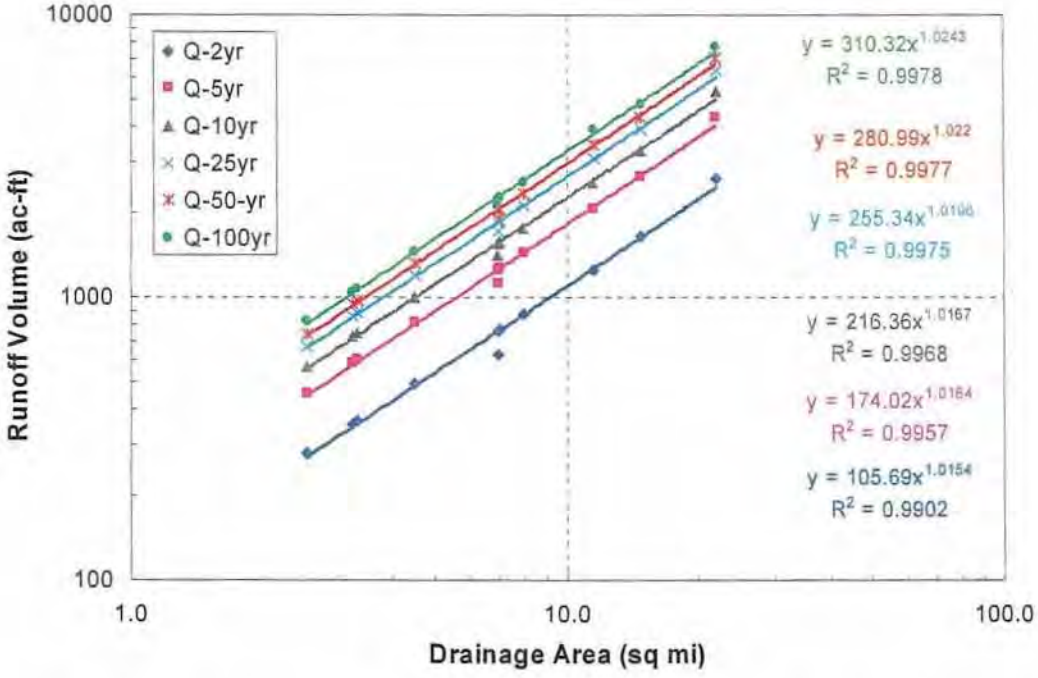

Figure 3.10. Computed storm volumes from the HEC-1 models for the primary tributaries as a function of contributing drainage area, and the resulting regression equations.

3.2.5. With-Dam Downstream Impacts

The effects of the proposed Ralph Hall Dam on downstream flows in the North Sulphur River will likely be significant due to the detention storage capacity available in the reservoir. Based on previous work (RJ Brandes Company, 2004), the 100-year peak discharge in the river below the dam will be reduced from about 38,000 cfs (Figure 3.7) to less than 10,000 cfs, with corresponding reductions in average velocities in the river channel from about 6 feet per second (fps) down to about 4 fps. The more frequent flood events also will be significantly reduced in terms of their peak discharge since runoff volumes for these lesser magnitude storms will be considerably less and subject to greater attenuation in the reservoir. When the reservoir is below its conservation storage capacity, inflows to the reservoir from smaller storms are likely to be entirely contained and stored, with no outflows passed downstream. The floodwater detention storage capabilities of the reservoir should result in significantly less erosion of the downstream channel below the dam.

Provisions are being incorporated into the operating plan for the reservoir to provide for the passage of sufficient low flows to maintain a proposed wetlands restoration project along approximately 14,000 feet of an abandoned segment of the original river channel within the southern floodplain of the river. Excess flows from this segment will be discharged back into the existing river channel approximately three miles below the dam; however, these flows are expected to be minimal. Because of the ephemeral natural of the existing river downstream of the proposed dam site, only very limited aquatic biological resources and habitat exist along the river channel, thus there is no great necessity for the passing substantial flows through the reservoir for environmental purposes.

4. HYDRAULICS

Hydraulic models were developed to quantify the hydraulic conditions (i.e., velocity, depth, water-surface elevation) within the project reach of the NSR and major tributaries over a range of flows up to and including the 100-year peak flow. The analysis was conducted using the U.S. Army Corps of Engineers 1-D HEC-RAS step-backwater program, Version 3.1.3 (USACE, 2005). A single model was developed for the mainstem NSR, and separate models were developed for each of the primary tributaries.

4.1. Hydraulic Model for the North Sulphur River

The HEC-RAS model for the mainstem NSR extends upstream from about 100 feet below the FM 904 bridge for a distance of about 11.8 miles to about 1 mile above SH 68, and includes 101 cross sections at an average spacing of 620 feet. The model geometry was based on cross sections that were cut from the Digital Terrain Model (DTM) of the project reach that was developed by CP&Y using aerial photography from February 2002. The cross sections were placed at representative locations along the channel, or at locations where hydraulic controls (i.e., bridges or other constrictions), extended across the entire main channel. HEC-RAS accounts for energy losses that result from roughness along the channel bed and banks with a roughness coefficient, or Manning's *n*-value. A vertical variation in *n*-values was used to account for the reduced roughness at higher flow depths that are typical in large channels such as the NSR. On the basis of field observations and previous experience with similar incised channels, the selected roughness values ranged from 0.040 at very low flows to about 0.022 at the 100-year peak flow in the main channel, and ranged from 0.048 to 0.070 in the overbanks. For the NSR model, the overbanks are defined as the region outside of the bank stations, which are established at the change in roughness that occurs at the boundary between the edge of vegetation and the exposed channel bed, and therefore do not typically coincide with the topographic top-of-bank. A normal-depth downstream boundary condition with a slope of 0.2 percent was used in the model based on the existing slope of the channel bed at the downstream limit of the model. All bridges were coded into the model using the most recent bridge design plans.

The model was run over a range of flows from 20 cfs (at downstream limit of model) to the 100-year event, with a flow distribution based on the MEI HEC-1 model (using wet antecedent runoff conditions) for mainstem flows at the dam and the unit discharge (discharge per unit drainage area) to estimate contribution from major tributaries since the individual tributary peak flows are likely not coincident with the mainstem peak flows.

4.1.1. Model Calibration

The model was calibrated to high-water marks that were identified and measured during the December 2005, field visit. Since the measured peak flows in 2004 and 2005 were relatively small (less than 8,950 cfs), and the measured high-water marks were between 9 and 13 feet above the channel bed, it was assumed that the field-observed high-water marks were associated with the 2002 and 2003 annual peaks. The 2002 and 2003 measured peak flows at the USGS Cooper gage were 60,400 and 72,200 cfs (corresponding to the 10- and 25-year peak flows, Figure 3.6), respectively, and were adjusted to flows at the dam and throughout the model reach based on the computed unit discharge. Using the roughness values and boundary conditions described above, the model calibrates well with the measured high-water marks (**Figure 4.1**).

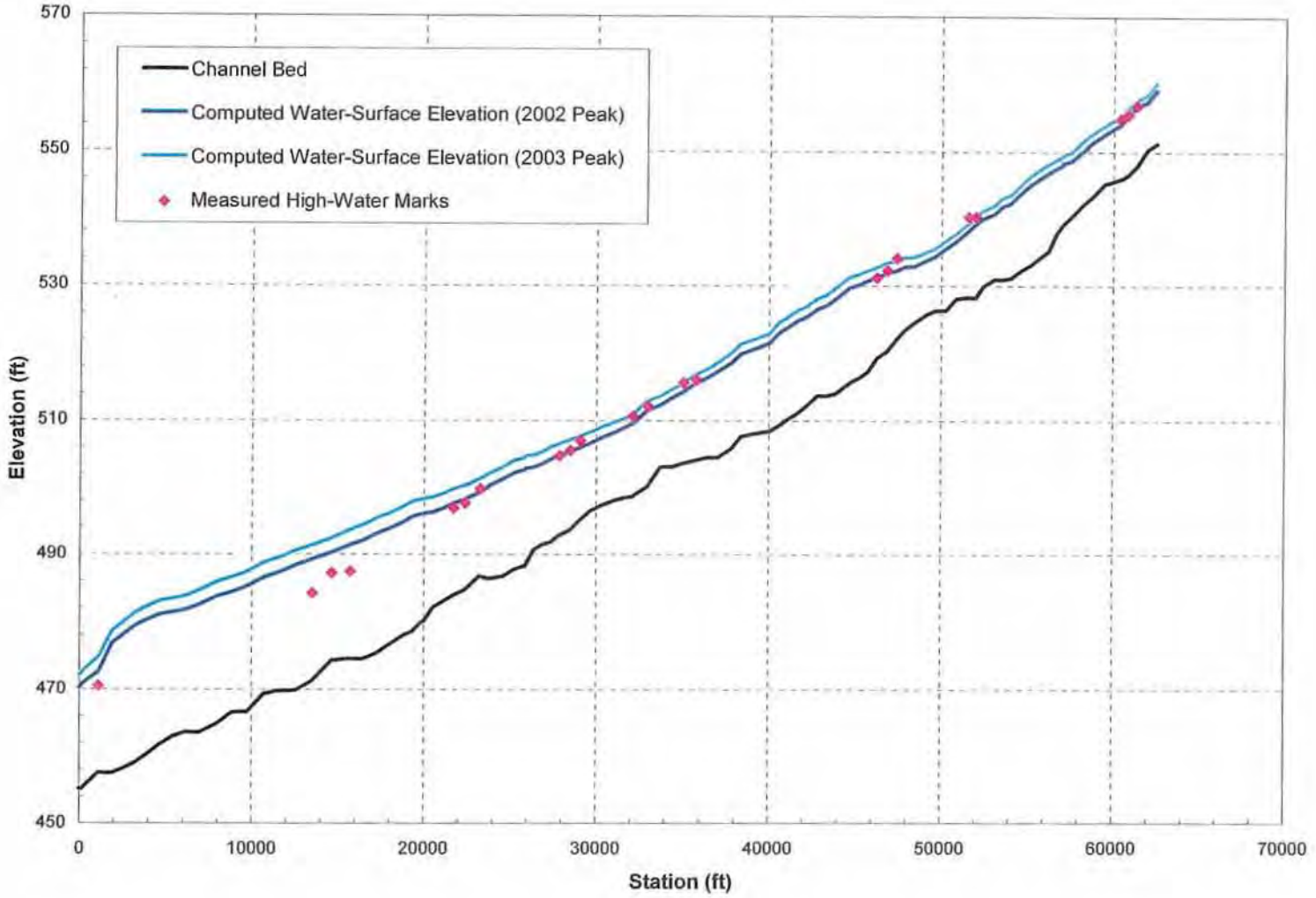

Figure 4.1. Measured high-water marks and computed water-surface elevations for the 2002 (Q=60,400 cfs) and the 2003 (72,200 cfs) flood peaks.

4.1.2. Reach-averaged Hydraulics

Subreach-averaged hydraulic conditions were evaluated by subdividing the model of the NSR into 10 subreaches, based on the locations of significant hydraulic controls and the location of the major tributaries (**Table 4.1, Figure 4.2**.) The average main channel velocity, hydraulic depth, effective (active channel) width, and total shear stress were computed for each of the subreaches over the range of modeled discharges (**Figures 4.3 through 4.6**). As expected, a general increasing trend of velocity, depth, and width occur in the downstream direction due to the effects of tributary inflows. Main channel velocities range from 4.8 to 9.7 fps at the 2-year peak discharge, and range from 5.6 to 11.6 fps at the 100-year peak discharge. Hydraulic depths in the main channel do not extend to the top of the channel over the range of modeled discharges, ranging from 3.7 to 10.1 feet at the 2-year event, and from 6.5 to 17.2 feet at the 100-year event. The effective widths are also limited to the main channel, ranging from 87 feet to about 190 feet at the 2-year peak discharge, and from about 130 feet to about 250 feet at the 100-year peak discharge. To evaluate the potential for the river to entrain bed material and to adjust the channel geometry (refer to Section 2.2.2), the total stream power (i.e., the amount of energy dissipated per unit length along the channel boundary) and unit stream power (stream power per unit width) were computed over the range of modeled flows (**Figures 4.7 and 4.8**). The total stream power averages about 600 lb/s at the 2-year event, ranging from 113 lb/s in the upstream subreaches to 2,460 lb/s in the downstream subreach, and averages about 1,560 lb/s at the 100-year peak discharge, ranging from 177 to 6720 lb/s. Unit stream powers also show a general increasing trend in the downstream direction, ranging from 0.9 to 15.9 lb/ft-s (average of 4.2 lb/ft-s) at the 2-year peak discharge, and from 0.8 to 26.9 lb/ft-s (average of 8.1 lb/ft-s) at the 100-year peak discharge. High unit-stream power in Subreach 5 corresponds to the high vertical, eroding banks in the subreach and indicates that further widening can be expected.

A critical grain-size analysis was carried out on a subreach-averaged basis to determine the size of sediment that can be mobilized at various discharges. The results indicate that the 2-year peak discharge will mobilize sediment sizes ranging from 48 to 68 mm, while the 100-year peak discharge will mobilize sediment sizes ranging from 74 to 120 mm (**Figure 4.9**). These results are consistent with evidence of transport of the gravel- and cobble-sized material that was observed at some locations along the channel bed.

Table 4.1. Summary of subreach delineations used for the reach-averaged hydraulic calculations.

Subreach	Description	Upstream Station (ft)	Downstream Station (ft)	Subreach Length (ft)
1	Upstream	61,966	59,106	2,861
2	Allen Creek to Bear Creek	59,106	54,342	4,764
3	Bear Creek to Brushy Creek	54,342	44,264	10,078
4	Brushy Creek to Pickle Creek	44,264	37,423	6,840
5	Pickle Creek to Davis Creek	37,423	32,513	4,910
6	Davis Creek to Leggets Branch	32,513	28,138	4,375
7	Leggets Branch to Bralley Pool Creek	28,138	22,786	5,352
8	Bralley Pool Creek to Merrill Creek	22,786	10,214	12,572
9	Merrill Creek to proposed dam location	10,214	7966	9,588
10	Proposed dam location to FM 904	7966	6	620

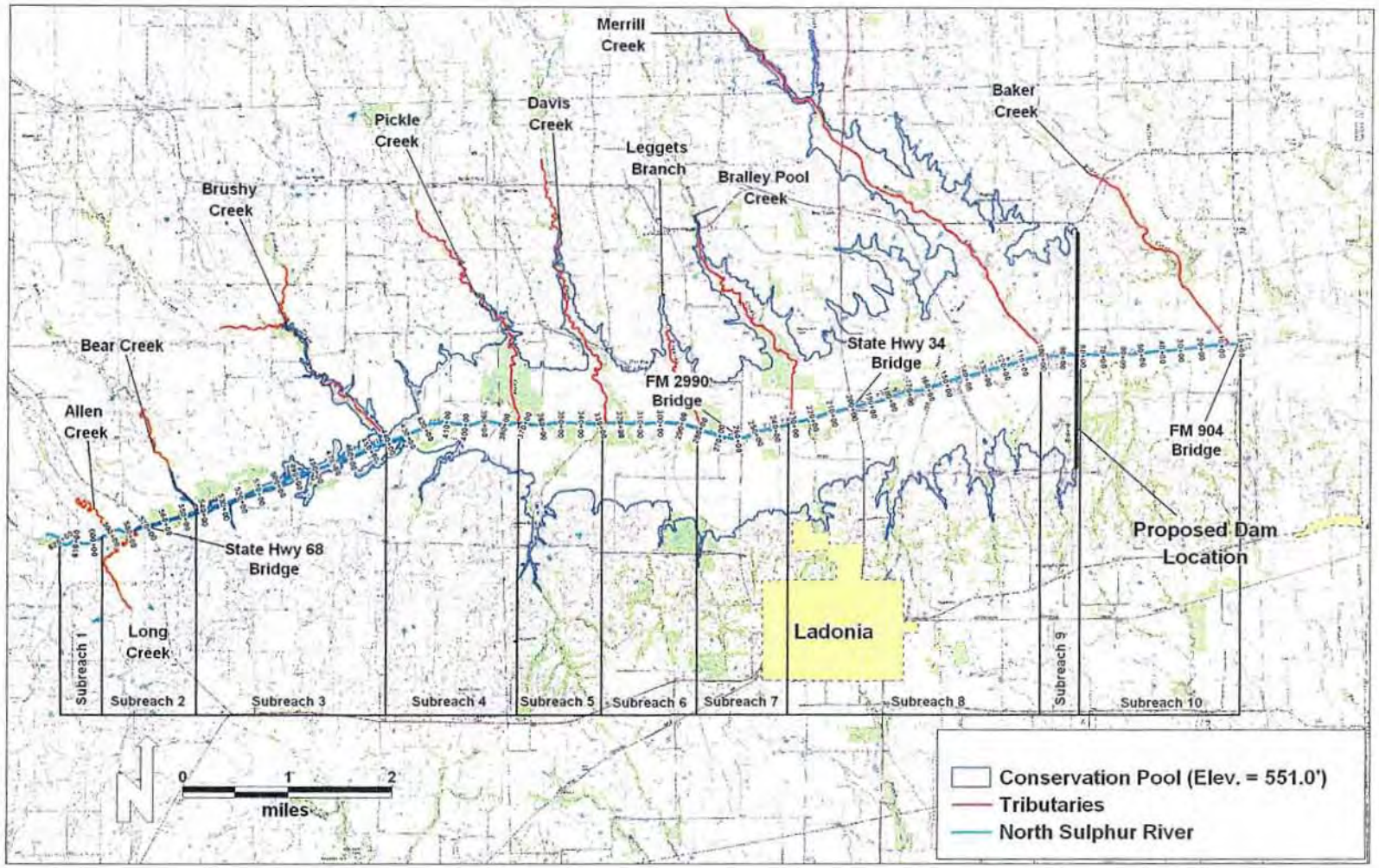

Figure 4.2. Subreach breakdown for the subreach-averaged hydraulic computations.

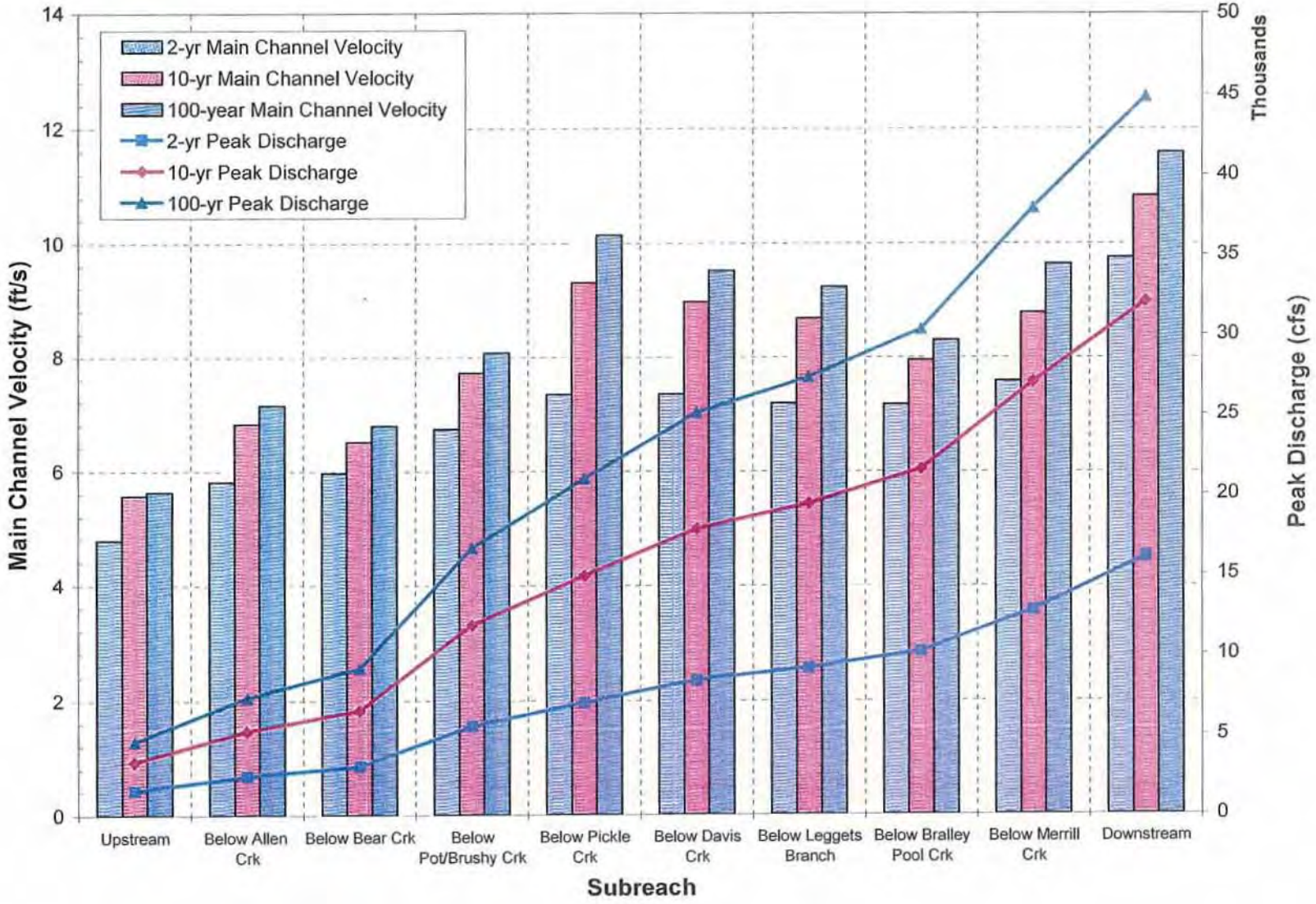

Figure 4.3. Subreach-averaged main channel velocities (bar graphs) for each of the subreaches for the 2-, 10-, and 100-year peak flows. Also shown are the peak discharges (curves).

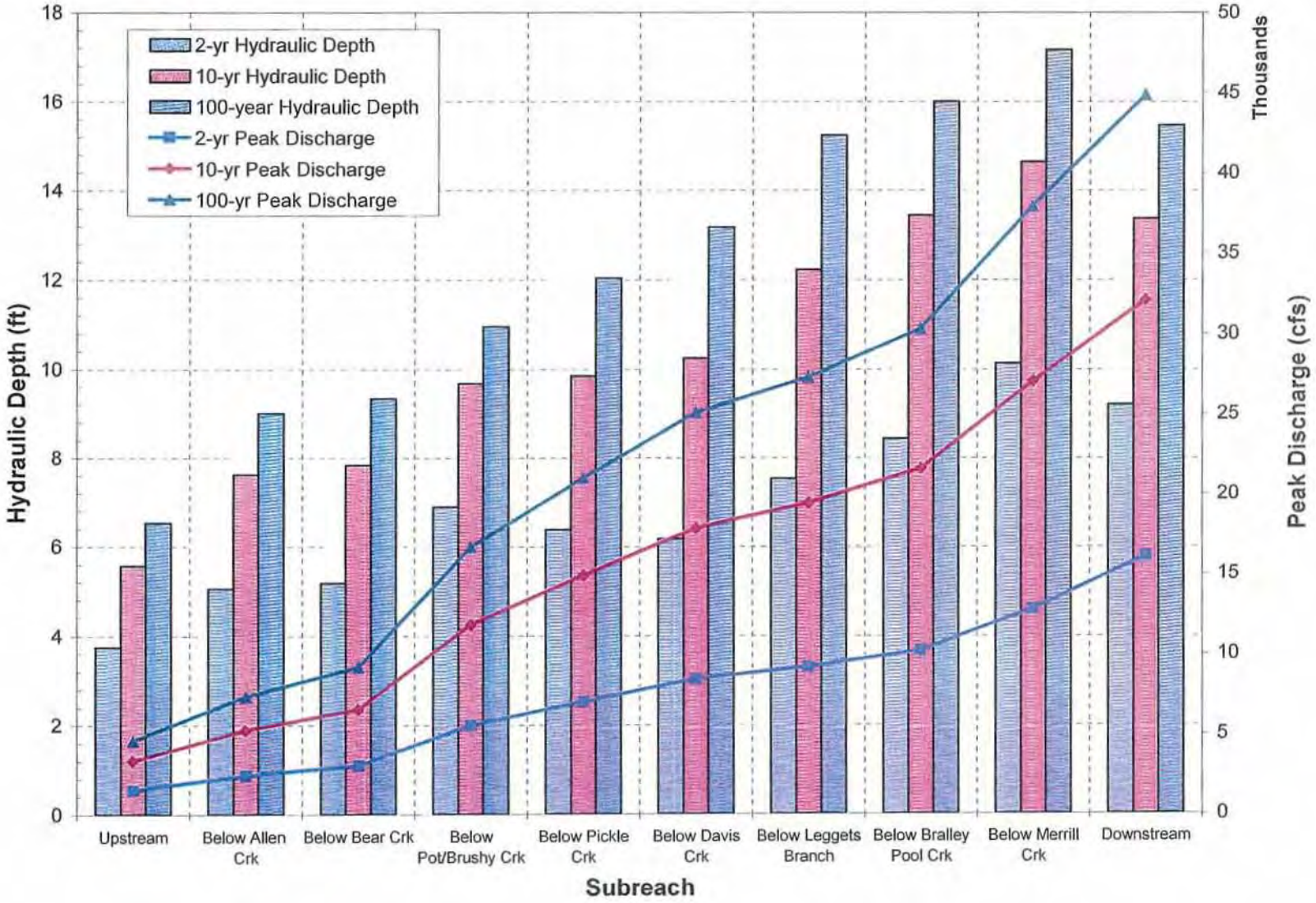

Figure 4.4. Subreach-averaged hydraulic depth (bar graphs) for each of the subreaches for the 2-, 10-, and 100-year peak flows. Also shown are the peak discharges (curves).

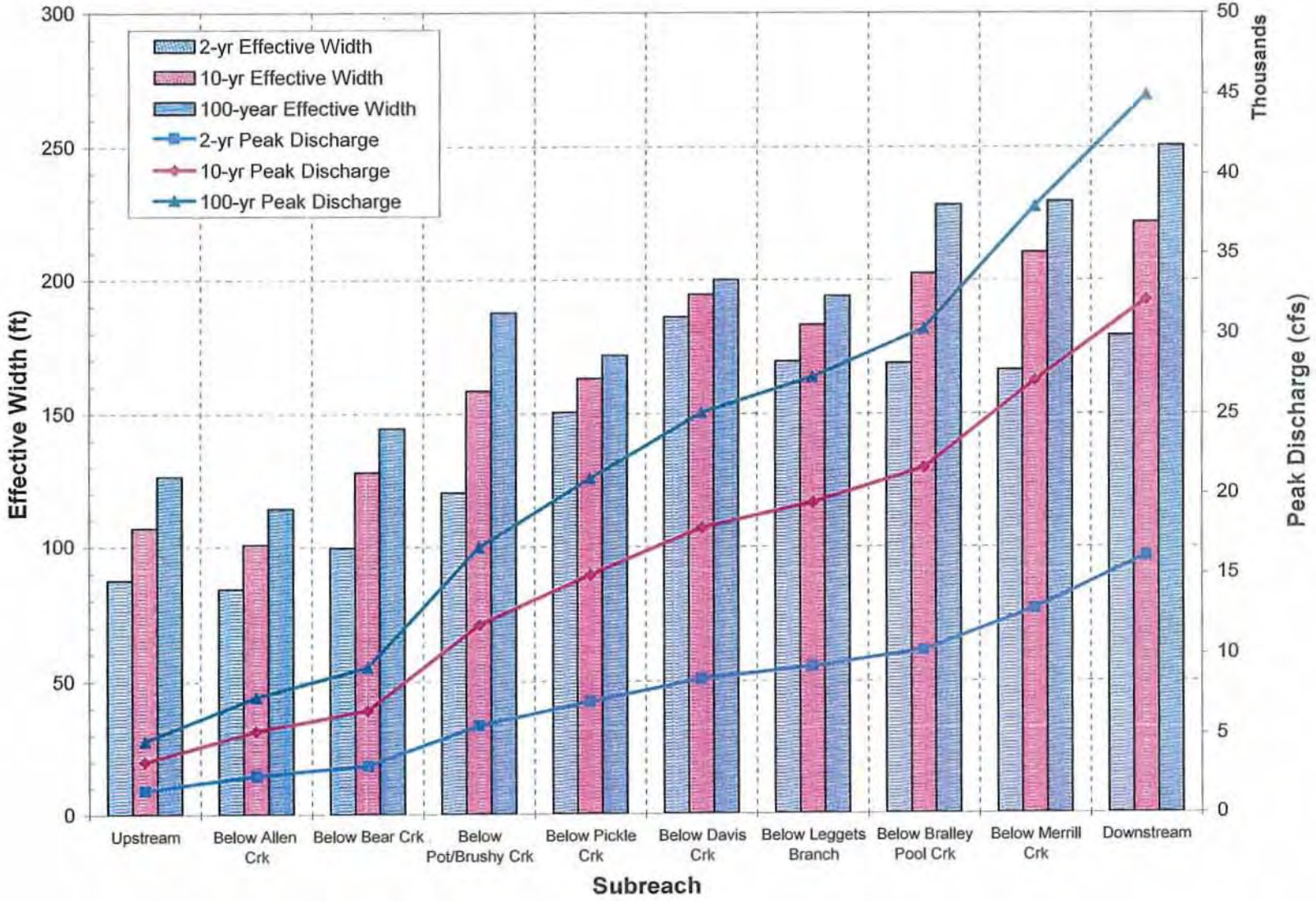

Figure 4.5. Subreach-averaged effective width (bar graphs) for each of the subreaches for the 2-, 10-, and 100-year peak flows. Also shown are the peak discharges (curves).

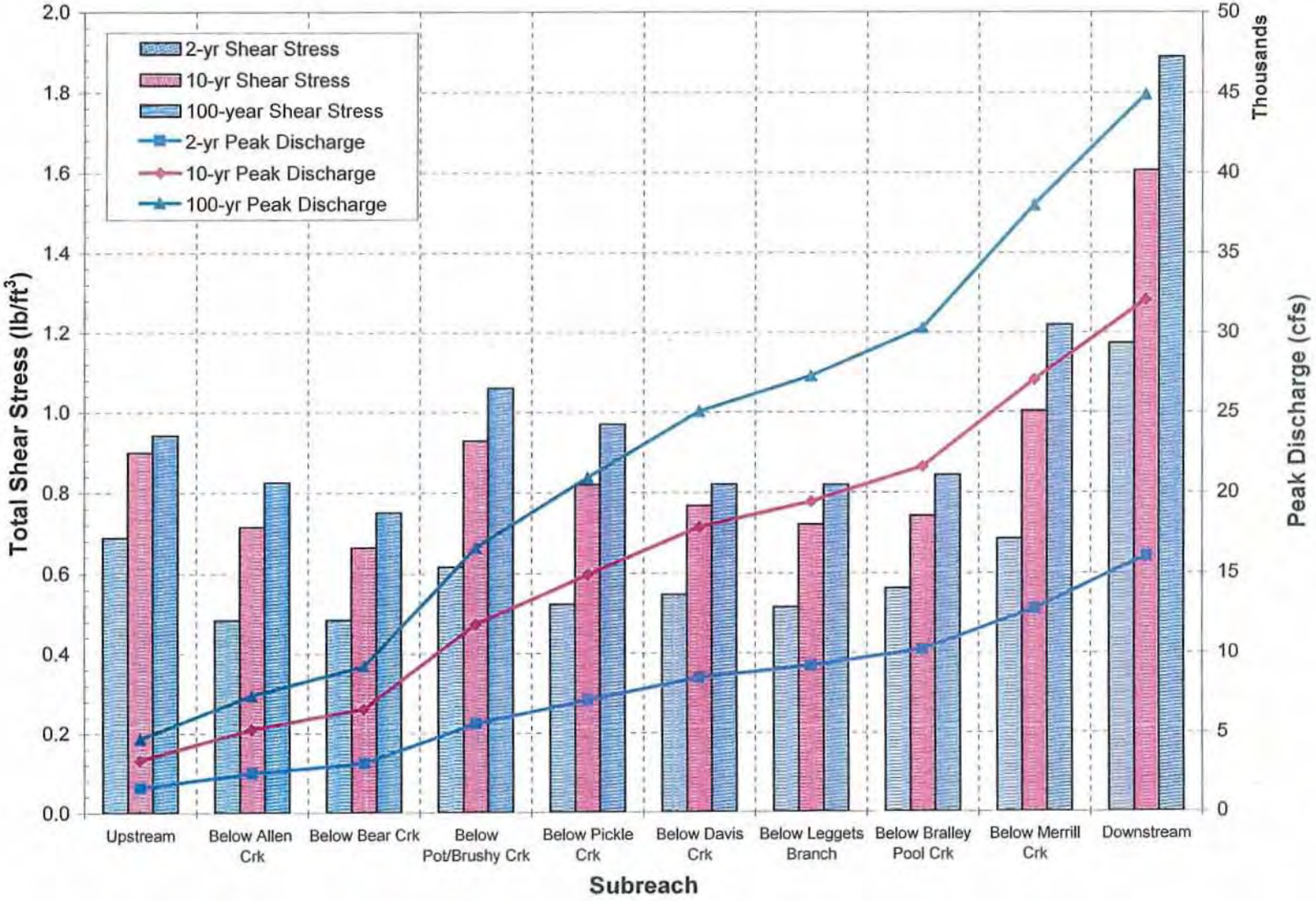

Figure 4.6. Subreach-averaged total shear stress (bar graphs) for each of the subreaches for the 2-, 10-, and 100-year peak flows. Also shown are the peak discharges (curves).

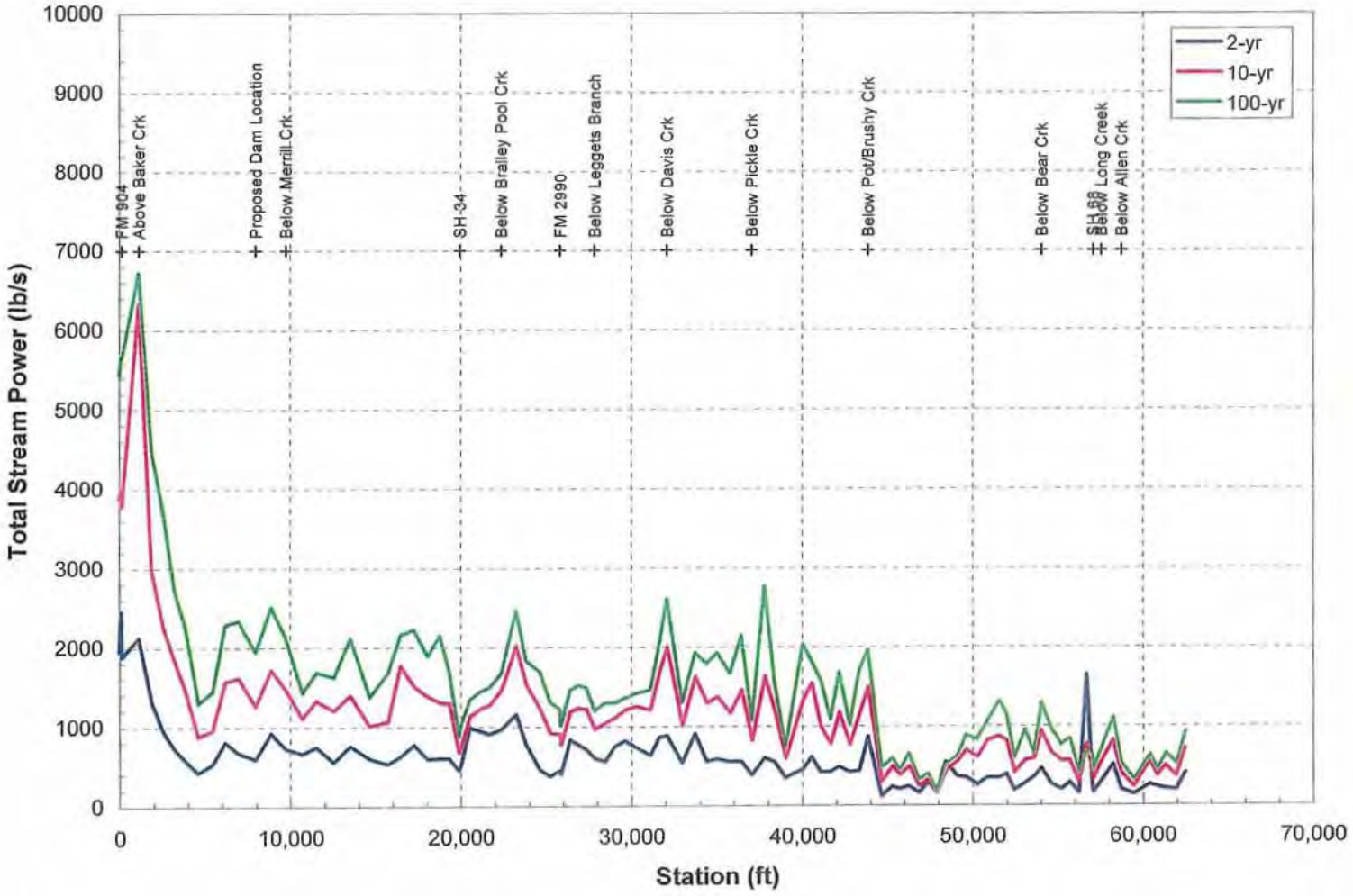

Figure 4.7. Computed total stream power along the modeled reach of the North Sulphur River for the 2-, 10-, and 100-year peak discharges.

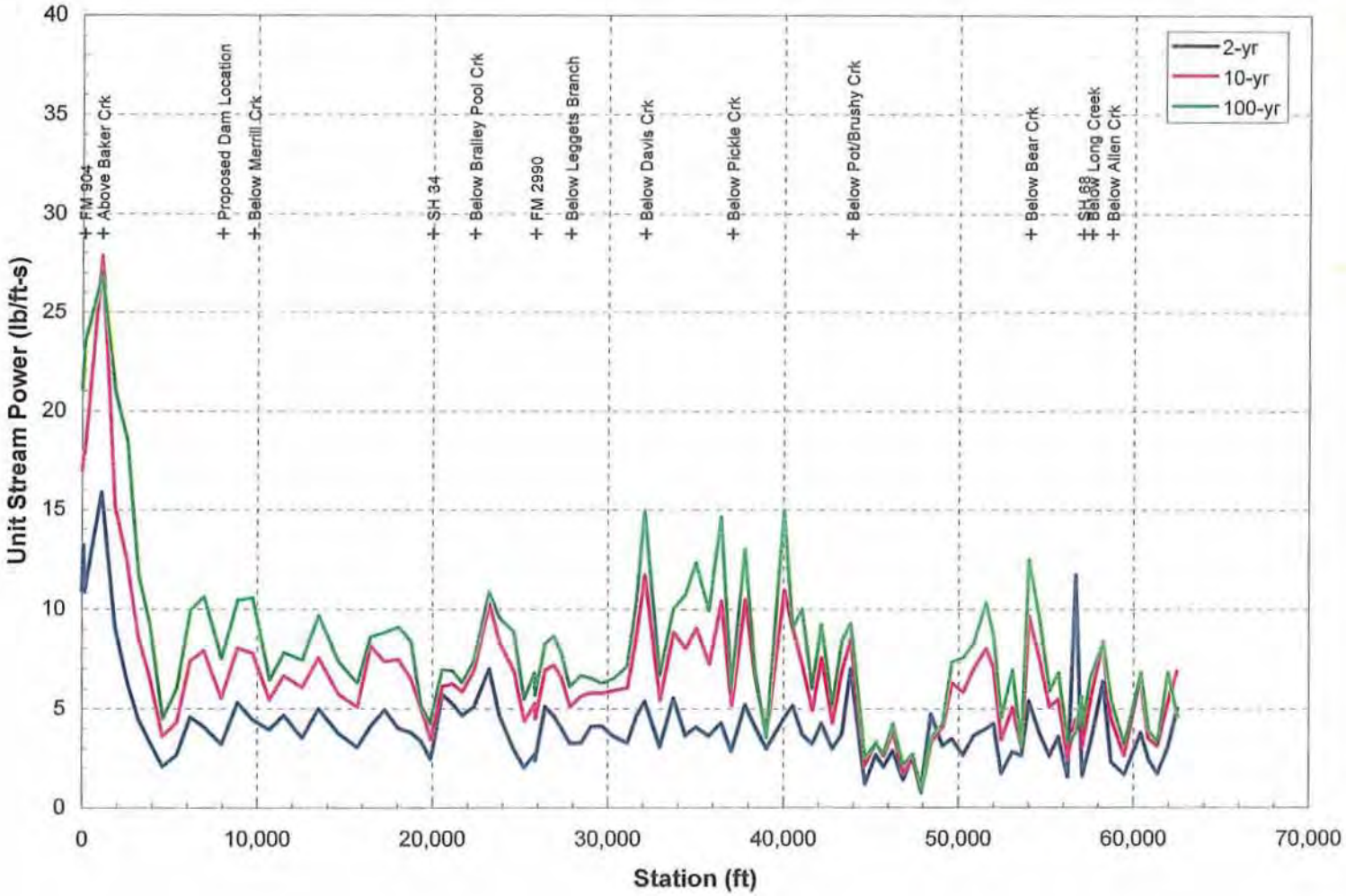

Figure 4.8. Computed unit stream power along the modeled reach of the North Sulphur River for the 2-, 10-, and 100-year peak discharges.

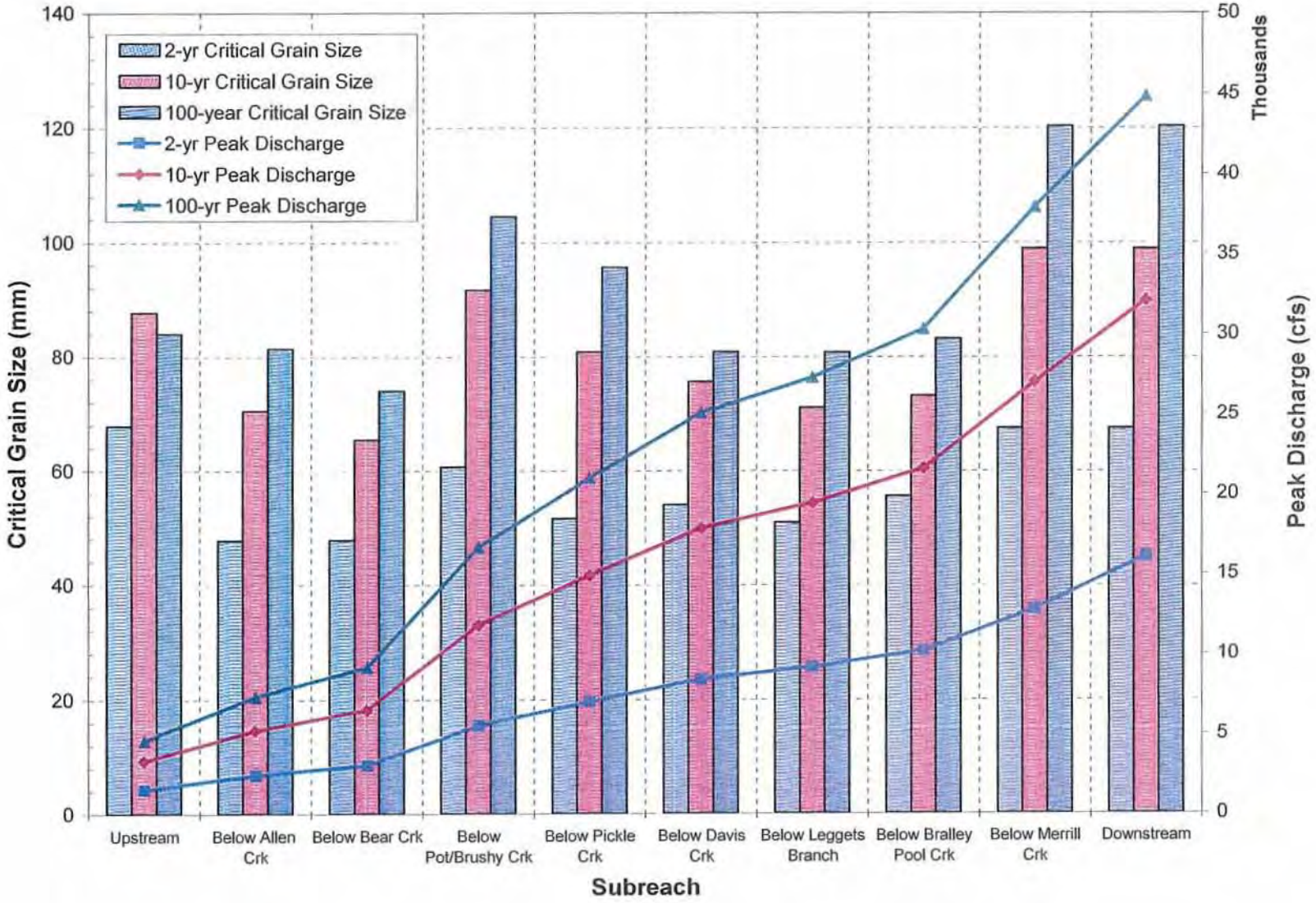

Figure 4.9. Subreach-averaged critical grain size (bar graphs) for each of the subreaches for the 2-, 10-, and 100-year peak flows. Also shown are the peak discharges (curves).

4.2. Hydraulic Models for the Primary Tributaries

Hydraulic models were developed for each of the primary tributaries in the project reach to estimate the hydraulic conditions to provide input to the sediment-transport calculations (Chapter 5). The modeled tributaries included Merrill Creek, Bralley Pool Creek, Leggets Branch, Davis Creek, Pickle Creek. Brushy Creek, Bear Creek, Long Creek, and Allen Creek. A model for Baker Creek was also developed to estimate hydraulic conditions in a typical tributary downstream from the location of the proposed dam. The model geometry was based on cross sections that were cut from the DTM developed by CP&Y. The length of the modeled reach and the number of sections in the model depended on the available topography covered by the DTM (**Table 4.2**). Model lengths ranged from 3,640 feet in Allen Creek to about 27,700 feet in Merrill Creek, and the number of sections in the models ranged from 20 in Allen Creek to 116 in Bralley Pool Creek, with average cross-sectional spacing ranging from 58 to 269 feet. In some cases, two models were developed for the individual tributaries, including one model for the portion of the tributary near the upstream limit of the DTM coverage and a separate model for the portion of the tributary near the confluence with the NSR. Consistent with the model for the mainstem, a vertical variation in the roughness was applied, resulting in Manning's *n*-values that ranged from 0.027 to 0.040 in the main channel, and from 0.049 to 0.070 in the overbanks. Downstream boundary conditions were based on normal depth conditions with a starting energy slope set equal to the average bed slope near the confluence with the mainstem NSR, and did not include backwater effects from the mainstem since the timing of the peaks in the tributaries is likely to be different than in the mainstem.

Table 4.2. Summary of hydraulic model information for the primary tributaries in the project reach.

Tributary	Model Length (ft)	Number of Cross Sections	Average Cross Section Spacing (ft)
Allen Creek	3,640	20	85/107*
Long Creek	7,032	22	58/64*
Bear Creek	7,338	46	154
Pot Creek	3,699	32	113
Brushy Creek	13,977	22	85/202*
Pickle Creek	15,963	24	99/117*
Davis Creek	17,301	95	182
Leggets Branch	6,886	28	254/269*
Bralley Pool Creek	21,393	116	182
Merrill Creek	27,729	106	258
Baker Creek	15,435	70	218

*Modeled upstream and downstream portion of tributary

Each of the tributary models was run over a range of flows up to and including the 100-year peak flow, based on results from the hydrologic (HEC-1) models.

4.2.1. Reach-averaged Hydraulics

Reach-averaged hydraulic conditions in the tributaries were computed using the results from the HEC-RAS models, and dividing each of the tributaries into up- and downstream (and in some cases, middle) subreaches. The reach-averaged discharge, velocity, depth, and topwidth for

the main channel at the 2-, 10-, and 100-year peak discharges are summarized in **Table 4.3**. At the 2-year event, a maximum reach-averaged velocity of 11.1 fps is indicated in Pickle Creek, and a maximum depth of 7.6 feet and maximum topwidth of 105 feet occur in Baker Creek. Maximum main-channel velocities, depths, and topwidths occur in the same tributaries at the 10- and 100-year events due to the relatively steep nature of Pickle Creek and the significant drainage area that contributes flow to Baker Creek. At the 10-year event, reach-averaged results indicate that velocities are as much as 15 fps (Pickle Creek), while maximum hydraulic depths are about 12 feet (Baker Creek), and topwidths exceed 130 feet (Baker Creek). Results for the 100-year event suggest maximum main channel velocities exceed 16 fps in Pickle Creek, maximum depths approach 15 feet in Baker Creek, and maximum topwidths exceed 140 feet in Baker Creek.

Table 4.3. Summary of reach-averaged hydraulic conditions for the 2-, 10-, and 100-year events for subreaches of the primary tributaries.															
Location	2-year Peak Discharge					10-year Peak Discharge					100-year Peak Discharge				
	Total Flow (cfs)	Main Channel Flow (cfs)	Main Channel Velocity (ft/s)	Main Channel Hydraulic Depth (ft)	Main Channel Top Width (ft)	Total Flow (cfs)	Main Channel Flow (cfs)	Main Channel Velocity (ft/s)	Main Channel Hydraulic Depth (ft)	Main Channel Top Width (ft)	Total Flow (cfs)	Main Channel Flow (cfs)	Main Channel Velocity (ft/s)	Main Channel Hydraulic Depth (ft)	Main Channel Top Width (ft)
Allen-DS	927	875	6.4	3.4	41.0	1,882	1,730	8.7	5.0	41.0	2,655	2,397	9.8	6.0	41.0
Allen-Mid	927	820	6.7	3.6	33.8	1,882	1,570	9.1	5.1	33.8	2,655	2,133	10.1	6.2	33.8
Allen-US	927	798	6.2	4.1	32.5	1,882	1,519	8.2	5.9	32.5	2,655	2,068	9.2	7.1	32.5
Long-DS	904	742	7.8	5.1	19.2	1,858	1,404	10.2	7.3	19.2	2,609	1,884	11.4	8.7	19.2
Long-Mid	904	820	7.9	4.8	21.8	1,858	1,563	9.8	7.3	21.8	2,609	2,122	11.2	8.7	21.8
Long-US	904	497	8.7	6.7	8.9	1,858	870	11.0	9.0	8.9	2,609	1,154	12.9	10.1	8.9
Bear-DS	811	765	7.1	3.5	30.7	1,646	1,483	9.5	5.2	30.7	2,315	2,020	10.5	6.3	30.7
Bear-Mid	811	747	6.8	3.7	30.6	1,646	1,448	9.1	5.2	30.6	2,315	1,975	10.2	6.4	30.6
Bear-US	811	648	7.0	4.1	24.1	1,646	1,203	8.8	6.0	24.1	2,315	1,612	9.7	7.2	24.1
Pot-DS	1,663	1,275	7.8	4.8	34.6	3,364	2,300	9.6	6.8	34.6	4,762	3,050	10.7	8.0	34.6
Pot-Mid	1,201	945	7.4	4.4	29.8	2,417	1,700	9.0	6.4	29.8	3,411	2,241	9.5	8.0	29.8
Pot-US	1,201	1,074	8.0	4.7	28.6	2,417	2,008	10.2	6.8	28.6	3,411	2,712	11.3	8.3	28.6
Brushy-US	1,696	1,411	8.8	5.9	28.2	3,408	2,660	11.4	8.6	28.2	4,799	3,623	12.9	10.2	28.2
Brushy-DS	3,093	2,837	8.0	5.7	63.4	6,364	5,581	10.1	8.9	63.4	9,043	7,744	11.2	11.1	63.4
Pickle-DS	1,592	1,385	9.3	5.6	27.5	3,320	2,686	11.5	8.7	27.5	4,715	3,656	12.7	10.6	27.5
Pickle-Mid	1,592	1,478	11.1	5.1	26.1	3,320	2,891	14.8	7.5	26.1	4,715	3,966	16.5	9.2	26.1
Pickle-US	1,592	1,012	9.8	6.9	14.9	3,320	1,806	12.0	10.1	14.9	4,715	2,377	13.2	12.1	14.9
Davis-DS	1,266	1,059	7.1	4.0	38.4	2,948	2,313	9.9	6.3	38.4	4,257	3,241	11.2	7.8	38.4
Davis-Mid	1,266	949	5.0	5.4	32.7	2,948	2,072	7.4	7.9	32.7	4,257	2,887	8.7	9.5	32.7
Davis-US	1,266	1,092	8.2	4.6	30.2	2,948	2,328	10.5	7.5	30.2	4,257	3,188	11.3	9.4	30.2
Leggetts-DS	648	645	7.1	3.1	29.5	1,304	1,281	8.8	4.5	32.9	1,838	1,779	9.7	5.5	34.1
Leggetts-US	648	483	5.3	2.8	33.8	1,304	790	6.4	3.7	33.8	1,838	1,017	7.1	4.3	33.8
Bralley-DS	1,482	1,400	7.6	4.6	40.5	3,052	2,758	10.0	6.9	40.5	4,328	3,809	11.2	8.4	40.5
Bralley-Mid	1,482	1,224	7.6	4.8	35.6	3,052	2,360	9.7	7.1	35.6	4,328	3,211	10.7	8.6	35.6
Bralley-US	1,482	1,268	9.3	5.5	24.9	3,052	2,329	10.6	7.9	24.9	4,328	2,983	10.9	9.8	24.9
Merrill-DS	2,123	1,990	7.8	5.2	49.8	4,459	3,998	10.3	7.9	49.8	6,795	5,915	12.0	10.0	49.8
Merrill-Mid	2,123	1,758	7.7	5.4	44.3	4,459	3,484	10.0	8.3	44.3	6,795	5,112	11.5	10.5	44.3
Merrill-US	2,123	1,686	8.4	5.5	37.5	4,459	3,146	10.2	7.8	37.5	6,795	4,219	11.4	9.7	37.5
Baker-DS	4,538	4,538	6.3	7.6	94.8	9,424	9,184	6.9	12.1	111.3	13,427	12,682	7.7	14.8	113.6
Baker-US	4,538	4,482	6.0	7.2	105.0	9,424	9,233	6.9	10.2	132.7	13,427	13,030	7.5	12.4	143.9

5. SEDIMENT TRANSPORT

The sediment-transport analysis was conducted under existing and with-dam (i.e., project) conditions to evaluate potential sediment loading to the proposed reservoir and to determine the effects of the dam on downstream channel conditions. Sediment transport is typically evaluated with two components:

1. Wash load: The portion of the sediment load that is primarily fine material and is not found in significant amounts in the bed material.
2. Bed-material load: The portion of the sediment load that is transported along the channel bed and makes up the material that is found in appreciable quantities on the channel bed.

The wash-load component of the overall sediment load includes the fine sediments that are delivered to the channel from the watershed (watershed sediment yield) and the fine material that is eroded from the bed and banks. Typically, the wash load is not morphologically significant. The bed-material load is typically made up of coarser material that is eroded from the bed and banks, and is considered to be morphologically significant. In the project reach of the NSR, the bed and lower banks are composed primarily of shale that, when entrained by the flow, enters the system as coarse bed-material load and breaks down into fine wash load as it is transported downstream due to cycles of wetting and drying that cause slaking (Chapter 2; Allen et al., 2002).

5.1. Watershed Sediment Yield

Evaluation of the watershed sediment yield requires an assessment of the sediment sources in the watershed, the cover (vegetation type and density) and management practices, and the types of erosion (sheet, rill, ephemeral gulley) that are prevalent. This information, combined with hydrologic information, can then be used to estimate the watershed sediment yield using empirically derived relationships. For this study, the Modified Universal Soil Loss Equation (MUSLE) was used to estimate the sheet-and-rill sediment yield to the location of the proposed dam under existing, and with-dam, conditions. Estimates of the ephemeral gulley sediment yield were developed from the soil erosion literature (Laflen et al., 1986).

5.1.1. Soil Characteristics, Cover and Management Practices

The types of soil in the NSR watershed were identified using maps from the Soil Survey of Fannin County, Texas (NRCS, 2001) and the NRCS online Web Soil Survey. In general, the watershed includes:

1. Clayey and loamy, slightly acid to moderately alkaline soils on uplands,
2. Loamy, very strongly acid to neutral soils on terraces,
3. Loamy and clayey, moderately acid to neutral soils on uplands, and
4. Clayey and loamy, moderately alkaline soils on floodplains.

Each of these soil types is relatively erodible due to the loamy properties. Specific soil types and their physical properties are outlined in the soil survey and can be found on the online Web Soil Survey.

Based on information from the Texas State Soil and Water Conservation Board (TSSWCB, 1997), land in Fannin County is primarily used for pasture, crops, and range. Under the assumption that the project watershed has a similar distribution of land-use practices to Fannin County, in general, about 42 percent of the watershed is used for pasture, 26 percent is used for cropping, 24 percent is rangeland, and only 2 percent is forested. These values are consistent with recent assessments of land use (written comm., Loretta Mokry, Alan Plummer and Associates, April 2006) that indicate about 21 percent of the project watershed is currently being used for cropping, and estimated rates of cropland loss of about 0.5 percent per year (personal comm., Randy Moore, NRCS, 1996). Because land used for crops typically has relatively low ground cover (especially during the non-growing season when the soil is essentially bare), and there is a significant amount of cropland in the watershed, the potential for surface erosion is relatively high in the Texas Blackland Prairie region (Harmel et al., 2006).

5.1.2. Modified Universal Soil Loss Equation

The Modified Universal Soil Loss Equation (MUSLE) was developed to estimate sediment yields from watersheds based on single storms. The equation, as presented by Williams and Berndt (1972), differs from the original Universal Soil Loss Equation by inclusion of a runoff factor in place of a rainfall energy factor. Since it directly considers the runoff associated with individual storms, it is more applicable to the ephemeral streams within the project watershed where runoff and sediment delivery to the channel system is primarily the result of rainfall. The MUSLE is given by:

$$Y_S = \alpha(Vq_p)^{\beta} KLSCP \tag{5.1}$$

where Y_s = sediment yield for the storm in tons,
K = soil erodibility factor,
LS = topographic factor representing the combination of slope length and slope gradient,
C = cover and management factor,
P = erosion-control practice factor,
V = runoff volume for the storm in ac-ft, and
q_p = peak discharge of the storm in cfs.

Values for α and β can be derived through calibration when sufficient data are available. The most commonly used values for α and β are 95 and 0.56, respectively, and were derived from data in experimental watersheds in Texas and Nebraska. Although the MUSLE was originally developed to represent the total watershed sediment yield, the equation likely accounts for only the fine sediment (wash load) yield for the project watershed. The bed-material component of the total sediment load is discussed later in this chapter.

The soil erodibility factor (K) was obtained from the Fannin County Soil Survey maps and tables (NRCS, 2001), which delineate the specific soil types and summarize the K-factors for each soil type. Area-weighted K-factors were computed for each subbasin (Figure 3.8) in the project watershed under existing and with-dam conditions, and are summarized in **Table 5.1**.

The basin shape and topography factor (LS) is computed as:

$$LS = \left(\frac{\lambda}{72.6}\right)^{n} \left(0.065 + 0.0454S + 0.0065S^2\right) \tag{5.2}$$

Table 5.1. Summary of MUSLE factors for the individual subbasins in the project watershed.													
Basin	ID	Existing Conditions						With Dam Conditions					
		Area (sq mi)	Slope (%)	Average Length (ft)	K	n	LS	Area (sq mi)	Slope (%)	Average Length (ft)	K	n	LS
Baker1	107	1.30	1.24	1167	0.38	0.3	0.30	1.30	1.24	1167	0.38	0.3	0.30
Baker2	92	2.08	1.10	1616	0.33	0.3	0.31	2.08	1.10	1616	0.33	0.3	0.31
Baker3 (Mclure)	94	4.76	0.79	2183	0.32	0.3	0.29	4.76	0.79	2183	0.32	0.3	0.29
Baker4 (Moss)	68	6.19	0.65	2297	0.32	0.3	0.27	6.19	0.65	2297	0.32	0.3	0.27
Baker5	66	0.85	0.80	1051	0.32	0.3	0.24	0.85	0.80	1051	0.32	0.3	0.24
Baker6	56	2.22	0.51	1363	0.32	0.3	0.22	2.22	0.51	1363	0.32	0.3	0.22
Baker7	57	4.68	0.52	2002	0.32	0.3	0.24	4.68	0.52	2002	0.32	0.3	0.24
DS1	147	2.41	1.37	2062	0.38	0.3	0.38	2.41	1.37	2062	0.38	0.3	0.38
HB	151	1.68	1.20	1124	0.38	0.3	0.29	1.68	1.20	1124	0.38	0.3	0.29
Merrill	110	11.49	0.82	3057	0.34	0.3	0.33	8.65	0.68	3057	0.32	0.3	0.30
LRH1	153	8.59	1.28	4541	0.36	0.3	0.46	3.97	1.46	4541	0.36	0.3	0.50
Bralley Pool	123	7.95	0.66	2125	0.33	0.3	0.27	7.05	0.55	2125	0.32	0.3	0.25
Leggetts	152	2.53	0.87	1402	0.35	0.3	0.27	1.32	0.89	1402	0.32	0.3	0.27
LRH2	163	2.41	1.76	1816	0.33	0.3	0.43	1.90	1.95	1816	0.33	0.3	0.47
LRH3	145	0.88	1.12	2472	0.36	0.3	0.36	0.24	2.02	2472	0.36	0.3	0.53
Davis	125	6.99	0.70	2457	0.34	0.3	0.29	6.32	0.64	2457	0.32	0.3	0.28
LRH4A	126	0.00	1.00	759	0.32	0.3	0.24	0.00	1.00	759	0.32	0.3	0.24
LRH5	132	0.42	0.84	623	0.32	0.3	0.21	0.07	1.11	623	0.32	0.3	0.24
LRH4	167	3.39	1.62	2259	0.33	0.3	0.44	2.90	1.66	2259	0.33	0.3	0.44
LRH6	133	1.03	0.74	1090	0.33	0.3	0.23	0.51	0.86	1090	0.33	0.3	0.24
Pickle	124	6.93	0.72	2434	0.33	0.3	0.29	6.37	0.70	2434	0.32	0.3	0.29
LRH8	136	1.38	0.83	1187	0.33	0.3	0.25	0.77	0.76	1187	0.33	0.3	0.24
LRH7	164	2.10	1.29	1502	0.32	0.3	0.33	1.97	1.24	1502	0.32	0.3	0.33
LRH9	170	4.73	1.11	2373	0.34	0.3	0.35	3.90	1.14	2373	0.34	0.3	0.36
Brushy1	128	1.44	0.88	1398	0.33	0.3	0.27	1.02	0.70	1398	0.33	0.3	0.24
Brushy2	103	6.37	0.63	2787	0.34	0.3	0.29	6.36	0.62	2787	0.34	0.3	0.29
Pot1	105	0.02	1.00	1827	0.32	0.3	0.31	0.00	1.00	1827	0.32	0.3	0.31
Pot2	102	2.01	0.76	1327	0.32	0.3	0.25	2.01	0.76	1327	0.32	0.3	0.25
Pot3	111	4.98	0.63	2345	0.33	0.3	0.27	4.97	0.63	2345	0.33	0.3	0.27
LRH9A	161	0.73	1.53	1025	0.32	0.3	0.33	0.68	1.40	1025	0.32	0.3	0.31
Bear	134	3.32	0.76	1569	0.34	0.3	0.26	3.29	0.74	1569	0.34	0.3	0.26
LRH10	142	0.02	1.00	2133	0.32	0.3	0.32	0.00	1.00	2133	0.32	0.3	0.32
Long	179	3.23	1.40	1849	0.32	0.3	0.37	3.22	1.40	1849	0.32	0.3	0.37
LRH11	146	0.11	0.97	13236	0.32	0.3	0.55	0.11	0.97	13236	0.32	0.3	0.55
Allen	139	4.49	0.54	1870	0.32	0.3	0.24	4.48	0.54	1870	0.32	0.3	0.24
LRH12	148	0.69	0.95	897	0.32	0.3	0.24	0.69	0.94	897	0.32	0.3	0.24
LRH13	174	2.93	1.28	1977	0.32	0.3	0.36	2.93	1.28	1977	0.32	0.3	0.36
LRH14A	141	0.02	1.00	2193	0.32	0.3	0.32	0.02	1.00	2193	0.32	0.3	0.32
LRH15	135	2.52	0.66	1446	0.32	0.3	0.24	2.52	0.66	1446	0.32	0.3	0.24
LRH14	166	2.03	1.07	1939	0.32	0.3	0.32	2.03	1.07	1939	0.32	0.3	0.32
LRH16	160	4.03	1.03	2798	0.32	0.3	0.35	4.03	1.03	2798	0.32	0.3	0.35

where λ = slope length (distance from the point of overland flow origin to the point where the water enters a well-defined channel),

S = percent slope, and n is an exponent depending upon the slope.

The exponent *n* is given by: *n*=0.3 for slope <= 3 percent

n=0.4 for slope <= 4 percent

n=0.5 for slope >= 5 percent

The slope length and the basin slope were measured from the DTM developed by CP&Y for each of the subbasins (Figure 3.8) that make up the contributing watershed to the dam site.

The measured values, the exponent (n) and the resulting LS factors are summarized for existing and with-dam conditions in Table 5.1.

The cover and management factor (C) is based on the vegetation type, height and percentage of ground cover, and is derived from SCS Agriculture Handbook Number 537 (1978). For the project watershed, a composite C-factor of 0.17 was computed for the overall watershed assuming that the percentage of cropland, rangeland, pastureland, and forestland is similar to the values reported by TSSWCB (1997) based on the individual land-use C-factors presented in **Table 5.2**.

Table 5.2. Summary of selected C-factors for the individual land-use types in the project watershed.

Type of Land Use	Percent (%)	C-factor
Forest	24.0	0.01
Row Crops	3.8	0.20
Close Crops	22.3	0.17
Pasture	41.9	0.17
Rangeland	24.0	0.17
Not Identified/Misc	5.8	0.20
Composite C-Value:		**0.17**

The erosion-control practice factor (P) accounts for the effect of conservation practices such as contouring, strip cropping, and terracing on erosion. It is defined as the ratio of soil loss using one of these practices to the loss using straight row farming up and down the slope. To be conservative, a P-factor of 1.0 was selected for the MUSLE calculations in this study, even though there are significant erosion-control measures in the basin.

Processes of erosion and sedimentation are cumulative over the long term, so it is necessary to evaluate sediment transport not only for a specific flood event, but also for the intervening smaller flows. For purposes of analyzing the long-term erosion potential, the representative annual event can be more accurately defined by considering individual storm events independently and weighting the effect of each based on their probability of occurrence. This is accomplished by integrating the flow-duration curve over discrete intervals resulting in the following equation (Mussetter et al., 1994):

$$Y_m=0.015Y_{100}+0.015Y_{50}+0.04Y_{25}+0.08Y_{10}+0.2Y_5+0.4Y_2 \quad (5.3)$$

where Y_m = magnitude of the average annual event (i.e., sediment yield) and
Y_i = magnitude of the event for the 2-, 5-, 10-, 25-, 50-, and 100-year return period storms.

Watershed sheet-and-rill sediment yields were computed from each subbasin (Figure 3.8) for the 2- through 100-year storm events using the MUSLE with the above factors and the results from the hydrologic analysis (peak flow and storm volume) that were developed using the HEC-1 models or from the rating curves (Chapter 3). Annual sediment yields were computed using Equation 5.3. Although previous studies (Smith et al., 1984) have indicated that the sediment yields predicted by the MUSLE are reasonable for Blackland Prairie soils, computed annual sediment yields using the identified parameters in the MUSLE (Table 5.1) are about 37 percent

of observed rates of sheet-and-rill erosion in the Blackland Prairie region that are about 2.0 t/ac/yr (Alan Plummer and Associates, 2005). Therefore, the value of the alpha coefficient (95) in the MUSLE was adjusted by a factor of 2.7, resulting in a new alpha coefficient of about 257 that is similar to values successfully used in other areas with high erosion rates (Mussetter et al., 1994).

5.1.3. Ephemeral Gully Erosion

The overall watershed sediment yield includes not only the portion that is accounted for by the MUSLE calculations (sheet-and-rill erosion), but also the portion of fine sediments that are eroded by ephemeral gullies. Ephemeral gullies are defined as small channels that form in croplands or nonvegetated, exposed soils at locations where the rills join and the macrotopography allows for concentrated flow. Ephemeral gullies are formed by the shearing forces of concentrated flow, and are typically removed (filled) on an annual basis through tilling and other crop-related practices (Laflen et al., 1986).

Initial estimates of sediment yield from ephemeral gulley erosion were computed using the SCS Ephemeral Gulley Erosion Model (Woodward, 1999), and indicated that a maximum annual detachment rate of about 0.4 t/ac would result from ephemeral gulley erosion within the project watershed. This estimate is believed to somewhat under-predict the actual sediment load that results from ephemeral gullies (pers. comm., Randy Moore, NRCS, 2006). The soil erosion literature indicates that ephemeral gullies may produce as much as 1.5 times the amount of sediment that is predicted by the Universal Soil Loss Equation (USLE), but typically the range is a factor of 0.25 to 1.0 (Laflen et al., 1986). Therefore, the amount of fine sediment volume that is eroded from ephemeral gullies was estimated as 1.0 times the sheet-and-rill erosion predicted by the MUSLE for the portion of land used for cropping, where ephemeral gullies form. The resulting ephemeral gulley erosion rates are 0.26 times the MUSLE (sheet-and-rill) erosion rates since approximately 26 percent of the project watershed is cropland.

5.1.4. Sediment Delivery Ratios

The portion of the gross sheet-and-rill erosion that is delivered to an outlet in a channel depends on the drainage area, watershed slope, drainage density, and runoff (Gottschalk, 1964). The sediment delivery ratio (SDR) expresses the percentage of on-site eroded material that reaches a designated downstream location. Renfro (1975) developed an equation for the SDR in the Blackland Prairie using measured gross erosion rates and watershed sediment yields:

$$\log_{10}SDR=1.8768-0.141911(\log_{10}(10(A))) \quad (5.4)$$

where SDR = sediment delivery ratio percentage, and
A = drainage area in square miles.

Compared with other relationships and estimates of the SDR (Shen and Julien, 1993; Alan Plummer and Associates, 2005), the relationship presented in Equation 5.4 produces the largest SDR values, and was therefore adopted to conservatively estimate the fine sediment yield resulting from sheet-and-rill erosion in this study.

The concept of the SDR also applies to sediment yields resulting from ephemeral gullies, but the percentage of eroded material is typically higher than for sheet-and-rill erosion because the fine material eroded from gullies is transported as suspended load by concentrated flow. Previous work indicates that the SDR for ephemeral gulley erosion in the Blackland Prairie should be about 0.67 (Alan Plummer and Associates, 2005). To compute the SDR for

sediments eroded in ephemeral gullies, the relationship between SDR and drainage area provided by Shen and Julien (1993) was adopted, and the coefficient was adjusted to compute a basin area-weighted SDR of 0.67. The resulting equation for estimating the SDR for ephemeral gullies is given by:

$$SDR_{ege}=0.43(A)^{-0.31} \quad (5.5)$$

where SDR_{ege} = sediment delivery ratio for ephemeral gulley erosion, and
A = basin area in square miles.

5.1.5. Existing Conditions Watershed Sediment Yield

Gross sheet-and-rill and gross ephemeral gulley erosion volumes were computed for each sub-basin (Figure 3.8) for the 2-, 5-, 10-, 25-, 50-, and 100-year events, and annual sediment yields were computed using Equation 5.3. Details of the computations are provided in **Appendix** E. The computed SDR values were then applied to the annual gross sheet-and-rill and gross ephemeral gulley erosion volumes to obtain the overall sediment yield from the project watershed. The results indicate that about 81,000 t/yr of fine sediment will be eroded from the watershed upstream from the location of the proposed dam (**Figure 5.1**).

5.1.6. With-Dam Sediment Yield

The estimates of the sheet-and-rill and ephemeral gulley erosion were revised to include the effects of the reservoir on watershed sediment yield. The basin parameters (i.e., basin area, watershed slope and slope length) that were used as input to the existing conditions sheet-and-rill (MUSLE) calculations were adjusted using the reservoir area at a conservation pool elevation of 551 feet (Appendix E). Compared to existing conditions, the basins located partially or entirely within the conservation pool have reduced basin areas and slopes, but the slope lengths are similar (Table 5.1). The procedures for estimation of sediment yield from ephemeral gulley erosion and application of the SDR under existing conditions were used for with-dam conditions, and indicate that the total watershed sediment yield would be reduced from 81,000 tons under existing conditions to about 69,000 tons under project conditions (Figure 5.1).

5.1.7. Worst-Case Sediment Yield

To determine the worst-case sediment yield from the project watershed, an estimate of the sheet-and-rill erosion was developed by assuming that the entire watershed was composed of cropland, and by using the highest measured annual sheet-and-rill erosion rates in the Blackland Prairie (Greiner, 1982). The measured annual sheet-and-rill erosion rates (3.74 t/ac) were applied uniformly over the watershed and the methods for estimating ephemeral gulley erosion and the SDR described above were incorporated into the computations for worst-case watershed sediment yields (Appendix E). The results indicate that the worst-case annual sediment yield delivered to the dam site would be about 147,000 tons under existing conditions, and about 90,000 tons under with-dam conditions (**Figure 5.2**).

5.2. Total Sediment Yield

The total sediment yield to the proposed dam location includes the watershed sediment yield (transported as wash load) and the sediment yield that results from erosion of the bed and banks of the mainstem NSR and its tributaries (channel sediment yield). In systems such as the NSR that have a sediment supply that is less than the hydraulic capacity of the channel to

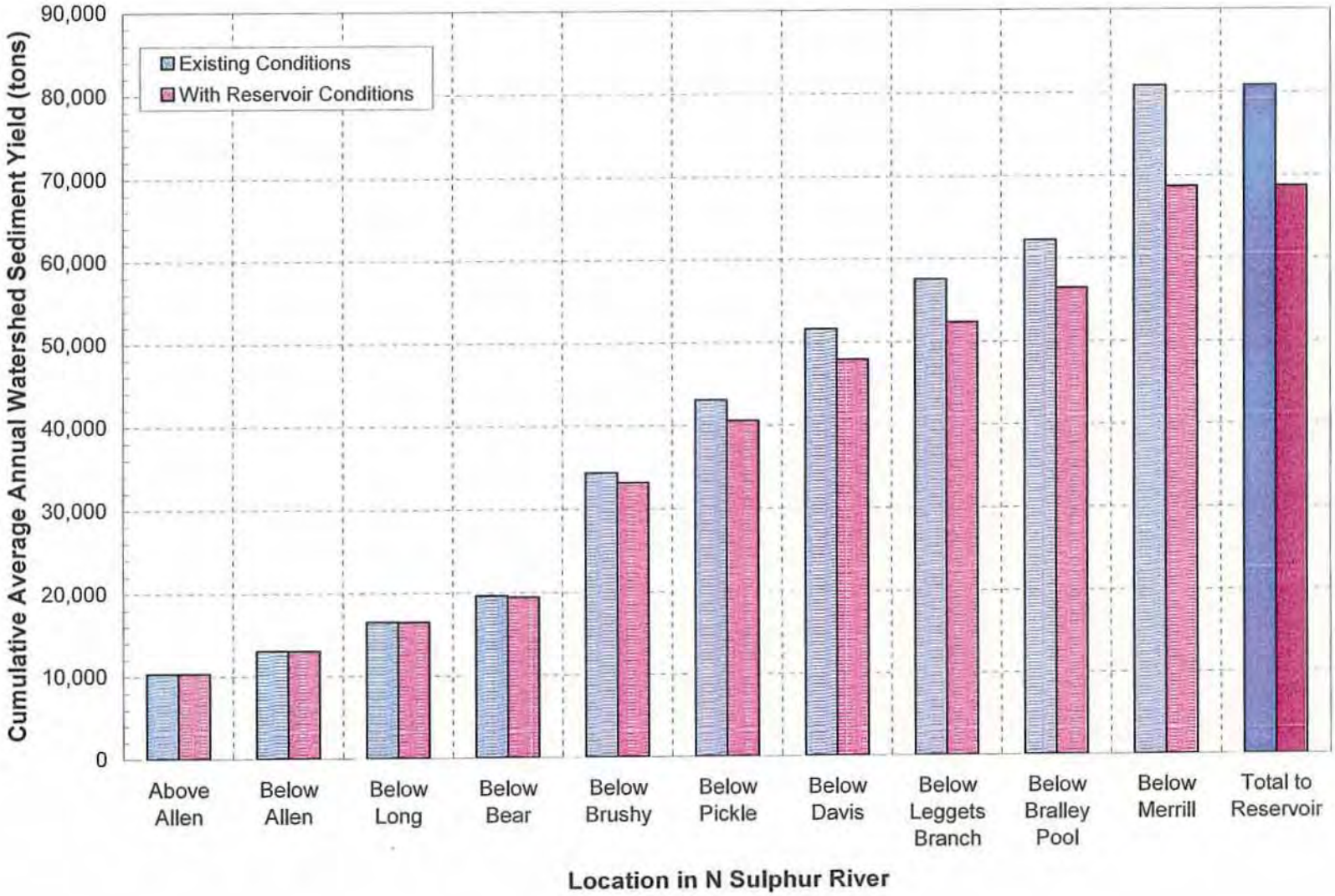

Figure 5.1. Cumulative total watershed sediment yield from the contributing basin at various locations within the project reach under existing and with-dam conditions.

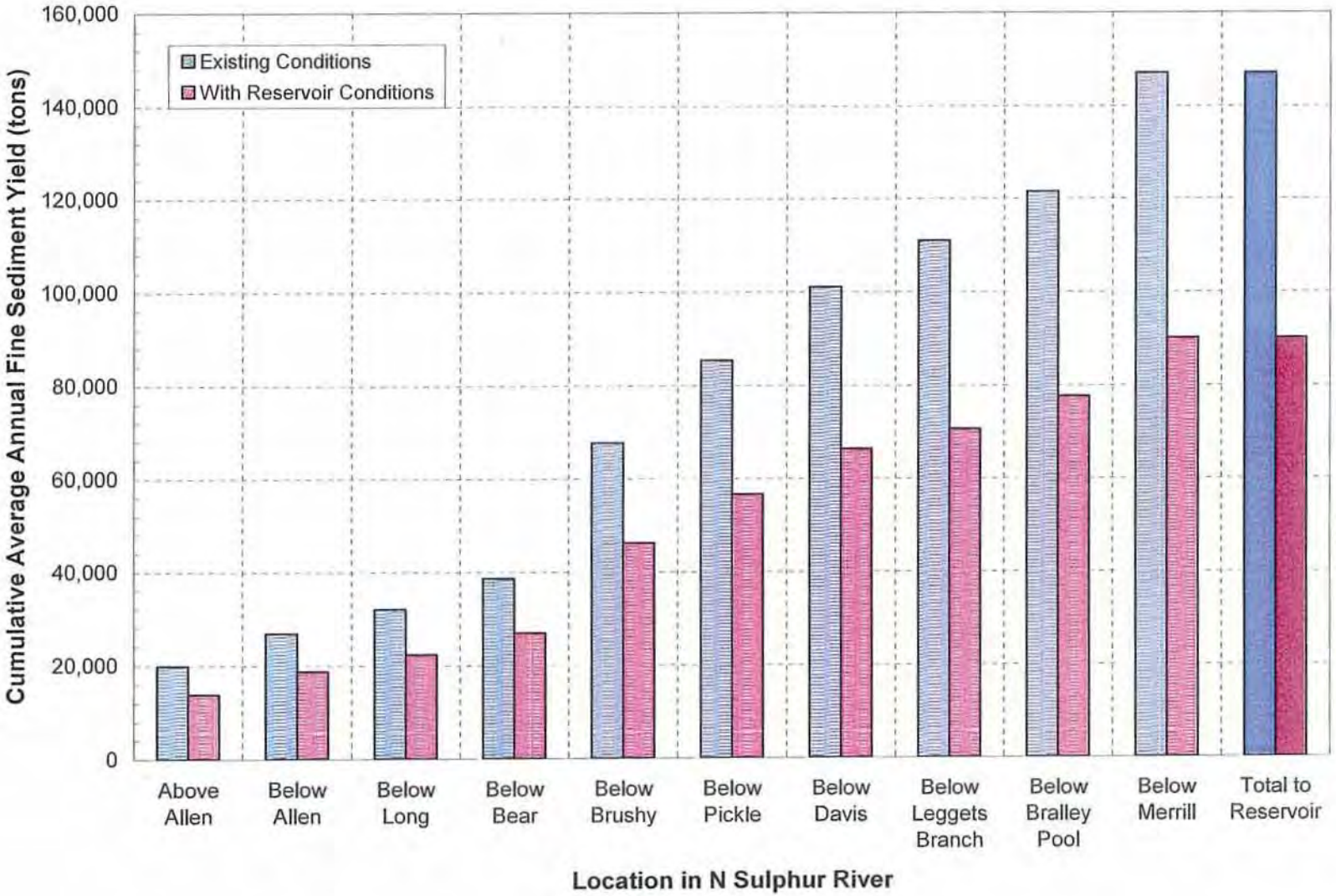

Figure 5.2. Cumulative total watershed sediment yield from the contributing basin at various locations within the project reach for the worst-case watershed sediment yields under existing and with-dam conditions.

convey sediment load (i.e., supply-limited conditions), the channel geometry typically responds through bed incision and/or erosion of the banks. In systems that have a sediment supply that exceeds the hydraulic capacity (i.e., capacity-limited conditions), net aggradation due to sediment deposition is typically expected. For the project reach of the NSR, a sediment-routing analysis was conducted to evaluate the expected total sediment yields by accounting for the observed supply-limited conditions. To evaluate the total sediment yield under capacity-limited conditions (worst-case sediment loading), a sediment-continuity analysis was performed. These two analyses are discussed in the following sections.

5.2.1. Bed-material Capacity Calculations

An estimation of the bed-material transport capacity was necessary to verify the assumption of supply-limited conditions for the sediment-routing analysis and to perform the sediment-continuity analysis for capacity-limited (worst-case) conditions. The bed-material capacity of each subreach in the mainstem NSR (Table 4.1; Figure 4.2) and in the tributaries was computed using the Meyer-Peter and Müller bed-load transport equation (Meyer-Peter and Müller, 1948) and Einstein's depth-integration of the suspended-bed sediment discharge (Einstein, 1950). Input for the capacity calculations included representative sediment gradations and specific gravities of the shale-derived material, and hydraulic data from the HEC-RAS model. The representative gradation for the mainstem shale material was based on the average of the dry sieve gradations from Samples NSR2 through NSR8 (Figure 2.38), and the representative tributary gradation was based on the average dry sieve gradations from Samples BP1, BP2, and BC1 (Figure 2.41). Specific gravity values for the mainstem were based on average bulk specific gravities of Samples NSR2 through NSR8, and an average bulk specific gravity from Samples BP1, BP2, and BC1 was used for the tributaries. The D_{16} (size with 16-percent passing), D_{50} (median diameter), D_{84} (size with 84-percent passing), and the specific gravity values are summarized in **Table 5.3**.

Bed-material transport capacity rating curves were developed for each subreach in the mainstem and the downstream subreaches in the primary tributaries by computing the bed-material load for a range of discharges using the reach-averaged hydraulic data presented in Chapter 4. The computed rating curves for the mainstem and the primary tributaries are presented in **Figures 5.3 and 5.4**. The rating curves were then integrated over the subreach hydrographs (Chapter 3) for the 2- through 100-year events and average annual bed-material capacities were computed using Equation 5.3.

5.2.2. Sediment-Routing Analysis

A sediment-routing analysis was performed using the subreaches developed for the reach-averaged hydraulic computations (Table 4.1 and Figure 4.2), estimated upstream and tributary sediment supplies, and estimated annual bed-and-bank erosion rates. The sediment-routing analysis was performed on an **annual** basis using the steps outlined in **Figure 5.5** as follows:

1. The upstream sediment supply was estimated by multiplying the computed hydraulic capacity of the upstream subreach (Subreach 1) by the percent area of the channel bed in Subreach 1 that is composed of depositional bars. The percent area with depositional bars is believed to represent the portion of the capacity that is supplied to the subreach (Struiksma, 1999), and was measured by delineating vegetated or topographically discernible bars using digital orthophotographic images taken in February 2002.

Table 5.3. Summary of gradation information used in the sediment-transport analysis.										
Subreach	Bed material capacity calculations					Shale break down to sand/washload Calculations				
	Sample	D16 (mm)	D50 (mm)	D84 (mm)	S.G.	Sample	D16 (mm)	D50 (mm)	D84 (mm)	% Sand
1	Average of All Mainstem (Dry) Sample Gradations	0.58	2.38	7.52	2.50	NSR #2 (Wet)	0.30	1.72	6.76	14%
2		0.58	2.38	7.52	2.50	NSR #2 (Wet)	0.30	1.72	6.76	14%
3		0.58	2.38	7.52	2.50	NSR #2 (Wet)	0.30	1.72	6.76	14%
4		0.58	2.38	7.52	2.50	Avg NSR#3,#4 (Wet)	0.67	3.19	10.52	56%
5		0.58	2.38	7.52	2.50	Avg NSR#3,#4 (Wet)	0.67	3.19	10.52	56%
6		0.58	2.38	7.52	2.50	Avg NSR#5,#6 (Wet)	0.52	2.33	6.91	65%
7		0.58	2.38	7.52	2.50	Avg NSR#5,#6 (Wet)	0.52	2.33	6.91	65%
8		0.58	2.38	7.52	2.50	Avg NSR#5,#6 (Wet)	0.52	2.33	6.91	65%
9		0.58	2.38	7.52	2.50	NSR #7 (Wet)	0.75	2.33	6.50	73%
10		0.58	2.38	7.52	2.50	NSR #8 (Wet)	0.69	2.18	6.16	86%
Allen	Average of All Tributubutary (Dry) Sample Gradations	0.65	2.79	9.75	2.53	Average of All Tributubutary (Wet) Sample Gradations	0.65	2.79	9.75	49%
Long		0.65	2.79	9.75	2.53		0.65	2.79	9.75	49%
Bear		0.65	2.79	9.75	2.53		0.65	2.79	9.75	49%
Pot		0.65	2.79	9.75	2.53		0.65	2.79	9.75	49%
Brushy		0.65	2.79	9.75	2.53		0.65	2.79	9.75	49%
Pickle		0.65	2.79	9.75	2.53		0.65	2.79	9.75	49%
Davis		0.65	2.79	9.75	2.53		0.65	2.79	9.75	49%
Leggetts		0.65	2.79	9.75	2.53		0.65	2.79	9.75	49%
Bralley Poc		0.65	2.79	9.75	2.53		0.65	2.79	9.75	49%
Merrill		0.65	2.79	9.75	2.53		0.65	2.79	9.75	49%
Baker		0.65	2.79	9.75	2.53		0.65	2.79	9.75	49%

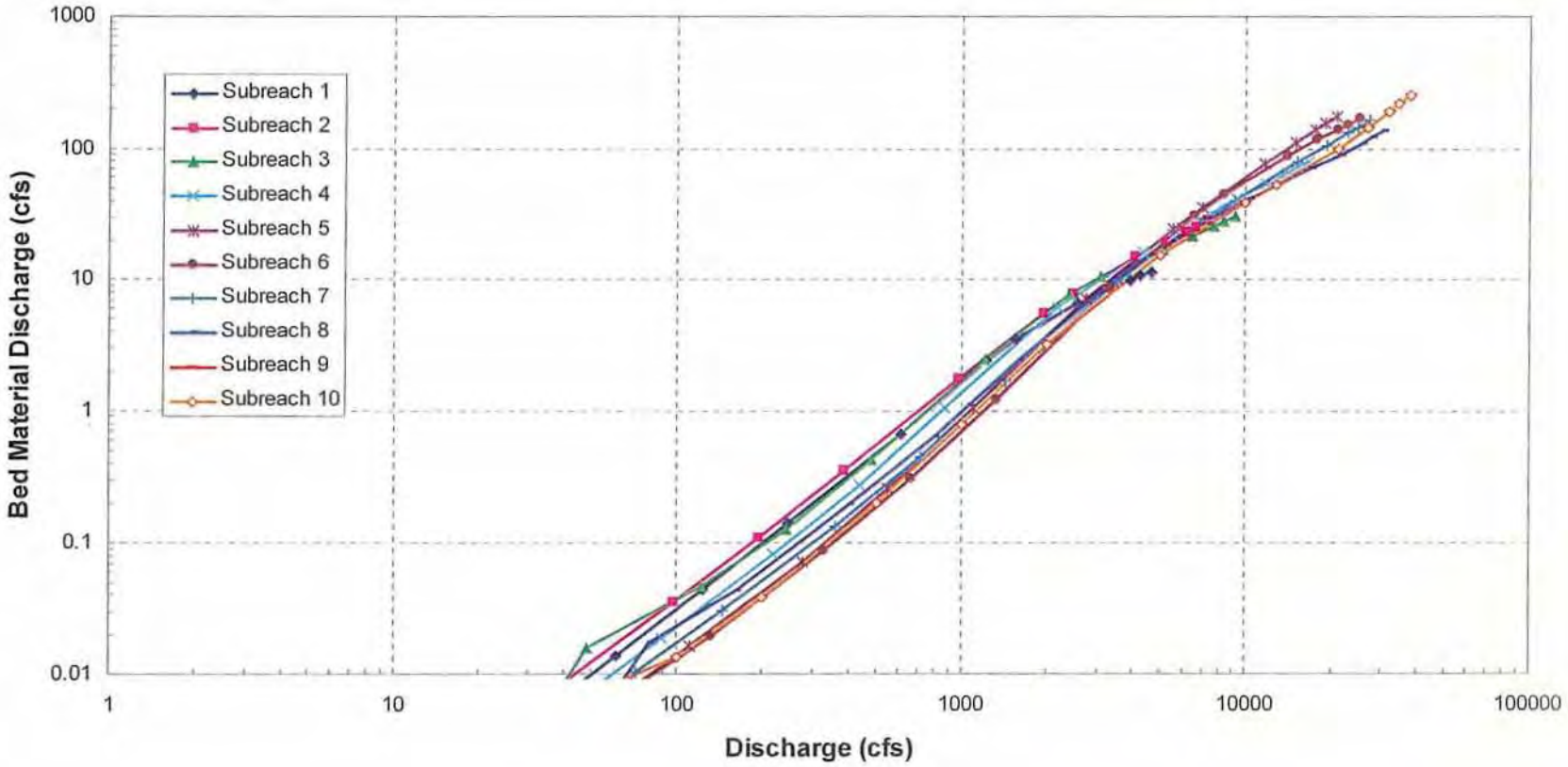

Figure 5.3. Computed bed-material transport capacity rating curves for the 10 subreaches in the mainstem North Sulphur River using MPM-Einstein equation.

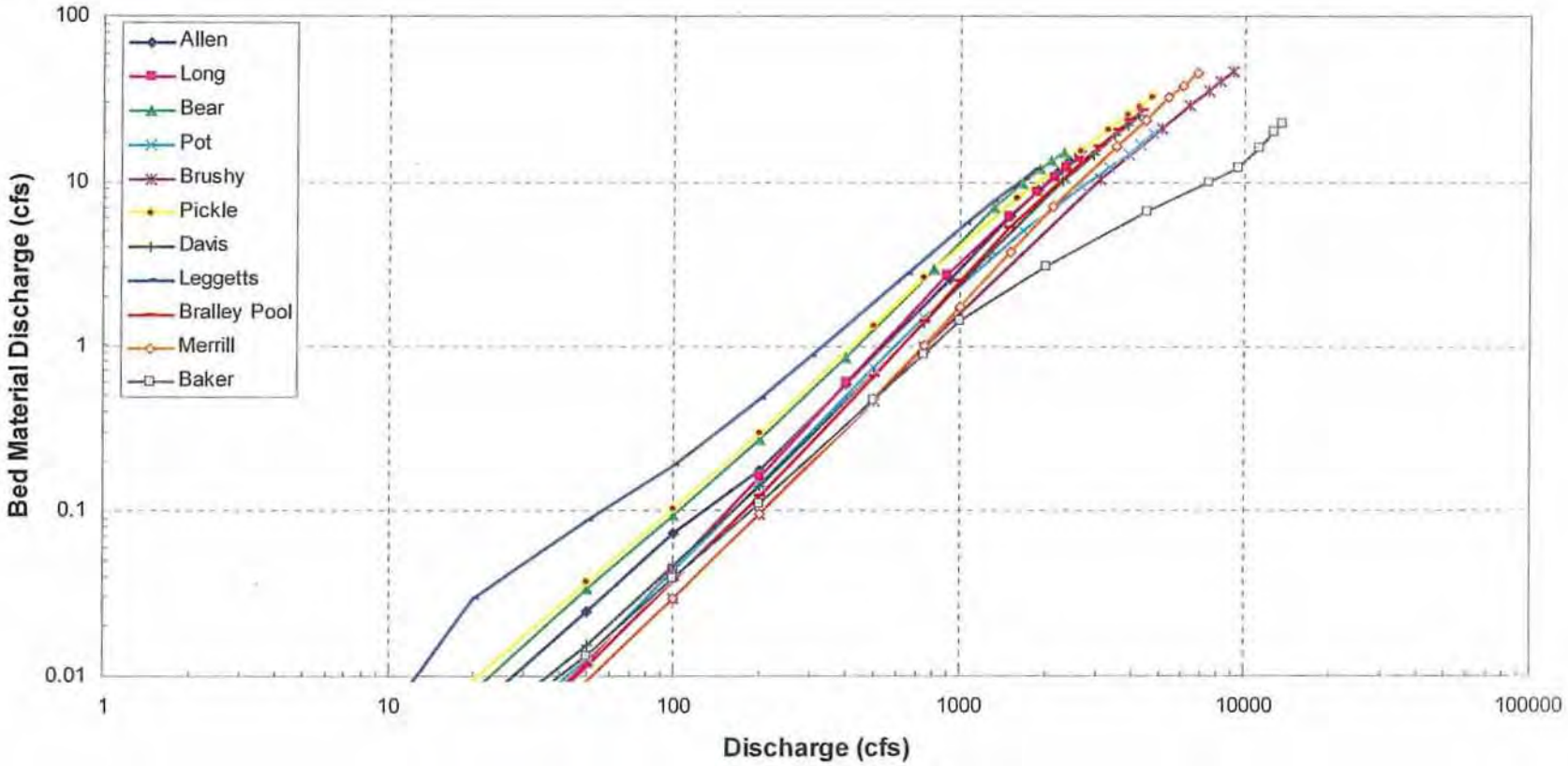

Figure 5.4. Computed bed-material transport capacity rating curves for the primary tributaries to the North Sulphur River using MPM-Einstein equation.

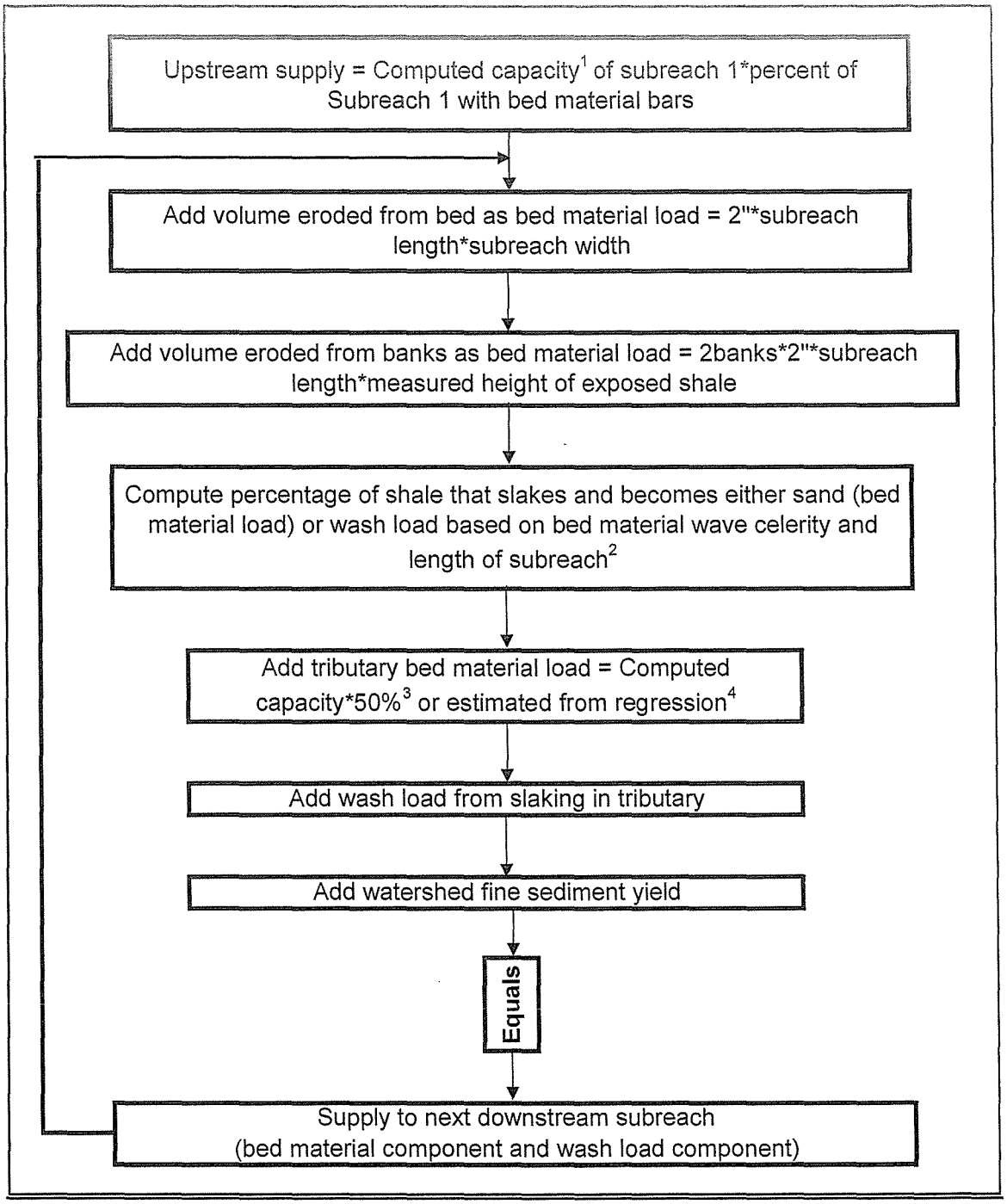

[1]Computed capacity based on representative dry gradation.

[2]Portion of shale that does not slake to wash load or sand remains shale bed material load.

[3]For primary tributaries: 50% is average of measured percentage of tributary bed that had bed material bars.

[4]For secondary tributaries: estimated from regression on computed primary tributary load as function of drainage area.

Figure 5.5. Flow chart for the sediment-routing computations.

2. The annual volume of material eroded from the shale bed was estimated using an annual degradation volume of 2 inches (Allen et al., 2002) distributed uniformly over the bed area of the subreach.

3. The annual volume of material eroded from the shale banks was estimated using an annual bank retreat of 2 inches (i.e., 4 inches of channel widening) (Allen et al., 2002), the measured (field-observed) height of the exposed shale, and the length of the subreach.

4. The percentage of shale that slakes and becomes either sand (bed-material load) or wash load was estimated using the celerity of the bed-material wave, the length of the subreach, and the time period over which the material is transported. The bed-material wave celerity (C_n) was computed from Li et al. (1988):

$$C_n=2.33(a(b-c)V^b d^{(c-1)})^{0.96} \quad (5.6)$$

where V and d = the main channel velocity and depth of flow, respectively (obtained from the reach-averaged hydraulic calculations), and
a, b, and c are solved by performing a multiple regression analysis on the relation:

$$q_s=aV^b d^c \quad (5.7)$$

where q_s = the unit bed-material sediment-transport rate computed using the total rate in Step 1 and the reach-averaged topwidth.

The distance that a shale particle travels before breaking down was estimated by multiplying the computed bed-material wave celerity by the time that the particle is subjected to transport by flowing water. This was estimated as the average time period for which flow is greater than 100 cfs at the gage times two cycles. Based on the unit discharge, a discharge of 100 cfs at the gage would represent about 40 cfs at the dam site, and was selected because the computed rating curves (Figure 5.3) indicate that flows below this discharge do not transport appreciable amounts of bed material. Two cycles were selected because previous work indicates that it requires two wetting-drying cycles for a particle of the Taylor/Ozan shale to lose about 50 percent of its weight (Allen et al., 2002).

After computing the percentage of shale bed material that breaks down within the subreach, the volume of remaining sand was computed using the percent of sand material based on the wet sieve analysis of the representative subreach sample (Figure 2.39, Table 5.3). It should be noted that the computations in this step do not affect the total sediment load estimates, since the overall volume of material is the same whether it is transported as wash load or bed-material load.

5. The bed-material load from the primary tributaries entering the subreach was estimated by multiplying the computed hydraulic capacity of the tributary by the percent area of the tributary that is composed of depositional bars. Similar to the upstream supply in Step 1, the percent area was measured by delineating vegetated or topographically-discernible bars using digital orthophotographic images taken in February 2002. However, because the orthophoto was not of sufficient resolution to delineate the bars in the smaller tributaries, the percent area calculations were conducted for the five largest tributaries (Brushy Creek, Davis Creek, Bralley Pool Creek, Merrill Creek and Baker Creek), and

resulted in an average of 27.6-percent area with depositional bars. To be conservative, the computed average was replaced with a value of 50 percent for each of the tributaries. The bed-material load from the smaller, un-named tributaries was estimated by performing a linear regression on the computed bed material load from the primary tributaries as a function of basin area, and resulted in the following regression equation:

6.

$$G_b = 351.42 * A + 54.174 \quad (5.8)$$

where G_b = tributary bed-material load in tons and
A = basin area in square miles.

The coefficient of determination (R^2) value for the regression was 0.91, indicating that tributary drainage area is a reasonable predictor for tributary bed material load.

7. The portion of the tributary bed-material load that breaks down into sand or wash-load material was not computed, since the time period over which it is subjected to transport by flowing water is not known. This simplification does not affect the overall amount of sediment supplied by the tributaries, because the volume of material is the same whether it is transported as wash load or bed-material load.

8. The bed-material and wash-load components of the total sediment load in Steps 1 through 6 are added to the computed watershed fine sediment yield from the subbasins that contribute to the subreach (Section 5.1). This total sediment load represents the supply to the next downstream subreach, and replaces Step 1 for all of the subreaches below Subreach 1.

The sediment-routing analysis was carried out under existing conditions (pre-project) to provide the best estimate of the total annual sediment yield, and indicates that about 174,000 t/yr (86 ac-ft/yr) will be transported to the proposed location of the dam. To verify the assumption that the system is supply-limited, the annual sediment loads at the downstream limit of each of the subreaches were compared to the computed hydraulic capacities, which indicated that supply-limited conditions occur throughout the project reach (i.e., the annual sediment loads were less than the computed capacities). An additional verification of this approach was carried out by comparing the measured percent area with depositional bars to the ratio of the computed sediment load to the hydraulic capacity as a percentage for each subreach (**Figure 5.6**). The comparison indicates that the ratio of the computed sediment load to the hydraulic capacity is generally greater than the percent area composed of depositional bars, and, therefore, the estimates are conservatively high.

The sediment routing was also carried out for with-dam conditions. This analysis assumed that the bed-material transport capacity is negligible within the reservoir, so bed-material transport occurs only in Subreaches 1 (upstream from the reservoir) and 10 (downstream from the reservoir). All sand material that results from slaking was deposited in the subreach. For the tributary sediment loading, the bed-material sediment loads computed for existing conditions were converted to wash load or deposited sands, since the bed material would be transported to the conservation pool, where it would be subjected to wetting and drying cycles as the pool elevation fluctuates. The results indicate that the total sediment load deposited upstream from the dam will be about 104,000 t/yr (~51 ac-ft/yr), of which about 20,000 t/yr is sand and the remainder is fine material.

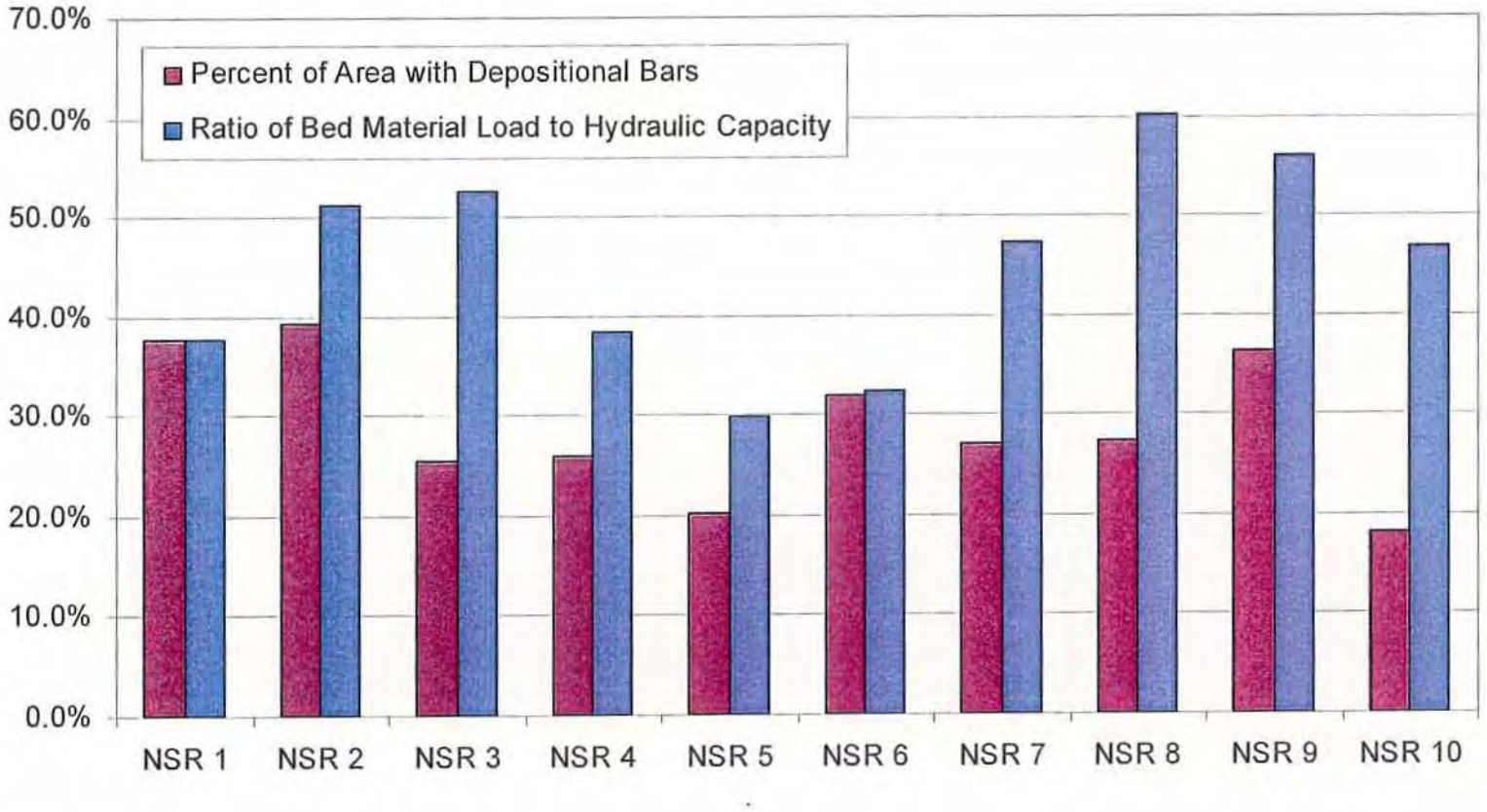

Figure 5.6. Measured percent area composed of depositional bars and the ratio (as percentage) of computed annual bed-material load to the hydraulic capacity for each subreach from the sediment routing analysis.

5.2.3. Capacity-Limited Sediment-Continuity Analysis

Worst-case channel sediment yields would result if the amount of bed-material supply to the system exceeds the hydraulic capacity. Although capacity-limited conditions are clearly not representative of the NSR, a sediment-continuity analysis was performed to evaluate maximum channel sediment yields. The sediment-continuity analysis involves comparing the upstream and tributary supply to a given subreach with the computed hydraulic capacity. If the supply exceeds the capacity, deposition occurs and the supply to the next downstream subreach is limited by the capacity of the current subreach. If the capacity exceeds the supply, degradation is indicated and the deficit is balanced through erosion of the channel bed and banks. The analysis was carried out using the bed-material capacity rating curves for the mainstem NSR and for the primary tributaries (Figures 5.3 and 5.4), and the wash-load component was accounted for by adding the watershed fine sediment yields (Section 5.1.5) and the amount of wash load that would result from breakdown of the shale material. To be conservative, it was assumed that the upstream bed-material supply for each subreach completely breaks down to wash load (or sand), and that erosion of the channel bed and banks balances the reduction in sediment load, thereby maintaining a sediment load that equals the hydraulic capacity at the downstream limit of the subreach Results from the analysis indicate that the total volume delivered to the proposed dam site could be about 373,000 t/yr (184 ac-ft/yr) if there was an unlimited supply of bed material to the system. Aggradation/degradation depths for each subreach were computed by dividing computed volume of deposited or eroded sediments by the bed area of each subreach. The results indicate that net aggradation rates of less than 0.2 in./yr would occur with an unlimited supply of bed material. Net aggradation in the project reach is clearly not representative of observed conditions, indicating the assumption of unlimited bed-material supply overestimates actual supply rates (**Figure 5.7**).

The sediment-continuity analysis was also carried out for with-dam conditions to evaluate worst-case channel sediment yields. Consistent with the sediment-routing analysis for with-dam conditions, it was assumed that the bed-material capacity is negligible within the reservoir, so bed-material transport occurs only in Subreaches 1 (upstream from the reservoir) and 10 (downstream from the reservoir). All sand material that results from break down of the shale was deposited in the subreach. For the tributary sediment loading, the bed-material sediment loads computed for existing conditions were converted to wash load or deposited sand, since the bed material would be transported to the conservation pool, where it would be subjected to wetting and drying cycles as the pool elevation fluctuates. The results indicate that the total sediment load deposited upstream from the dam will be about 128,000 t/yr (63.3 ac-ft/yr), of which about 20,000 t/yr is sand and the remainder is fine material.

5.2.4. Worst-Case Watershed Sediment Yield and Summary of Total Sediment Yields

The worst-case watershed fine sediment yields were incorporated into the sediment-routing and sediment-continuity analyses to determine the impacts of extreme watershed erosion on the total sediment loading to the proposed dam site. The analysis was carried out for existing and with-dam conditions, and indicates that for the best-estimate of the channel yield (bed-material supply limitations), the worst-case watershed sediment yield increases the total sediment yield to the dam by a factor of 1.4 under existing conditions and 1.2 under with-dam conditions. For the worst-case channel yield (unlimited bed-material supply), the worst-case watershed sediment yield increases the total sediment yield to the dam by a factor of 1.2 under existing and with-dam conditions (**Figure 5.8**).

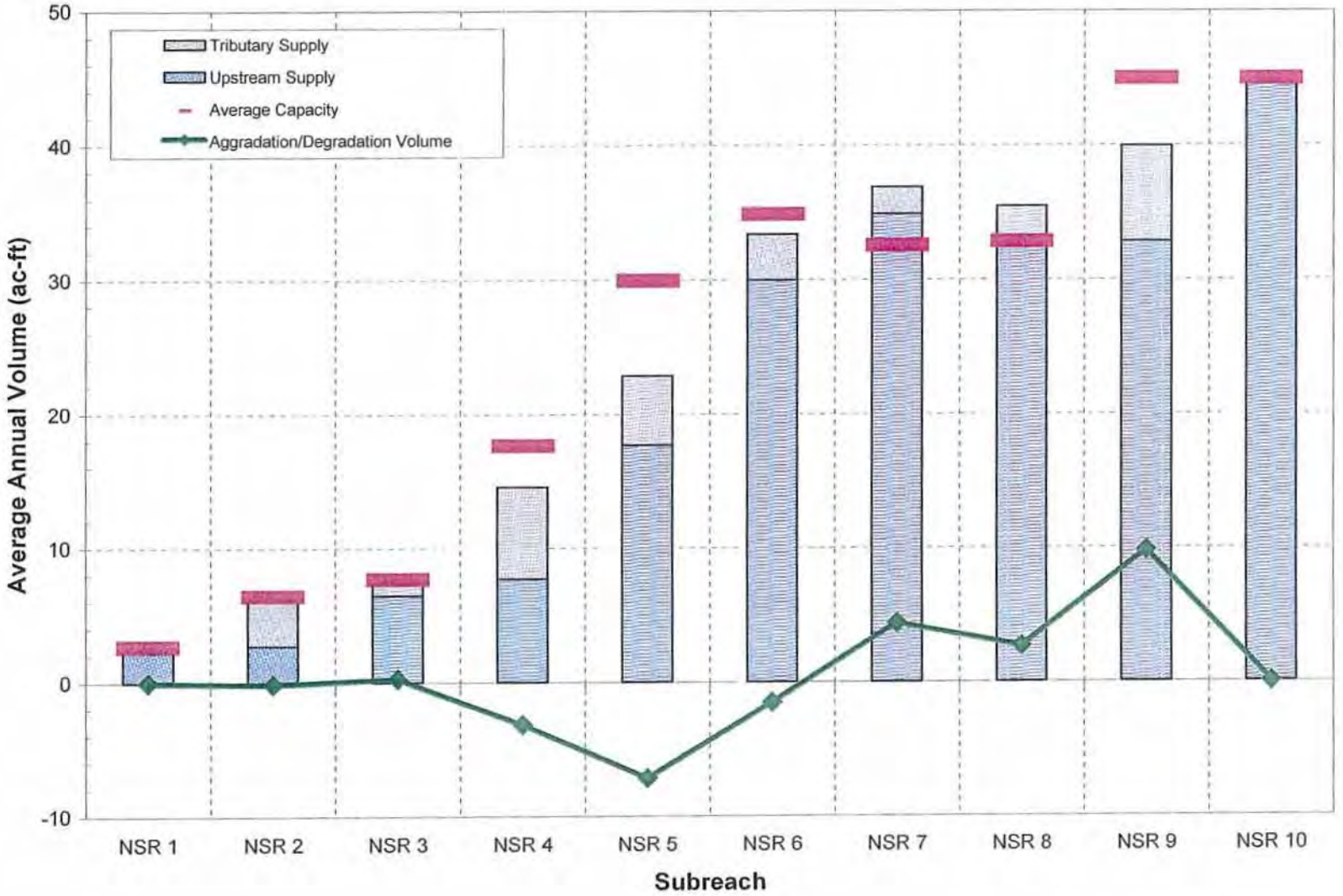

Figure 5.7. Computed upstream and tributary bed-material supply, hydraulic capacity, and the resulting aggradation/degradation volume for the sediment-continuity analysis (worst-case channel sediment yield with no supply limitations).

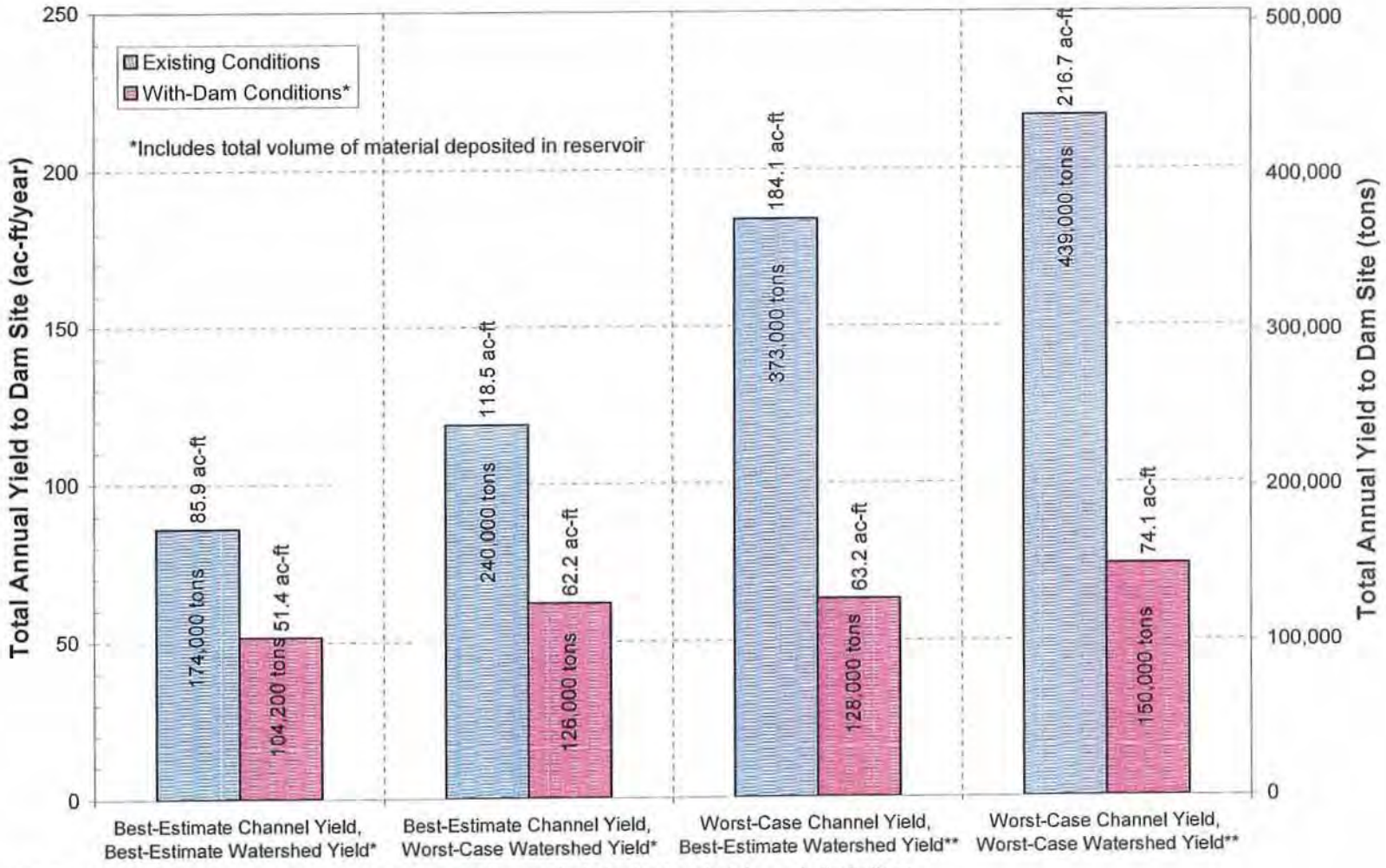

*Best-estimate of channel yield from sediment-routing analysis for bed material supply limitations.
**Worst-case channel yield from sediment-continuity analysis for unlimited bed material supply.

Figure 5.8. Summary of total sediment yield to the proposed location of the dam for the best-estimates and worst-case watershed and channel sediment yields under existing and with-dam conditions.

5.2.5. Summary

In summary, under conservative assumptions regarding existing conditions in the watershed, and assuming that the channel is supply limited, which is the most appropriate assumption based on the observed geomorphic conditions, the best estimate of annual sediment yield to the dam site under pre-project (without-dam) conditions is 85.9 ac-ft (174,000 tons). With the reservoir in place, the contributing watershed area is reduced as is the length of channel that is supplying sediment, and therefore, the annual sediment yield to the reservoir reduces to 51.4 ac-ft (104,000 tons). Therefore, the best conservative estimate of sediment delivery to the 160,235 ac-ft reservoir over the project life of 50 years is about 2,570 ac-ft which represents a loss of reservoir storage of approximately 1.6 percent over the project life. Under the assumptions of the worst case, and highly improbable, watershed (100 percent of the watershed under cultivation with no soil conservation measures) and channel sediment yields (transport capacity limited assumption) the estimated annual yield to the dam site is 217 ac-ft (439,000 tons). With the reservoir in place, this reduces to an annual yield of 74 ac-ft (150,000 tons). Therefore, the worst-case estimate of sediment delivery to the 160,235 ac-ft reservoir over the 50-year project life is about 3,700 ac-ft, which represents a loss of reservoir storage capacity of approximately 2.3 percent.

To put the estimated annual sediment yields at the dam site into perspective, a review was conducted of other sediment yield studies in the Blackland Prairie region of Texas (**Table 5.4**).

Table 5.4. Comparison of estimated sediment yields from Texas Blackland Prairie watersheds.

Source	Annual Sediment Yield at Dam Site (t/yr)	Unit Annual Sediment Yield (t/sq mi)	Unit Annual Sediment Yield (t/ac)	Annual Sediment Yield (ac-ft)
MEI best estimate	174,000	1,740	2.7	86
MEI worst-case estimate	439,000	4,390	6.9	217
Alan Plummer and Associates (2005) reservoir surveys	100,000	1,000	1.6	49
Greiner (1982) sheet, rill, gully and channel erosion	105,600	1,056	1.7	51
Simon et al. (2004) Blackland ecoregion analysis	25th Perc. 25,500 50th Perc. 179,000 75th Perc. 375,300	255 1,790 3,753	0.4 2.8 5.9	13 88 188
Coonrod et al. (1998) suspended sediment yields in Texas watersheds	104,900	1,049	1.6	52
Texas Dept. Water Resources (1979) maximum suspended sediment load, Sulphur River at Talco, Texas (1968)	264,200	2,642	4.2	130
NRCS, Birket (1994) Mill Creek sediment analysis	108,220	1,082	1.7	53

With the exception of the Simon et al. (2004) ecoregion analysis 50th and 75th percentile values that were based on only six data points, and the highest suspended sediment value measured at the Talco gage (TDWB, 1974), when there was likely a much higher channel erosion

component, the conservatively based MEI best estimate of annual sediment yield is significantly higher than other reported data for the Texas Blackland region. The MEI worst-case estimate significantly exceeds any measured or estimated values, and can be, therefore, considered to represent an upper limit that would encompass all likely sediment sources in the watershed.

One of the concerns about the Lake Ralph Hall project is the potential downstream effects of the dam on channel conditions and channel capacity. Potential problems could include sediment accumulation in the bed of the channel since operation of the reservoir will affect the magnitude and frequency of flows in the downstream channel, but will not affect sediment supply from the watershed tributaries and channel sources downstream of the dam. Field and helicopter reconnaissance of the NSR from its confluence with the South Sulphur River to the headwaters indicates that the channel of the NSR is deeply incised for its entire length, and that the bed of the channel is composed of shale bedrock. Locally, near the mouths of some of the large tributaries downstream of the dam site (e.g., Hickory and Big Sandy Creeks) there are alternate bars in the bed of the channel, but these reflect local sediment supply and do not extend downstream for any distance. Under existing conditions, the best estimate of the annual total sediment yield to the dam site is about 174,000 tons (Figure 5.7), but only about 25 percent is composed of bed material, the remainder being wash load. Therefore, construction of the dam will reduce the morphologically-significant sediment yield to the channel downstream of the dam by about 25 percent. Since the sediment-transport capacity greatly exceeds the sediment supply, this level of reduction in supply will have an insignificant effect on downstream channel morphology.

Based on the geologic map (Figure 2.2), and field observations, the characteristics of the shale exposed in the mainstem and tributaries downstream of the dam site are similar to those upstream of the site, and therefore, it can be assumed that the sediment characteristics are also similar. This being the case, the bulk of the sediments being delivered to the NSR by the tributaries downstream of the dam will be composed of shale clasts that break down into wash-load size materials as they are exposed to transport and weathering processes (slaking). Furthermore, the NSR is a supply-limited system that has the capacity to transport considerably more bed material than is currently being supplied to the channel. Consequently, it is unlikely that significant amounts of sediment will accumulate in the bed of the NSR downstream of the dam. If sediment accumulation does occur it is highly unlikely that there will be significant loss of channel capacity since flows far greater than the 100-year flood peak can be conveyed in-bank.

6. SEDIMENT MANAGEMENT

Although estimated sediment yields to the Lake Ralph Hall reservoir are relatively low, the sediment yields could be further reduced by implementation of soil conservation measures on the watershed and by reducing the exposure of shale in the mainstem of the NSR and the tributaries between the upstream end of the reservoir and the Roxton/Gober Chalk outcrop (Figure 2.2).

6.1. Watershed Sediment Reduction

The percentage of the NSR watershed area under cultivation has reduced from about 75 percent in the late 1920s (Williams, 1928) to about 26 percent presently (TSSWCB, 1997; Loretta Mokry, pers. comm., 2006), and the percentage in cropland is reducing at a rate of about 0.5 percent per year (Randy Moore, NRCS Fannin Co., pers. comm., 2006). Data from Reisel, Texas in the Blackland Prairie have shown that net soil losses with conservation management range from 0.2 to 1.0 t/ac/yr on cultivated soils (Harmel et al., 2006). In contrast, under native meadow grasses net soil losses are as low as 0.05 t/ac/yr (Richardson, 1993). Therefore conversion of cropland to native grassland could reduce the net soil loss by factors of 4 to 20.

Review of the aerial photography of the NSR watershed indicates that significant areas of the watershed have been improved with soil conservation measures including contour cultivation and terracing in the past. Field observation indicates that many of the measures have not been maintained. Therefore, sediment yields from the watershed, especially in those areas still under cultivation, could be reduced by maintaining the soil conservation structures. Additionally, a number of SCS floodwater retarding structures (FWRS) have been built within the watershed. A number of the structures have been breached as a result of baselevel-lowering-induced channel erosion, and others appear to have lost much of their storage capacity due to sedimentation. Replacement and rehabilitation of the FWRS will reduce sediment yield from the watershed. A relatively high number of gulleys were observed in areas adjacent to the incised tributary channels, especially on the south side of the watershed. Gully stabilization measures, including installation of gully plugs to store sediment on the gulley floors, revegetation, and construction of water diversion structures around the head of the gulleys to reduce erosion would reduce sediment yields from this source.

Riparian tree and shrub buffers are located along many of the channel segments in the NSR tributaries, and these tend to trap sheet-and-rill erosion-derived sediments and prevent them being delivered to the channel system. Further, the presence of a robust riparian buffer tends to increase the stability of the upper banks, both as a result of root reinforcement and development of positive matric suction when the soils are wet (Simon et al., 1999). Therefore, re-establishment of a riparian buffer zone along channel segments that have been cleared of woody vegetation is likely to reduce sediment yield to the channels.

6.2. Channel Sediment Reduction

Erosion of the shale exposed in the bed and banks of the NSR and its incised tributaries is due primarily to weathering processes (slaking) that are controlled by the frequency of wetting and drying cycles (Allen et al., 2002). As shown in the sediment-transport calculations, removal of long segments of the channel due to reservoir construction reduces the volume of channel-derived sediments by about 40 percent. Further reduction in the shale-derived channel sediment yield could be achieved by preventing further weathering of the shale. This could be

achieved by inundating the currently exposed shale outcrop on a year-round basis by constructing a number of small in-channel check structures that pond water. The extent of the exposed shale upstream of the reservoir boundaries is determined by the distance between the elevation of the top of the conservation pool and the in-channel outcrop of the Roxton/Gober Chalk (Table 2.1). The HEC-RAS models of the tributaries indicate that they easily contain the 100-year peak flow within-bank, and therefore, construction of in-channel check structures is not likely to cause out-of-bank flooding. Spacing and sizing of the check structures for the individual tributaries can be done with the HEC-RAS models (Appendix D).

A number of concrete box culverts have been constructed at road crossings on the incised tributaries to the NSR and these structures provide a measure of grade control in the channels. However, downstream erosion has caused damage to many of the structures and these will need to be maintained if they are to provide grade control in the future. A concrete box culvert at the FM 2990 crossing of Leggetts Branch that has prevented a significant amount of degradation from progressing upstream will be inundated by the reservoir, but the box culvert crossing of FM 1550 is upstream of the reservoir and will provide grade control for the upstream channel (Figure 2.25). Similarly, the box culvert at the FM 2990 crossing of Davis Creek will be inundated but the FM 1550 crossing will provide grade control provided that the structure is maintained (Figure 2.26). The box culvert at the FM 1550 crossing of Pickle Creek is also providing grade control and it too must be maintained (Figure 2.27). The H-pile and concrete beam grade-control structure below the FM 1550 bridge on Brushy Creek (Figure A.22) appears to be a successful structure, and similar structures may need to be constructed downstream of many of the other bridge and culvert crossings in the watershed.

7. SUMMARY AND CONCLUSIONS

7.1. Summary

The Upper Trinity Regional Water District (UTRWD) is proposing to build a 160,235-ac-ft water supply reservoir, Lake Ralph Hall, on the NSR about 3.5 miles north of Ladonia in Fannin County, Texas (Figure 1.1). Fannin County is located within the Texas Blackland Prairie physiographic area (NRCS, 2001). The NSR and its tributaries, within the boundaries of the proposed reservoir, as well as upstream and downstream, are deeply incised and eroding. Current conditions are the result of channelization and straightening of the sinuous, meandering river and the lower reaches of its tributaries to prevent frequent overbank flooding on the NSR floodplain in the late 1920s (Williams, 1928; Avery, 1974). Prior to channelization, the NSR was a sinuous (1.7) meandering stream with a slope of about 4.3 ft/mi. In the vicinity of the proposed dam site, the natural channel was about 48 feet wide and 6 feet deep and had a hydraulic capacity of between 700 and 1,000 cfs. The channelized and straightened channel had a top width of 16 to 30 feet, and a depth of 9 to 12 feet with a slope of 6.5 ft/mi (Avery, 1974; Chiang, Patel & Yerby, Inc., 2004; AR Consultants, Inc., 2005) and a hydraulic capacity of about 700 cfs. Currently, at the proposed dam site the NSR is 300 feet wide and about 40 feet deep, the bed and lower portions of the banks of the channel are composed of erodible shale (Ozan Formation), and the channel contains flows well in excess of the 100-year flood peak (38,000 cfs). Between the late 1920s and the present about 28M tons of sediment have been eroded from the mainstem NSR and its tributaries upstream of the proposed dam site. At the time of the channelization in the late 1920s about 75 percent of the watershed was under cultivation (Williams, 1928), and consequently soil erosion rates were probably very high (up to 16 t/ac/yr) (Baird, 1948, 1964), which may have contributed to loss of channel capacity and increased frequency of overbank flooding that occasioned the channelization. Currently about 21 percent of the watershed that contributes water and sediment to the proposed reservoir is cultivated (Texas State Soil and Water Conservation Board, 1997).

The primary objectives of this geomorphic and sedimentation study of the Lake Ralph Hall project were:

1. Quantification of the sediment delivery to the reservoir site for the 50-year project life under pre- and post-project conditions,
2. Evaluation of the downstream effects of the dam on channel conditions and flow capacity, and
3. Assessment of the potential for reducing or managing the upstream sediment supply to the reservoir.
4. Assessment of future conditions in the North Sulphur River and tributaries upstream of the dam site in the absence of the project.

Future loss of reservoir capacity due to sedimentation is the primary issue of concern for this investigation of the Lake Ralph Hall project and, therefore, estimates of sediment yield from the 100-square-mile watershed upstream of the proposed dam were required. Potential sources of sediment identified included channel erosion in the mainstem NSR and the incised tributaries (bed and banks) and watershed erosion (sheet, rill, ephemeral gully). Hydrologic analyses of the gage record at the USGS North Sulphur River near Cooper gage (USGS Gage No. 07343000) and HEC-1 models were used to estimate peak flow frequencies (Figures 3.7, 3.9),